Title

Genomic perspectives on the pathogenic chytrid fungus and persisting amphibian hosts

Author

Byrne, Allison Q

Publication Date

2020

Peer reviewed|Thesis/dissertation

Genomic perspectives on the pathogenic chytrid fungus and persisting amphibian hosts

By

Allison Q Byrne

A dissertation submitted in partial satisfaction of the

requirements for the degree of

Doctor of Philosophy

in

Environmental Science, Policy, and Management

in the

Graduate Division

of the

University of California, Berkeley

Committee in charge:

Professor Erica Bree Rosenblum, Chair
Professor Ian J. Wang
Professor Rasmus Nielsen

Summer 2020

Genomic perspectives on the pathogenic chytrid fungus and persisting amphibian hosts

by Allison Q Byrne

Abstract

Genomic perspectives on the pathogenic chytrid fungus and persisting amphibian hosts

By

Allison Q Byrne

Doctor of Philosophy in Environmental Science, Policy, and Management

University of California, Berkeley

Professor Erica Bree Rosenblum, Chair

My dissertation research is focused on using molecular tools to advance amphibian conservation and better understand the drivers of amphibian declines. My work is centered around the amphibian chytrid fungus *Batrachochytrium dendrobatidis* (Bd), which has been linked to catastrophic amphibian declines around the world. During my time as a PhD student I developed and implemented a new method to genotype Bd from noninvasive swab samples (Chapters 1 and 2). I also used genomic tools to understand how one critically endangered amphibian species is recovering after a Bd outbreak in Panama (Chapter 3).

First, I developed a new molecular method to genotype noninvasive Bd DNA samples. The most common non-invasive method for sampling Bd from natural populations is to swab amphibian skin. As a result, hundreds of thousands of swabs have been collected from amphibians around the world. However, Bd DNA collected via swabs is often low in quality and/or quantity. Working with a team in the Rosenblum lab at UC Berkeley, I developed a custom Bd genotyping assay that uses microfluidic PCR technology to amplify many carefully selected regions of the Bd genome. Here I show that this new assay has the power to accurately discriminate among the major Bd clades. Additionally, I show that this method can genotype swabs taken from preserved museum specimens, opening the possibility of retrospective Bd surveys to investigate historic pathogen dynamics.

Next, I used this new genotyping method to unveil cryptic diversity of Bd to reveal new threats for amphibians. Bd consists of distinct genetic lineages that vary in geographic extent and virulence. Most surveys for Bd report only the presence or absence of the pathogen, but some regions of the world have endemic Bd lineages and simply testing for Bd presence is not particularly informative. Using the new genotyping method for Bd described above, we can elucidate the historic relationship between amphibian communities and Bd and document recent lineage spread. By forming an opportunistic, collaborative network with amphibian biologists around the world I was able to genotype 222 new Bd samples collected from 24 different countries. This study presents the discovery of a new divergent lineage of Bd, highlights areas where divergent Bd lineages are coming into secondary contact and advances our understanding of the global distribution of this pathogen.

Finally, I used whole exome sequencing to understand mechanisms of persistence in the variable Harlequin frogs of Panama *(Atelopus varius, Atelopus zeteki*). The Panamanian golden frog (*Atelopus varius*) declined precipitously in the early 2000's due to an outbreak of Bd in Panama. Once thought to be extirpated from Panama, *A. varius* populations have recently been

rediscovered in multiple locations across their historic range. Using tissue samples collected from *A. varius* before and after the Bd outbreak in Panama, I sequenced whole exomes with the goal of describing potential genetic mechanisms of persistence. In my study I document the genetic diversity of contemporary populations in the wild and in captivity and search for genes under positive selection in wild, persistent populations. My research aims to inform conservation and captive management of these species as well as evaluate the potential for genetic rescue in imperiled amphibians.

For my mom, Sheri. Thank you for your endless support and love.

Table of Contents

Acknowledgements

First and foremost, I would like to thank my advisor Dr. Erica Bree Rosenblum. At the beginning of my graduate career I never could have dreamed of all the growth I would do as a person and scientist due to your mentorship and friendship. I am forever grateful for the doors you have opened for me, and for the ones you have encouraged me to open myself. I will carry the lessons I learned from you close to my heart always.

Also, thank you Bree for gathering some of the most amazing people and scientists and creating the wonderful RoLab community. It has made all the difference to know that I have the unwavering support of my lab in all my endeavors. Thanks specifically to Tom Poorten for teaching me so much when I was a naïve first-year. Thanks also to all the undergraduates that I have worked with at UC Berkeley – you all are inspiring and working with you was one of my favorite parts of this job.

Thank you to my committee – Dr. Rasmus Nielsen and Dr. Ian Wang. Your insights and guidance have helped shape me as a biologist and have inspired confidence and wonder in my scientific practice. Thanks also to additional faculty at UC Berkeley that have allowed me to grow as a mentor, teacher, and researcher including Dr. John Battles, Dr. Stephanie Carlson, Dr. Michelle Koo, Dr. Carol Spencer, and Dr. David Wake.

I would like to thank my funding sources including the National Science Foundation, the Department of Environmental Science, Policy and Management at UC Berkeley, and the Museum of Vertebrate Zoology (MVZ). A special acknowledgement to the MVZ community for fostering a supportive and rigorous intellectual community and for getting me started on my academic journey at UC Berkeley.

Thank you to all the people I worked with in Panama including John Morgan, Gonçalo Rosa, Andi Levorse, Kristen Charles, Angie Estrada, Rachel Perez, Kimberly Terrell, Heidi Ross, and Edgardo Griffith. Thanks specifically to Dr. Jamie Voyles and Dr. Cori Richards-Zawacki. Your mentorship has been empowering and inspiring and I hope to continue working with you until the end of time.

Thank you to Gabbi for endless laughs and encouragement. Thanks to my brothers Adam and Mike and to my Dad for always being supportive and encouraging.

Finally, thank you to the frogs for providing inspiration, skin swabs, and the occasional toe. Ultimately, this is all for you.

General introduction to the amphibian chytrid fungus and mechanisms of host resilience

The study of emerging pathogens is critical to understanding the conservation challenges of a rapidly changing, global ecosystem. Emerging infectious diseases have been increasing in prevalence and severity over time (Jones et al., 2008). In addition, the loss of biodiversity frequently increases disease transmission within an ecosystem, exacerbating disease-related declines in wildlife populations (Keesing et al., 2010). Emerging infectious diseases involve a complex interplay of the host organism, the pathogen, and the environment in which they interact. One recently emerged infectious disease that has had devastating impacts on biodiversity is the amphibian chytrid fungus *Batrachochytrium dendrobatidis* (Bd). Bd is an aquatic fungus that infects the skin of amphibians and infection often leads to death in susceptible hosts, making this emerging pathogen a significant contributor to worldwide amphibian declines (Wake & Vredenburg, 2008). While Bd research has been a top priority in the conservation community since its description in 1999 (Longcore, Pessier, & Nichols, 1999), many unanswered question remain. For example, researchers have not been able to answer why certain amphibian species are susceptible to chytridiomycosis, while others are tolerant or resistant. Consequently, our abilities to mitigate the impacts of Bd have not kept pace with its spread and destruction.

Conservation efforts to mitigate the impacts of Bd on amphibian species have focused on captive breeding, a costly and controversial practice (Griffiths & Pavajeau, 2008). Other experimental conservation practices, such as bathing amphibians in antifungal solutions, have been tested in the field but have not yielded promising results (Harris et al., 2009). As biologists have continued to study and monitor populations affected by *Bd* outbreaks, more instances of population resilience and recovery have been documented (e.g. Perez et al. 2014; Knapp et al. 2016; Barrio-Amorós et al. 2020). Understanding the mechanisms and dynamics of population recovery with respect to *Bd* is essential to inform management practices, as well as predict extinction risk and conduct viability analyses. Many drivers of population persistence and recovery have been hypothesized. Here I synthesize current research on Bd and post-outbreak amphibian populations, focusing on the proposed mechanisms for persistence, ways in which these populations have been studied in terms of host-pathogen coevolution, and implications for future management and conservation outcomes. By analyzing how the research on this system has addressed the relative contributions of the host, pathogen, and the environment, I lay the groundwork for deeper investigations into these questions in subsequent chapters.

Pathogen

Bd has been thoroughly studied under laboratory conditions using controlled infection experiments and genomic sequencing technologies. Initial research on Bd showed that the life cycle of this fungus involves a free-living, flagellated zoospore which colonizes host tissue and encysts to form a sporangia (Longcore et al., 1999). Death in susceptible hosts results from the disruption of skin integrity due to Bd invasion and the inability of amphibian hosts to exchange ions across this physiologically important membrane (Voyles et al., 2009). Recent genomic and phenotypic profiling has revealed several distinct lineages of Bd with different growth and virulence characteristics (O'Hanlon et al., 2018), including one lineage that has been linked to almost all Bd-related declines – the Global Panzootic Lineage (GPL, Farrer et al., 2011). While it is hypothesized that Bd originated in Asia (O'Hanlon et al., 2018), the precise origin of the GPL

has not been identified. Many studies have indicated that Bd lineage identity is important for disease risk (O'Hanlon et al., 2018). One important characteristic that differs among lineages is temperature-mediated growth. Bd grows within a relatively narrow range temperatures that varies slightly among lineages (Voyles et al., 2017). Additionally, whole-genome sequencing has shown that Bd has an unusually dynamic genome and some genes linked to Bd virulence have been identified (Farrer et al., 2013; Refsnider, Poorten, Langhammer, Burrowes, & Rosenblum, 2015; Rosenblum, Poorten, Joneson, & Settles, 2012). Finally, a recent study in a natural systems showed that Bd did not attenuate in virulence after becoming enzootic, indicating that changes in the pathogen cannot explain host persistence in some areas (Voyles et al., 2018). Given this finding, researchers have looked to environmental and host-related factors to explain relic populations of susceptible species.

Environment

As discussed above, Bd is temperature sensitive and tends to prefer cooler environments. Some studies have shown that Bd stops growing at 28°C and dies at 30°C (Piotrowski et al. 2004). Recent studies have shown that Bd is highly plastic in response to temperature and that this plasticity varies among lineages (Muletz-Wolz et al., 2019). Altogether, evidence of temperature sensitivity, in combination with the temperature-dependence of amphibian immune systems (Raffel, Rohr, Kiesecker, & Hudson, 2006), indicates the environment has a significant impact on disease outcomes in this system. Furthermore, specific examples of persistent amphibian species indicate that environment does play an important role in Bd outcomes.

In Australia the armored mist frog, *Litoria lorica*, was thought to have gone extinct in the early 1990's after *Bd* devastated populations in its known range. In 2008 this frog was rediscovered in a patch of habitat adjacent to its known range (Puschendorf et al., 2011). This habitat was characterized by less canopy cover and higher temperatures than the rainforest habitat that *L. lorica* typically inhabits, leading the researchers to hypothesize that an environmental refuge was responsible for the survival of this species. As a follow-up, Daskin and colleagues (2011) simulated in laboratory conditions the temperatures that would be available *L. lorica* in their hypothesized refugia. They concluded that these higher temperatures arrested the exponential growth of Bd, adding evidence that an environmental refugia may explain persistence in this species. In a related study of *Lithobates yavapaiensis*, researchers found that the probability of Bd infection was significantly negatively related to the water temperature at which the frog was caught (Forrest & Schlaepfer, 2011). Furthermore, Zumbado-Ulate and colleagues (2014) used distribution models to analyze the environmental space occupied by persisting *Craugastor punctariolus* populations to show that environmental variables appear to be very important for the persistence of this amphibian species. Altogether, studies indicate that environment is important for host-Bd interactions. However, given the limited range of many imperiled species, researchers have increasingly investigated changes in host biology that may be linked to persistence in hopes of unlocking the key to amphibian resilience.

Host

The ways in which host populations have responded to Bd has been investigated in both field and laboratory conditions. One study showed that *Atelopus zeteki* – now thought to be extinct in the wild –behaviorally thermoregulated during an outbreak of Bd (Richards-Zawacki,

2010). The study reported that frogs during the outbreak were found at consistently higher temperatures than before the outbreak. At the cellular level, studies have shown that Bd has an inhibitory effect on the immune system of some amphibian species. One study showed that Bd cells and supernatants impaired lymphocyte proliferation and induced apoptosis; however, fungal recognition and phagocytosis by macrophages and neutrophils was not impaired (Fites et al., 2013). Corroborating this finding, another study found that Bd suppress adaptive immune responses and that this mechanism of suppression is shared across distantly related susceptible species (Rosenblum, Poorten, Settles, & Murdoch, 2012).

Recently, studies have used advances in genome sequencing technologies to look for regions of the genome that might be linked to differential susceptibility in host populations. Of particular interest is the region of the genome that codes for the major histocompatibility complex II (MHCII) genes. This region is known to be linked to adaptive immunity in vertebrates. One study demonstrated that selection for certain MHCII conformations predicted survival in Bd-infected amphibians (Bataille et al., 2015). Another study combined environmental and genetic factors into a single analysis and found that host population genetics is a significant predictor of disease dynamics (Savage, Becker, & Zamudio, 2015). They considered the entire selective, genetic, and environmental landscape in determining the reason that a population of *Lithobates yavapaiensis* had differential survival in the field. They found that environment predicted infection intensity and proportion, while genetics, and specifically the MHCII conformation, was the best predictor of mortality. These finding suggest that there may be a genetic basis for resistance in some host populations.

One more example of host-mediated factors influencing Bd outcomes is that of the variable harlequin toad (*Atelopus varius* – one of the focal species in Chapter 3). This critically endangered amphibian species was previously thought to be extirpated from its range in Costa Rica and Panama. One population of *A. varius* was rediscovered in Costa Rica in 2004, then a second population was discovered in 2008 (González-Maya et al., 2013). In Panama, *A. varius* was found in both highland and lowland sites, indicating that environmental refugia may not be driving persistence in this species (Perez et al., 2014). Frogs in the genus *Atelopus* are known to be extremely susceptible to Bd (Bustamante, Livo, & Carey, 2010), so it was hypothesized that host-mediated changes may be important for this species. Indeed one study found that persisting *A. varius* produced anti-microbial peptides that were more effective at killing Bd than secretions from pre-Bd individuals (Voyles et al., 2018).

Conclusions

Despite the ever-increasing frequency of research on Bd-related amphibian declines, biologists have yet to develop a truly effective way to prevent Bd spread and the resulting impacts. Consequently, much of the field research in this system has involved observing and documenting Bd intensity and recording dwindling population numbers. Recently, however, field surveys have brought news of populations that are persisting in the wake of a Bd outbreak. These discoveries have opened a new line on inquiry in this system; what mechanisms are at play in each instance of resilience and are there similarities and differences among each? In the future, more integrative studies that account for all potential contributions of the host, pathogen, and environment will allow scientists to build a complete picture of Bd disease dynamics in a post-

outbreak ecosystem. Using advances in technology, researchers will be able to understand how and why populations can persist and inform management practices.

First, researchers must quantify the environmental space in which an amphibian host is persisting to determine what effect that the environment is having on Bd dynamics. In addition to collecting standard abiotic measurements, researchers can also use high-resolution remote sensing data and niche modeling techniques to predict where populations might be persisting and highlight areas of special conservation concern. Researchers can use eDNA techniques (as done in Chestnut et al., 2014) to filter water and use qPCR to quantify the amount of free-living Bd persisting in amphibian habitats. Next, identifying the lineages of Bd that are present in an environment will be a key insight for answering these questions. The status quo for sampling Bd has been to use qPCR to quantify fungal load on an amphibian, however, advances in genome sequencing technologies, along with an increased understanding of the Bd genome, has opened the possibility of genotyping Bd from swabs (see Chapter 1). With this technology, we can begin to understand the heterogeneity of Bd within and between populations and make predictions of virulence and spread (see Chapter 2). Finally, genomic techniques can also be used to look at host population dynamics. Using techniques such as exome capture to sequence the coding regions of persisting populations and scanning this genome for signs of adaptation will be key to understanding the genetic basis of resistance (see Chapter 3). Building an integrative approach to understanding amphibian resilience will be a critical step in taking informed management actions to save amphibian populations on the brink of extinction.

References

Barrio-Amorós, C. L., Costales, M., Vieira, J., Osterman, E., Kaiser, H., & Arteaga, A. (2020). Back from extinction: rediscovery of the harlequin toad *Atelopus mindoensis* Peters, 1973 in Ecuador. *Herpetology Notes*, *13*, 325–328.

Bataille, A., Cashins, S. D., Grogan, L., Skerratt, L. F., Hunter, D., McFadden, M., … Waldman, B. (2015). Susceptibility of amphibians to chytridiomycosis is associated with MHC class II conformation. *Proceedings of the Royal Society B: Biological Sciences*, *282*(1805), 20143127.

Bustamante, H. M., Livo, L. J., & Carey, C. (2010). Effects of temperature and hydric environment on survival of the Panamanian Golden Frog infected with a pathogenic chytrid fungus. *Integrative Zoology*, *5*(2), 143–153.

Chestnut, T., Anderson, C., Popa, R., Blaustein, A. R., Voytek, M., Olson, D. H., & Kirshtein, J. (2014). Heterogeneous Occupancy and Density Estimates of the Pathogenic Fungus *Batrachochytrium dendrobatidis* in Waters of North America, *PLoS One*, *9*(9), e106790.

Daskin, J. H., Alford, R. A., & Puschendorf, R. (2011). Short-term exposure to warm microhabitats could explain amphibian persistence with *Batrachochytrium dendrobatidis*. *PLoS One*, *6*(10), e26215.

Farrer, R. A., Henk, D. A., Garner, T. W. J., Balloux, F., Woodhams, D. C., & Fisher, M. C. (2013). Chromosomal copy number variation, selection and uneven rates of recombination

reveal cryptic genome diversity linked to pathogenicity. *PLoS Genet*, *9*(8), e1003703.

Farrer, R. A., Weinert, L. A., Bielby, J., Garner, T. W. J., Balloux, F., Clare, F., … Fisher, M. C. (2011). Multiple emergences of genetically diverse amphibian-infecting chytrids include a globalized hypervirulent recombinant lineage. *Proceedings of the National Academy of Sciences*, *108*(46), 18732–18736.

Fites, S. ., Ramsey, J. ., Holden, W. ., Collier, S. ., Sutherland, D. M., Reinert, L. ., … Rollins-Smith, L. (2013). The invasive chytrid fungus of amphibians paralyzes lymphocyte responses. *Science*, *342*(6156), 366–369.

Forrest, M. J., & Schlaepfer, M. a. (2011). Nothing a hot bath won't cure: Infection rates of amphibian chytrid fungus correlate negatively with water temperature under natural field settings. *PLoS ONE*, *6*(12), e28444.

González-Maya, J. F., Escobedo-Galván, A. H., Wyatt, S. a., Schipper, J., Belant, J. L., Fischer, A., … Corrales, D. (2013). Renewing hope: the rediscovery of *Atelopus varius* in Costa Rica. *Amphibia-Reptilia*, *34*, 573–578.

Griffiths, R. A., & Pavajeau, L. (2008). Captive breeding, reintroduction, and the conservation of amphibians. *Conservation Biology*, *22*(4), 852–861.

Harris, R. N., Brucker, R. M., Walke, J. B., Becker, M. H., Schwantes, C. R., Flaherty, D. C., … Minbiole, K. P. C. (2009). Skin microbes on frogs prevent morbidity and mortality caused by a lethal skin fungus. *ISME J*, *3*(7), 818–824.

Jones, K. E., Patel, N. G., Levy, M. A., Storeygard, A., Balk, D., Gittleman, J. L., & Daszak, P. (2008). Global trends in emerging infectious diseases. *Nature*, *451*(7181), 990–993.

Keesing, F., Belden, L. K., Daszak, P., Dobson, A., Harvell, C. D., Holt, R. D., … Mitchell, C. E. (2010). Impacts of biodiversity on the emergence and transmission of infectious diseases. *Nature*, *468*(7324), 647–652.

Knapp, R. A., Fellers, G. M., Kleeman, P. M., Miller, D. A. W., Vredenburg, V. T., Rosenblum, E. B., & Briggs, C. J. (2016). Large-scale recovery of an endangered amphibian despite ongoing exposure to multiple stressors. *Proceedings of the National Academy of Sciences* , *113*(42), 11889–11894.

Longcore, J. E., Pessier, A. P., & Nichols, D. K. (1999). *Batrachochytrium Dendrobatidis* gen. et sp. nov., a Chytrid Pathogenic to Amphibians. *Mycologia*, *91*(2), 219–227.

Muletz-Wolz, C. R., Barnett, S. E., DiRenzo, G. V, Zamudio, K. R., Toledo, L. F., James, T. Y., & Lips, K. R. (2019). Diverse genotypes of the amphibian-killing fungus produce distinct phenotypes through plastic responses to temperature. *Journal of Evolutionary Biology*, *32*(3), 287–298.

O'Hanlon, S. J., Rieux, A., Farrer, R. A., Rosa, G. M., Waldman, B., Bataille, A., … Fisher, M. C. (2018). Recent Asian origin of chytrid fungi causing global amphibian declines. *Science*,

360(6389), 621 LP-627.

Perez, R., Richards-zawacki, C. L., Krohn, A. R., Robak, M., Griffith, E. J., Ross, H., … Voyles, J. (2014). Short Communication Field surveys in Western Panama indicate populations of Atelopus varius frogs are persisting in regions where *Batrachochytrium dendrobatidis* is now enzootic, *Amphibian & Reptile Conservation*, *8*(2), 30–35.

Puschendorf, R., Hoskin, C. J., Cashins, S. D., Mcdonald, K., Skerratt, L. F., Vanderwal, J., & Alford, R. a. (2011). Environmental Refuge from Disease-Driven Amphibian Extinction. *Conservation Biology*, *25*(5), 956–964.

Raffel, T. R., Rohr, J. R., Kiesecker, J. M., & Hudson, P. J. (2006). Negative effects of changing temperature on amphibian immunity under field conditions. *Functional Ecology*, *20*(5), 819–828.

Refsnider, J. M., Poorten, T. J., Langhammer, P. F., Burrowes, P. A., & Rosenblum, E. B. (2015). Genomic Correlates of Virulence Attenuation in the Deadly Amphibian Chytrid Fungus, *Batrachochytrium dendrobatidis*. *G3: Genes, Genomes, Genetics*, *5*(11), 2291–2298.

Richards-Zawacki, C. L. (2010). Thermoregulatory behaviour affects prevalence of chytrid fungal infection in a wild population of Panamanian golden frogs. *Proceedings. Biological Sciences / The Royal Society*, *277*(1681), 519–528.

Rosenblum, E. B., Poorten, T. J., Joneson, S., & Settles, M. (2012). Substrate-Specific Gene Expression in *Batrachochytrium dendrobatidis*, the Chytrid Pathogen of Amphibians. *PLoS ONE*, *7*(11), e49924.

Rosenblum, E. B., Poorten, T. J., Settles, M., & Murdoch, G. K. (2012). Only skin deep: Shared genetic response to the deadly chytrid fungus in susceptible frog species. *Molecular Ecology*, *21*(13), 3110–3120.

Savage, A. E., Becker, C. G., & Zamudio, K. R. (2015). Linking genetic and environmental factors in amphibian disease risk. *Evolutionary Applications*, *8*(6), 560–572.

Voyles, J., Johnson, L. R., Rohr, J., Kelly, R., Barron, C., Miller, D., … Rosenblum, E. B. (2017). Diversity in growth patterns among strains of the lethal fungal pathogen *Batrachochytrium dendrobatidis* across extended thermal optima. *Oecologia*, *184*(2), 363–373.

Voyles, J., Woodhams, D. C., Saenz, V., Byrne, A. Q., Perez, R., Rios-Sotelo, G., … Richards-Zawacki, C. L. (2018). Shifts in disease dynamics in a tropical amphibian assemblage are not due to pathogen attenuation. *Science*, *359*(6383), 1517 LP-1519.

Voyles, J., Young, S., Berger, L., Campbell, C., Voyles, W. F., & Dinudom, A. (2009). Pathogenesis of Chytridiomycosis, a Cause of Catastrophic Amphibian Declines. *Science*, *326*(5952), 582–585.

Wake, D. B., & Vredenburg, V. T. (2008). Colloquium paper: are we in the midst of the sixth mass extinction? A view from the world of amphibians. *Proceedings of the National Academy of Sciences of the United States of America*, *105 Suppl 1*, 11466–73.

Zumbado-Ulate, H., Bolaños, F., Gutiérrez-Espeleta, G., & Puschendorf, R. (2014). Extremely Low Prevalence of *Batrachochytrium dendrobatidis* in Frog Populations from Neotropical Dry Forest of Costa Rica Supports the Existence of a Climatic Refuge from Disease. *EcoHealth*, *11*(4), 593–602.

Chapter 1: Unlocking the story in the swab: A new genotyping assay for the amphibian chytrid fungus *Batrachochytrium dendrobatidis*

Abstract

One of the most devastating emerging pathogens of wildlife is the chytrid fungus, *Batrachochytrium dendrobatidis* (Bd), which affects hundreds of amphibian species around the world. Genomic data from pure Bd cultures has advanced our understanding of Bd phylogenetics, genomic architecture, and mechanisms of virulence. However pure cultures are laborious to obtain and whole genome sequencing is relatively expensive, so relatively few isolates have been genetically characterized. Thus we still know little about the genetic diversity of Bd in natural systems. The most common non-invasive method of sampling Bd from natural populations is to swab amphibian skin. Hundreds of thousands of swabs have been collected from amphibians around the world, but Bd DNA collected via swabs is often low in quality and/or quantity. In this study, we developed a custom Bd genotyping assay using the Fluidigm Access Array platform to amplify 192 carefully-selected regions of the Bd genome. We obtained robust sequence data for pure Bd cultures and field-collected skin swabs. This new assay has the power to accurately discriminate among the major Bd clades, recreating the basic tree topology previously constructed using whole genome data. Additionally, we established a critical value for initial Bd load for swab samples (150 Bd genomic equivalents) above which our assay performs well. By leveraging advances in microfluidic multiplex PCR technology and the globally distributed resource of amphibian swab samples, non-invasive skin swabs can now be used to address critical spatial and temporal questions about Bd and its effects on declining amphibian populations.

Introduction

Emerging infectious diseases (EID) are increasingly recognized as a critical threat to wildlife. EIDs have been responsible for catastrophic declines in many natural systems, for example chytridiomycosis in amphibians, white-nose syndrome in bats, avian malaria in Hawaii, and chronic wasting disease in cervids (Atkinson & Samuel, 2010; Foley, Clifford, Castle, Cryan, & Ostfeld, 2011; Saunders, Bartelt-Hunt, & Bartz, 2012; Skerratt et al., 2007). To further understand the origin, spread, and transmission dynamics of EIDs of wildlife, biologists have increasingly turned to genetic and genomic tools (Archie, Luikart, & Ezenwa, 2009; Grogan et al., 2014). Advances in DNA extraction, amplification and sequencing technologies can inform wildlife management by allowing effective and timely disease monitoring, identification of disease transmission pathways, and reconstruction of evolutionary relationships among pathogens.(e.g. Beja-Pereira et al. 2009; Schloegel et al. 2012; Wallace et al. 2007).

Of the many documented wildlife EIDs, few have had such a devastating impact as the amphibian chytrid fungus, *Batrachochytrium dendrobatidis* (Bd). Bd is a generalist pathogen that infects hundreds of amphibian species around the world. Chytridiomycosis - the disease caused by Bd - has been linked to mass mortality events in many of the most diverse amphibian communities in the world (Berger et al., 1998; Crawford, Lips, & Bermingham, 2010). To date, the most detailed genetic and genomic studies of Bd have relied on pure cultures of the pathogen, which are isolated from infected wild amphibians. Once isolated, pure cultures can be cryoarchived for use in future experiments (Boyle et al., 2003) and can be grown in the lab to provide enough genetic material for the application of genome-scale molecular approaches.

Molecular studies from pure Bd isolates have been used to produce a Bd phylogeny, reveal complex structural variation in the Bd genome, identify putative virulence genes, and catalogue Bd strains that likely result from hybridization (Farrer et al., 2011; Jenkinson et al., 2016; Rosenblum et al., 2013; Rosenblum, Poorten, Joneson, & Settles, 2012). However, pure cultures are laborious to isolate, require access to a sterile laboratory, and often necessitate destructive amphibian sampling (Longcore, Pessier, & Nichols, 1999). While some pure Bd cultures have been isolated from less destructive toe clips, toe-clipping can cause stress to individual amphibians (McCarthy and Parris 2004) and still requires access to a sterile laboratory for processing. Therefore, studies using pure isolates generally suffer from limited sample sizes and lack of isolates from remote locations.

An alternative sampling method to collect Bd genetic material is the use of sterile swabs (Hyatt et al., 2007; Retallick, Miera, Richards, & Field, 2006). Bd infects the epidermal cells of amphibians and the keratinized mouthparts of tadpoles (Berger et al., 1998; Fellers, Green, & Longcore, 2001). By swabbing amphibian skin or tadpole mouthparts, Bd genetic material can be collected in an inexpensive and non-invasive manner, allowing for large sample sizes and minimal impacts on host species. Swabs are then typically screened for Bd using a quantitative PCR assay (Boyle, Boyle, Olsen, Morgan, & Hyatt, 2004; Hyatt et al., 2007). To date, Bd swabs have most commonly been used to track Bd prevalence and load in natural populations, infection intensity during laboratory infection experiments, and Bd presence in museum specimens (e.g. Cheng et al. 2011; Zhu et al. 2014). Amphibian researchers have collected hundreds of thousands of swabs from myriad host species, geographic localities, and time-points during Bd outbreaks (Olson et al., 2013). However, the use of swabs for more detailed population genetics studies has been limited by the low quality and quantity of DNA collected using this method. A handful of studies have sequenced genetic markers from swabs, but these have been limited to one or few loci (e.g. Bai et al. 2012; Garland et al. 2011; Goka et al. 2009) and have lacked resolution for addressing key questions about the origin, spread, and transmission of Bd.

Here we present a new method for rapid, cost-effective, multi-locus genotyping for Bd swab samples. We selected 192 target regions of the Bd genome based on their ability to capture variation within and between the major clades of the Bd phylogeny. We then developed a custom Bd assay using the Fluidigm Access Array System. This microfluidic multiplex PCR platform amplifies selected regions of the Bd genome and tags individual samples so they can be pooled for Illumina sequencing. The assay is specifically designed to amplify Bd DNA of low quantity and/or quality and is highly scalable for large sample sizes. By leveraging advances in DNA amplification and sequencing technology and the globally distributed resource of amphibian swab samples, we can begin to understand Bd genetic diversity across temporal and spatial scales and finally unlock the story in the swab.

Materials and Methods

Genomic loci selection and primer design

We used genomic datasets consisting of 29 globally distributed Bd isolates from Rosenblum et al. (2013) and 20 Bd isolates from Farrer et al. (2011) as the basis for developing our genotyping assay. We integrated these two datasets to obtain 76,515 single nucleotide polymorphisms (SNPs) and infer a whole genome phylogeny (see Rosenblum et al. 2013). Using the genomes of these 49 isolates, we selected 192 genomic regions for our new assay (Supplementary Table 1). We targeted 150-200 base pair regions (rather than particular SNPs) to

increase the power of our assay and to avoid issues of ascertainment bias. We selected target regions based on three primary criteria:

First, we selected genomic regions that had discriminatory power at different nodes of the Bd phylogeny. Specifically, we chose regions with SNPs that showed high genetic differentiation (F_{ST} values) between clades of interest. We captured variation across five Bd lineages including two main clades within the globally distributed Global Panzootic Lineage (GPL), divergent lineages from South Africa (Bd-Cape) and Europe (Bd-CH), and a deeply divergent group of isolates from Brazil (Bd-Brazil) (Farrer et al., 2011; Rosenblum et al., 2013).

Second, we selected genomic regions in putative mutational hotspots to increase the resolution within the GPL. Using a sliding window analysis, we searched for clusters of informative SNPs that were enriched for rare alleles (defined as a minor allele frequency (MAF) <0.15 in the Rosenblum et al. (2013) genomic dataset). In addition, we chose genomic targets that were well dispersed across different chromosomal segments.

Third, we selected several genomic regions to provide a direct comparison to previous Bd studies. We targeted genomic regions previously sequenced in other studies (James et al., 2009; Morehouse et al., 2003; Morgan et al., 2007; Schloegel et al., 2012) and designed additional primers for these regions to fit our target amplicon size and design parameters. In addition, we included a single primer pair to target, *Batrachochytrium salamandrivorans,* a recently described relative of Bd that is particularly deadly to salamanders (Martel et al., 2013). We selected *B. salamandrivorans* specific primers for the ITS1, 5.8S rRNA, ITS2 region (Genbank: KC762295) based on Martel et al. (2013). This single *B. salamandrivorans* marker will most likely function as a detection locus rather than as a marker for comparative purposes, but additional *B. salamandrivorans* markers can be added as genomic resources are developed for this species.

Primer validation

We designed primers *in silico* using Primer3 version 0.4.0 (Koressaar & Remm, 2007) using Bd isolate JEL423 (Broad Institute, broadinstitute.org) as a reference genome. We optimized for conditions as required for the Fluidigm Access Array System (Fluidigm, South San Francisco, CA) including a melting temperature of 60°C and a 3bp maximum length for mononucleotide repeats. We selected amplicons of 150-200bp to increase the potential for informative linked SNPs within regions while keeping amplicon sizes small. We excluded all known polymorphisms from the primer binding sites to maximize probability of successful primer binding to all Bd samples.

We subsequently tested all designed primers using *in silico* PCR in *Geneious* version 7.1.2 (Kearse et al., 2012) to assess specificity and confirm that targets were single-copy loci. We ensured no overlap between forward and reverse primers of nearby target regions, we verified inclusion of SNPs in the target sequences, and we confirmed that all primer-binding sites were located in conserved regions of the Bd genome. Finally, we assessed phylogenetic resolution of our assay by aligning target sequences from Bd strains in all major clades.

Primer pooling

Pooling primers allows more high-throughput workflows, but multiplex PCR methods can be prone to amplification failure if primer pools are not constructed carefully (e.g., dimer interactions among primers, amplification bias towards more robust amplicons, differences in

GC content among amplicons) (Baskaran et al., 1996; Markoulatos, Siafakas, & Moncany, 2002; Suzuki & Giovannoni, 1996). We therefore carefully assigned our primers to pools that minimized adverse interactions. We constructed primer pools in 48 wells (4 primer pairs per pool). As an initial screen for primer pooling, we sorted primer pairs based on target regions being on different chromosomal segments. We then screened for potential inter-primer interactions using Thermo Fisher Scientific multiple primer analyzer tool (https://www.thermofisher.com/us/en/home/brands/thermo-scientific/molecular-biology/molecular-biology-learning-center/molecular-biology-resource-library/thermo-scientific-web-tools/multiple-primer-analyzer.html). Additionally, we kept amplicon sizes within 20% of the average length within each primer pool to avoid amplification biases resulting from combining PCR products of different sizes. Furthermore, we calculated GC content of all amplicons using the Biostrings package in R (Pagès, Aboyoun, Gentleman, & DebRoy, 2016) to ensure combined primer pairs would target regions with GC content within 20% of the average GC content among amplicons in each well.

Sample selection and DNA isolation

Following genomic target selection and primer design, we selected samples for assay validation with two primary goals. Our first goal was to assess how accurately our 192 genomic targets could recover the basic topology of the Bd phylogeny presented in Rosenblum et al. (2013). Therefore, we selected 28 Bd isolates that were globally dispersed and from a variety of amphibian host species (Supplementary Table 2). Our sampling focused on the GPL and the divergent Bd-Brazil clade, but was not exhaustive and did not include *B. salamandrivorans*. We also included isolates from three non-Bd chytrids: *Homolaphlyctis polyrhiza, Entophlyctis helioformis,* and *Rhizophydium brooksianum* to test the specificity of the primers. We extracted isolate DNA using a modified version of a phenol-chloroform extraction protocol (Joneson, Stajich, Shiu, & Rosenblum, 2011; Zolan & Pukkila, 1986).

Our second goal was to test assay sensitivity to DNA quantity. We included three replicates each of serial diluted Bd DNA extractions at 0.1, 1, 10, and 100 genome equivalents (GE). We also included 48 field-collected swab samples ranging in Bd copy number from 1.6-116,706 (Supplementary Table 2). We extracted DNA from the swab samples using the manufacturer's recommendations for Qiagen DNeasy Kits (Qiagen, Valencia, CA). Copy number for the swabs was calculated by using a plasmid-based qPCR standard. Average copy number is a commonly-reported measure of Bd infection intensity, therefore we chose swab samples with different Bd loads to assess assay performance. See Supplementary Table 2 for the full list of 96 samples included in this study.

Microfluidic PCR and Illumina sequencing

The Fluidigm Access Array platform allows users to perform multiple (48 primer pairs) PCRs across multiple (48) DNA samples in parallel through a two-staged multiplex amplification (2,304 simultaneous PCR reactions). During PCR, all amplicons are tagged with 1) dual barcodes to distinguish each sample and 2) sequencing adapters suitable for downstream Illumina sequencing. After amplification, all samples are pooled for sequencing and can later be demultiplexed by their respective barcodes.

To improve microfluidic PCR success, we used a pre-amplification step that first enriches DNA template for the targeted genomic regions. Pre-amplification is especially beneficial when

working with low quantities of template DNA (e.g., swab samples). We performed pre-amplification reactions according to the manufacturer's protocol (Fluidigm, South San Francisco, CA). We cleaned pre-amplified products using ExoSAP-IT, followed by a 1:5 dilution in water.

We used both our pre-amplified diluted products and primer pair pools in Access Array amplification and Illumina sequencing. Briefly, samples and primer pools were loaded into Fluidigm's integrated fluidic circuits (IFC) and multiplex PCR reactions occurred in the Fluidigm FC1 Cycler at the University of Idaho IBEST Genomics Resources Core. Sequencing was performed on the Illumina MiSeq using the 300bp paired-end kits at the University of Idaho IBEST Genomics Resources Core. We processed our samples on a quarter of a sequencing plate (resulting in ~4 million reads) to generate ~200X coverage for each unique amplicon (i.e., each combination of sample and target). We chose a relatively high level of sequencing effort to increase number of reads per samples and minimize missing data given our input of samples of variable DNA quantity and quality.

SNP genotyping and analysis

Starting with raw sequences, we used dbcAmplicons (https://github.com/msettles/dbcAmplicons) to process reads and identify consensus sequences and putative alleles for each sample and primer pair. Briefly, each read was demultiplexed for each sample and primer, using the sample-specific dual barcode combinations (edit-distance <= 1bp) and target specific primers (Levenshtein distance <=4 with final 4 bases as perfect matches, resulting in firm ends). Primer sequences were then removed. Representative sequences for each sample and amplicon were then identified using the reduce_amplicons R script within the dbcAmplicons repository (https://github.com/msettles/dbcAmplicons/blob/master/scripts/R/reduce_amplicons.R). Paired reads were overlapped and joined into a single continuous sequence using FLASH2 (https://github.com/dstreett/FLASH2). Lastly, reads for each sample and primer pair were collapsed to their most often occurring amplicon length variant (all other reads were not included in the consensus or ambiguity sequences). Ambiguity sequences contain IUPAC ambiguity codes at positions with possible polymorphisms. Consensus sequences (with and without ambiguities) were generated when each variant was present in at least 5 reads and at least 5% of the total number of reads.

Whole genome data from 25 isolates was cleaned and analyzed as done in Rosenblum et al. (2013). This dataset contained 22 isolates previously published in Rosenblum et al. (2013) and 3 isolates from Panama that have not been published (Campana, JEL410, Rio Maria). Briefly, variants were called using the best practices for the GATK v.3.4 pipeline (McKenna et al., 2010). The GATK tools RealignerTargetCreator and IndelRealigner were used to realign reads around insertions/deletions, and the HaplotypeCaller and GenotypeGVCFs tools were used to call variants. Custom R scripts were used to filter genotypes based on quality and depth. SNPs were encoded to represent homozygous for ancestral allele (0), heterozygous (1), and homozygous for derived allele (2). A dataset consisting of 20,535 SNPs was used to create a maximum parsimony phylogenetic tree with 100 bootstraps using the phangorn package in R (Schliep, 2011). For the Bd Fluidigm Access Array data, the consensus sequences for all shared amplicons were concatenated to form a single consensus sequence. These sequences were then aligned using MUSCLE v3.8 (Edgar, 2004) and alignments were visually inspected to check for errors. A maximum parsimony phylogenetic tree with 100 bootstrap replicates was created using

the phangorn package (Schliep, 2011) in R (version 3.2.2) with UM142 as the designated outgroup. Each phylogenetic tree was plotted in R using the phytools package (Revell, 2012) to create a cophylogeny that is rotated to minimize the distance between each sample pair. Three of the 28 isolates included in the Bd Fluidigm Access Array study were omitted from this analysis because whole genome sequences were not available. Finally, to assess swab performance, we conducted a local regression comparing the ln Bd copy number to the number of unique amplicons returned. We used the loess function in R and then a recursive decision tree in the R package rpart (Therneau, Atkinson, & Ripley, 2010) to classify swabs into higher-performing and lower-performing groups.

Results

General Assay Performance

Of the 192 target loci, 190 (99%) successfully amplified (produced a consensus sequence) for at least one of the 96 samples (Figure 1). The vast majority of target loci amplified consistently across the pure Bd culture samples. For the pure Bd isolates, we obtained an average of 182.5 (95%) loci per sample, resulting in concatenated consensus sequences of more than 20,000 base pairs in length. All pure Bd isolates, including the most divergent UM142 and LFT001, had similar amplification profiles and low locus dropout rates. We also used standard dilutions of pure Bd culture to test assay sensitivity. Number of loci successfully sequenced increased predictably with Bd genomic equivalents (GE). An average of 2.3 loci were returned for 0.1 GE, 29.3 for 1 GE, 41 for 10 GE, and 93.3 for 100 GE. Also as expected, the non-Bd isolates amplified only a small number of target regions. We obtained an average of 8 loci for *Homolaphlyctis polyrhiza*, 23 loci for *Entophlyctis helioformis,* and 24.5 loci for *Rhizophydium brooksianum*.

Swab Performance

The number of loci successfully sequenced was positively associated with swab Bd load (LOESS span α=0.75, degree of polynomial fit λ=2, Figure 2). The break between the higher-performing and lower-performing groups of swabs fell at a Bd load of 5.073 ln Bd copy numbers (or 159.5 Bd DNA copies). All of the samples in the higher performing group returned at least 100 loci and an average of 169.6 loci (n=17, standard deviation=23.8). The lower performing group returned an average of 41.2 loci (n=30, standard deviation=39.7). However, there were some outliers in each group. One swab sample that would be included in the high-performing group (average copy number of 91,698) only returned a single locus. This outlier was excluded from the curve fit and decision tree calculation displayed in Figure 2, as well as the average loci data presented above. Additionally, two samples grouped with the lower-performing swabs (average copy number of 35.6 and 59.0) returned a surprisingly large number of loci (149 and 163, respectively).

Phylogenetic Discriminatory Power

Our sequence data recapitulated the known phylogenetic relationships of Bd isolates based on whole-genome data. For example, all isolates previously described as GPL (Rosenblum et al., 2013) were correctly assigned to the GPL clade using our amplicon data (Figure 3). Additionally, the two isolates previously described as belonging to the Bd-Brazil clade were correctly placed outside of the GPL. Overall, almost all of the nearest-neighbor relationships

were conserved in the phylogeny produced from the amplicon dataset and the phylogeny produced from the whole-genome dataset. However, placement of isolates into GPL subclades was not always consistent across each dataset (Figure 3).

Discussion

Here, we present a new genotyping assay for the pathogenic fungus Bd that uses a microfluidic PCR approach optimized for low quality/quantity DNA. We targeted a carefully-curated set of 192 highly polymorphic regions of the Bd genome (each 150-200 bp long). Our amplicon approach reduces ascertainment bias that can be problematic in other SNP-based genotyping approaches (e.g., Albrechtsen *et al.* 2010). The new assay performed exceptionally well not only for pure Bd cultures but also for samples collected non-invasively from swabbing host skin (Figures 1 and 2). Swabs with a reasonable starting amount of Bd (more than 150 Bd genomic equivalents) returned robust sequence data. Our assay also has the power to accurately discriminate among major Bd clades, and 192 markers were sufficient to reconstruct the basic Bd tree topology generated previously from whole-genome sequence data (Figure 3). Our approach is highly-scalable (samples are individually barcoded and pooled before sequencing), and can support much larger sample sizes than alternative sequencing approaches. Additionally, the per-sample cost for our assay (~$25) is more than an order of magnitude smaller than for whole genome sequencing (see Supplementary Table 3). Other studies have successfully implemented a similar microfluidic workflow to genotype low-quality DNA from noninvasively collected samples, including historical fish scales (Smith et al., 2011) and bird feathers (Ruegg et al., 2014).

Given its low cost, high scalability, and reliable data generation for low DNA quantity samples, our new assay will help address many outstanding questions in the Bd disease system. In particular, swab samples will become a revitalized resource. Swabs have been the preferred method for large-scale collection of Bd DNA because they are minimally invasive, do not require a sterile lab for collection, and can be easily stored and transported for long periods of time. Hundreds of thousands of amphibian skin swab samples have already been collected (e.g. see Olson et al. 2013) and can now be genotyped to reveal spatial and temporal dynamics of Bd in natural systems. For example, one exciting spatial application of this genotyping assay is the potential to create a global Bd genotype map. Bd swabs from around the world can be affordably genotyped, and genotypes could be integrated into Bd mapping efforts (e.g., http://www.bd-maps.net/; Olson et al. 2013).

The result would be a public-access database that includes not only Bd presence/absence data but also genotype information. Each successive sample would add more resolution to the global Bd map, allowing Bd researchers to make more effective inferences and predictions about the distribution and spread of different Bd clades, as well as provide a tool for rapid disease surveillance. Understanding the spatial distribution of Bd clades is especially important given that certain strains of Bd are known to be more pathogenic than others (e.g. Berger et al. 2005) and could pose threats if introduced to novel areas.

In addition to using swab genotypes to understand the spatial distribution of Bd clades around the world, this assay can be used to answer key questions about temporal dynamics in the Bd system. For example, one promising application of this assay is to better infer the origin and introduction history of Bd in different parts of the world. To understand how long Bd has been present in an area and when it arrived, researchers have turned to swabbing the skin of preserved

museum specimens (e.g. Cheng et al. 2011; Zhu et al. 2014). Additionally, new DNA extraction techniques have opened the possibility of obtaining reliable Bd DNA from formalin-fixed specimens (Hykin, Bi, & McGuire, 2015; Richards-Hrdlicka, 2012). By integrating new extraction techniques with the genotyping assay described here, museum specimens can now be used to reveal the historical occurrence of Bd, document how and when Bd introductions occurred, and understand long-term temporal dynamics of the major Bd clades.

We expect this assay to contribute substantially to understanding Bd-related amphibian declines, but it is important to note limitations of the approach. The assay works best with at least a moderate amount of input Bd DNA. The threshold amount of Bd DNA for our higher performing swabs (~150 Genome equivalents/1ul) is higher than many positive Bd skin swabs, especially in areas where Bd appears to be endemic such as Asia (Bataille et al., 2013) and Brazil (Rodriguez, Becker, Pupin, Haddad, & Zamudio, 2014). This may introduce a bias towards recovering more virulent and/or faster growing strains if the assay is only applied to samples with high loads. Additionally, swab samples sometimes fail to detect Bd infection altogether and often underreport Bd infection loads (Shin, Bataille, Kosch, & Waldman, 2014). However, a subset of swabs in our study with very low Bd loads produced a robust set of amplicons, so some samples with lower Bd loads could be successfully analyzed using this platform. Further, one high-load swab failed for unknown reasons. The occasional sample failure with a PCR-based method is not surprising especially given that swab sample extracts often contain PCR inhibitors. The probability of sample success can be increased through precipitating and concentrating sample extracts. In addition, we cannot predict how well the current panel of primers will work for novel strains yet to be discovered. We designed primers to amplify across diverse Bd isolates, and we obtained high quality data from diverse isolates both within and outside the GPL. However, relatively few loci amplified for distantly-related non-Bd chytrids, so it remains to be seen how much deeper phylogenetic diversity can be captured by the current primer pool. Additionally, this study is limited in its power to assess the efficacy of our primer pool to distinguish among all major Bd clades, as we focused on samples from the GPL and Bd-Brazil clades (see Supplementary Table 2). Future applications will include samples from other Bd clades and from *B. salamandrivorans*. Finally, researchers have not yet thoroughly characterized genetic diversity in Bd populations over fine spatial or temporal scales. Although our target amplicons are effective for distinguishing among major Bd clades, they may not provide sufficient resolution for finer scale questions. However, there is room to expand the number of target loci as other Fluidigm Access Array designs have included up to 10 primer pairs per pool (for a total of 480 target loci) (e.g. Halbritter et al. 2012). By increasing the number of target regions and/or base pairs per target, this assay could be extended to address questions about Bd dynamics across deeper or finer temporal and spatial scales.

In summary, the genotyping assay described here uses microfluidic, multiplex PCR technology to create a highly-scalable workflow with the specific aim of garnering genotype data from Bd skin swabs. Our assay focuses on Bd genotyping, but skin swabs can also be used for population genetics studies of amphibians (e.g. Prunier et al., 2012). Thus extensions of our assay could be used to understand patterns of genetic variation in both host and pathogen simultaneously. Ultimately the approach described here expands the utility of noninvasive sampling methods for understanding disease-related amphibian declines, an important advance for studying imperiled amphibian species. The application of this tool to swab samples collected

across species, life stages, continents, and decades will be a critical step forward in the study of Bd and for amphibian conservation planning.

Acknowledgements

This work was co-authored by Andrew P. Rothstein, Thomas J. Poorten, Jesse Erens, Matthew L. Settles, and Erica Bree Rosenblum. This work was supported by an NSF GRFP to AQB and an NSF IOS grant to EBR (IOS-1354241). We thank Cori Richards-Zawacki for sharing Bd swab extracts. We thank Katy Richards-Hrdlicka and Andrew O'Guin at Fluidigm and Dan New and Alida Gerritsen at the University of Idaho IBEST Genomics Resources Core for assistance with troubleshooting.

Data Accessibility

Supporting data have been accessioned to Dryad (doi:10.5061/dryad.33st2).

References

Albrechtsen, A., Nielsen, F. C., & Nielsen, R. (2010). Ascertainment biases in SNP chips affect measures of population divergence. *Molecular Biology and Evolution*. *27*(11):2534-47.

Archie, E. A., Luikart, G., & Ezenwa, V. O. (2009). Infecting epidemiology with genetics: a new frontier in disease ecology. *Trends in Ecology & Evolution*, *24*(1), 21–30.

Atkinson, C. T., & Samuel, M. D. (2010). Avian malaria *Plasmodium relictum* in native Hawaiian forest birds: epizootiology and demographic impacts on ʻapapane Himatione sanguinea. *Journal of Avian Biology*, *41*(4), 357–366.

Bai, C., Liu, X., Fisher, M. C., Garner, T. W. J., & Li, Y. (2012). Global and endemic Asian lineages of the emerging pathogenic fungus *Batrachochytrium dendrobatidis* widely infect amphibians in China. *Diversity and Distributions*, *18*(3), 307–318.

Baskaran, N., Kandpal, R. P., Bhargava, A. K., Glynn, M. W., Bale, A., & Weissman, S. M. (1996). Uniform amplification of a mixture of deoxyribonucleic acids with varying GC content. *Genome Research*, *6*(7), 633–638.

Bataille, A., Fong, J. J., Cha, M., Wogan, G. O. U., Baek, H. J., Lee, H., … Waldman, B. (2013). Genetic evidence for a high diversity and wide distribution of endemic strains of the pathogenic chytrid fungus Batrachochytrium dendrobatidis in wild Asian amphibians. *Molecular Ecology*, *22*(16), 4196–209.

Beja-Pereira, A., Bricker, B., Chen, S., Almendra, C., White, P. J., & Luikart, G. (2009). DNA Genotyping Suggests that Recent Brucellosis Outbreaks in the Greater Yellowstone Area Originated from Elk. *Journal of Wildlife Diseases*, *45*(4), 1174–1177.

Berger, L., Marantelli, G., Skerratt, L. F., & Speare, R. (2005). Virulence of the amphibian chytrid fungus *Batrachochytrium dendrobatidis* varies with the strain. *Diseases of Aquatic Organisms*, *68*(1), 47–50.

Berger, L., Speare, R., Daszak, P., Green, D. E., Cunningham, A. A., Goggin, C. L., … Parkes, H. (1998). Chytridiomycosis causes amphibian mortality associated with population

declines in the rain forests of Australia and Central America. *Proceedings of the National Academy of Sciences* , *95*(15), 9031–9036.

Boyle, D. G., Boyle, D. B., Olsen, V., Morgan, J. A. T., & Hyatt, A. D. (2004). Rapid quantitative detection of chytridiomycosis (*Batrachochytrium dendrobatidis*) in amphibian samples using real-time Taqman PCR assay, *Diseases of Aquatic Organisms, 60*(2), 141–148.

Boyle, D. G., Hyatt, A. D., Daszak, P., Berger, L., Longcore, J. E., Porter, D., … Olsen, V. (2003). Cryo-archiving of *Batrachochytrium dendrobatidis* and other chytridiomycetes. *Diseases of Aquatic Organisms*, *56*(1), 59–64.

Cheng, T. L., Rovito, S. M., Wake, D. B., & Vredenburg, V. T. (2011). Coincident mass extirpation of neotropical amphibians with the emergence of the infectious fungal pathogen *Batrachochytrium dendrobatidis*. *Proceedings of the National Academy of Sciences* , *108*(23), 9502–9507.

Crawford, A. J., Lips, K. R., & Bermingham, E. (2010). Epidemic disease decimates amphibian abundance, species diversity, and evolutionary history in the highlands of central Panama. *Proceedings of the National Academy of Sciences* , *107*(31), 13777–13782.

Edgar, R. C. (2004). MUSCLE: multiple sequence alignment with high accuracy and high throughput. *Nucleic Acids Research*, *32*(5), 1792–7.

Farrer, R. A., Weinert, L. A., Bielby, J., Garner, T. W. J., Balloux, F., Clare, F., … Fisher, M. C. (2011). Multiple emergences of genetically diverse amphibian-infecting chytrids include a globalized hypervirulent recombinant lineage. *Proceedings of the National Academy of Sciences*, *108*(46), 18732–18736.

Fellers, G. M., Green, D. E., & Longcore, J. E. (2001). Oral Chytridiomycosis in the Mountain Yellow-Legged Frog (*Rana muscosa*). *Copeia*, *2001*(4), 945–953.

Foley, J., Clifford, D., Castle, K., Cryan, P., & Ostfeld, R. S. (2011). Investigating and managing the rapid emergence of white-nose syndrome, a novel, fatal, infectious disease of hibernating bats. *Conservation Biology*, *25*(2), 223–31.

Garland, S., TY, J., Blair, D., & Berger, L. (2011). Polymorphic repetitive loci of the amphibian pathogen *Batrachochytrium dendrobatidis* . *Diseases of Aquatic Organisms*, *97*(1), 1–9.

Goka, K., Yokoyama, J., Une, Y., Kuroki, T., Suzuki, K., Nakahara, M., … Hyatt, A. D. (2009). Amphibian chytridiomycosis in Japan: distribution, haplotypes and possible route of entry into Japan. *Molecular Ecology*, *18*(23), 4757–74.

Grogan, L. F., Berger, L., Rose, K., Grillo, V., Cashins, S. D., & Skerratt, L. F. (2014). Surveillance for Emerging Biodiversity Diseases of Wildlife. *PLoS Pathog*, *10*(5), e1004015.

Halbritter, J., Diaz, K., Chaki, M., Porath, J. D., Tarrier, B., Fu, C., … Otto, E. A. (2012). High-throughput mutation analysis in patients with a nephronophthisis-associated ciliopathy applying multiplexed barcoded array-based PCR amplification and next-generation

sequencing. *Journal of Medical Genetics* , *49*(12), 756–767.

Hyatt, A. D., Boyle, D. G., Olsen, V., Boyle, D. B., Berger, L., Obendorf, D., … Gleason, F. (2007). Diagnostic assays and sampling protocols for the detection of *Batrachochytrium dendrobatidis*. *Diseases of Aquatic Organisms*, *73*(3), 175–192.

Hykin, S. M., Bi, K., & McGuire, J. A. (2015). Fixing Formalin: A Method to Recover Genomic-Scale DNA Sequence Data from Formalin-Fixed Museum Specimens Using High-Throughput Sequencing. *PLoS ONE*, *10*(10), e0141579.

James, T. Y., Litvintseva, A. P., Vilgalys, R., Morgan, J. A. T., Taylor, J. W., Fisher, M. C., … Longcore, J. E. (2009). Rapid Global Expansion of the Fungal Disease Chytridiomycosis into Declining and Healthy Amphibian Populations. *PLoS Pathogens*, *5*(5), e1000458.

Jenkinson, T. S., Betancourt Román, C. M., Lambertini, C., Valencia-Aguilar, A., Rodriguez, D., Nunes-de-Almeida, C. H. L., … James, T. Y. (2016). Amphibian-killing chytrid in Brazil comprises both locally endemic and globally expanding populations. *Molecular Ecology*, *25*(13), 2978–96.

Joneson, S., Stajich, J. E., Shiu, S. H., & Rosenblum, E. B. (2011). Genomic transition to pathogenicity in chytrid fungi. *PLoS Pathogens*, *7*(11), e1002338.

Kearse, M., Moir, R., Wilson, A., Stones-Havas, S., Cheung, M., Sturrock, S., … Drummond, A. (2012). Geneious Basic: An integrated and extendable desktop software platform for the organization and analysis of sequence data. *Bioinformatics* , *28*(12), 1647–1649.

Koressaar, T., & Remm, M. (2007). Enhancements and modifications of primer design program Primer3. *Bioinformatics*, *23*(10), 1289–1291.

Longcore, J. E., Pessier, A. P., & Nichols, D. K. (1999). *Batrachochytrium Dendrobatidis* gen. et sp. nov., a Chytrid Pathogenic to Amphibians. *Mycologia*, *91*(2), 219–227.

Markoulatos, P., Siafakas, N., & Moncany, M. (2002). Multiplex polymerase chain reaction: a practical approach. *Journal of Clinical Laboratory Analysis*, *16*(1), 47–51.

Martel, A., Spitzen-van der Sluijs, A., Blooi, M., Bert, W., Ducatelle, R., Fisher, M. C., … Pasmans, F. (2013). *Batrachochytrium salamandrivorans* sp. nov. causes lethal chytridiomycosis in amphibians. *Proceedings of the National Academy of Sciences* , *110*(38), 15325–15329.

Mccarthy, M. A., & Parris, K. M. (2004). Clarifying the effect of toe clipping on frogs with Bayesian statistics. *Journal of Applied Ecology*, *41*(4), 780–786.

McKenna, A., Hanna, M., Banks, E., Sivachenko, A., Cibulskis, K., Kernytsky, A., … DePristo, M. A. (2010). The Genome Analysis Toolkit: A MapReduce framework for analyzing next-generation DNA sequencing data. *Genome Research* , *20*(9), 1297–1303.

Morehouse, E. a., James, T. Y., Ganley, A. R. D., Vilgalys, R., Berger, L., Murphy, P. J., & Longcore, J. E. (2003). Multilocus sequence typing suggests the chytrid pathogen of amphibians is a recently emerged clone. *Molecular Ecology*, *12*(2), 395–403.

Morgan, J. a T., Vredenburg, V. T., Rachowicz, L. J., Knapp, R. a, Stice, M. J., Tunstall, T., … Taylor, J. W. (2007). Population genetics of the frog-killing fungus Batrachochytrium dendrobatidis. *Proceedings of the National Academy of Sciences of the United States of America*, *104*(34), 13845–13850.

Olson, D. H., Aanensen, D. M., Ronnenberg, K. L., Powell, C. I., Walker, S. F., Bielby, J., … Group, T. B. M. (2013). Mapping the Global Emergence of Batrachochytrium dendrobatidis, the Amphibian Chytrid Fungus. *PLoS ONE*, *8*(2), e56802.

Pagès, H., Aboyoun, P., Gentleman, R., & DebRoy, S. (2016). String objects representing biological sequences, and matching algorithms. *R Package Version 2.36.4*.

Prunier, J., Kaufmann, B., Grolet, O., Picard, D., Pompanon, F., & Joly, P. (2012). Skin swabbing as a new efficient DNA sampling technique in amphibians, and 14 new microsatellite markers in the alpine newt (Ichthyosaura alpestris). *Molecular Ecology Resources*, *12*(3), 524–531.

Retallick, R. W. R., Miera, V., Richards, K. L., & Field, K. J. (2006). A non-lethal technique for detecting the chytrid fungus Batrachochytrium dendrobatidis on tadpoles . *Diseases of Aquatic Organisms*, *72*(1), 77–85.

Revell, L. J. (2012). phytools: an R package for phylogenetic comparative biology (and other things). *Methods in Ecology and Evolution*, *3*(2), 217–223.

Richards-Hrdlicka, K. L. (2012). Extracting the amphibian chytrid fungus from formalin-fixed specimens. *Methods in Ecology and Evolution*, *3*(5), 842–849.

Rodriguez, D., Becker, C. G., Pupin, N. C., Haddad, C. F. B., & Zamudio, K. R. (2014). Long-term endemism of two highly divergent lineages of the amphibian-killing fungus in the Atlantic Forest of Brazil. *Molecular Ecology*, *23*(4), 774–87.

Rosenblum, E. B., James, T. Y., Zamudio, K. R., Poorten, T. J., Ilut, D., Rodriguez, D., … Stajich, J. E. (2013). Complex history of the amphibian-killing chytrid fungus revealed with genome resequencing data. *Proceedings of the National Academy of Sciences of the USA*, *110*(23), 9385–90.

Rosenblum, E. B., Poorten, T. J., Joneson, S., & Settles, M. (2012). Substrate-Specific Gene Expression in *Batrachochytrium dendrobatidis*, the Chytrid Pathogen of Amphibians. *PLoS ONE*, *7*(11), e49924.

Ruegg, K., Anderson, E. C., Paxton, K. L., Apkenas, V., Lao, S., Siegel, R. B., … Smith, T. B. (2014). Mapping migration in a songbird using high-resolution genetic markers, *Molecular Ecology*, *23*(23), 5726-5739.

Saunders, S. E., Bartelt-Hunt, S. L., & Bartz, J. C. (2012). Occurrence, Transmission, and Zoonotic Potential of Chronic Wasting Disease. *Emerging Infectious Diseases*, *18*(3), 369–376.

Schliep, K. P. (2011). phangorn: phylogenetic analysis in R. *Bioinformatics* , *27*(4), 592–593.

Schloegel, L. M., Toledo, L. F., Longcore, J. E., Greenspan, S. E., Vieira, C. A., Lee, M., … James, T. Y. (2012). Novel, panzootic and hybrid genotypes of amphibian chytridiomycosis associated with the bullfrog trade. *Molecular Ecology*, *21*(21), 5162–5177.

Shin, J., Bataille, A., Kosch, T. A., & Waldman, B. (2014). Swabbing Often Fails to Detect Amphibian Chytridiomycosis under Conditions of Low Infection Load. *PLoS ONE*, *9*(10), e111091.

Skerratt, L. F., Berger, L., Speare, R., Cashins, S., McDonald, K. R., Phillott, A. D., … Kenyon, N. (2007). Spread of Chytridiomycosis Has Caused the Rapid Global Decline and Extinction of Frogs. *EcoHealth*, *4*(2), 125–134.

Smith, M. J., Pascal, C. E., Grauvogel, Z., Habicht, C., Seeb, J. E., & Seeb, L. W. (2011). Multiplex preamplification PCR and microsatellite validation enables accurate single nucleotide polymorphism genotyping of historical fish scales. *Molecular Ecology Resources*, *11*, 268–77.

Suzuki, M. T., & Giovannoni, S. J. (1996). Bias caused by template annealing in the amplification of mixtures of 16S rRNA genes by PCR. *Applied and Environmental Microbiology* , *62*(2), 625–630.

Therneau, T. M., Atkinson, B., & Ripley, B. (2010). rpart: Recursive partitioning. *R Package Version*, *3*, 1–46.

Wallace, R. G., HoDac, H., Lathrop, R. H., & Fitch, W. M. (2007). A statistical phylogeography of influenza A H5N1. *Proceedings of the National Academy of Sciences* , *104*(11), 4473–4478.

Zhu, W., Bai, C., Wang, S., Soto-Azat, C., Li, X., Liu, X., & Li, Y. (2014). Retrospective survey of museum specimens reveals historically widespread presence of *Batrachochytrium dendrobatidis* in China. *EcoHealth*, *11*, 241–250.

Zolan, M. E., & Pukkila, P. J. (1986). Inheritance of DNA methylation in Coprinus cinereus. *Molecular and Cellular Biology* , *6*(1), 195–200.

Figures

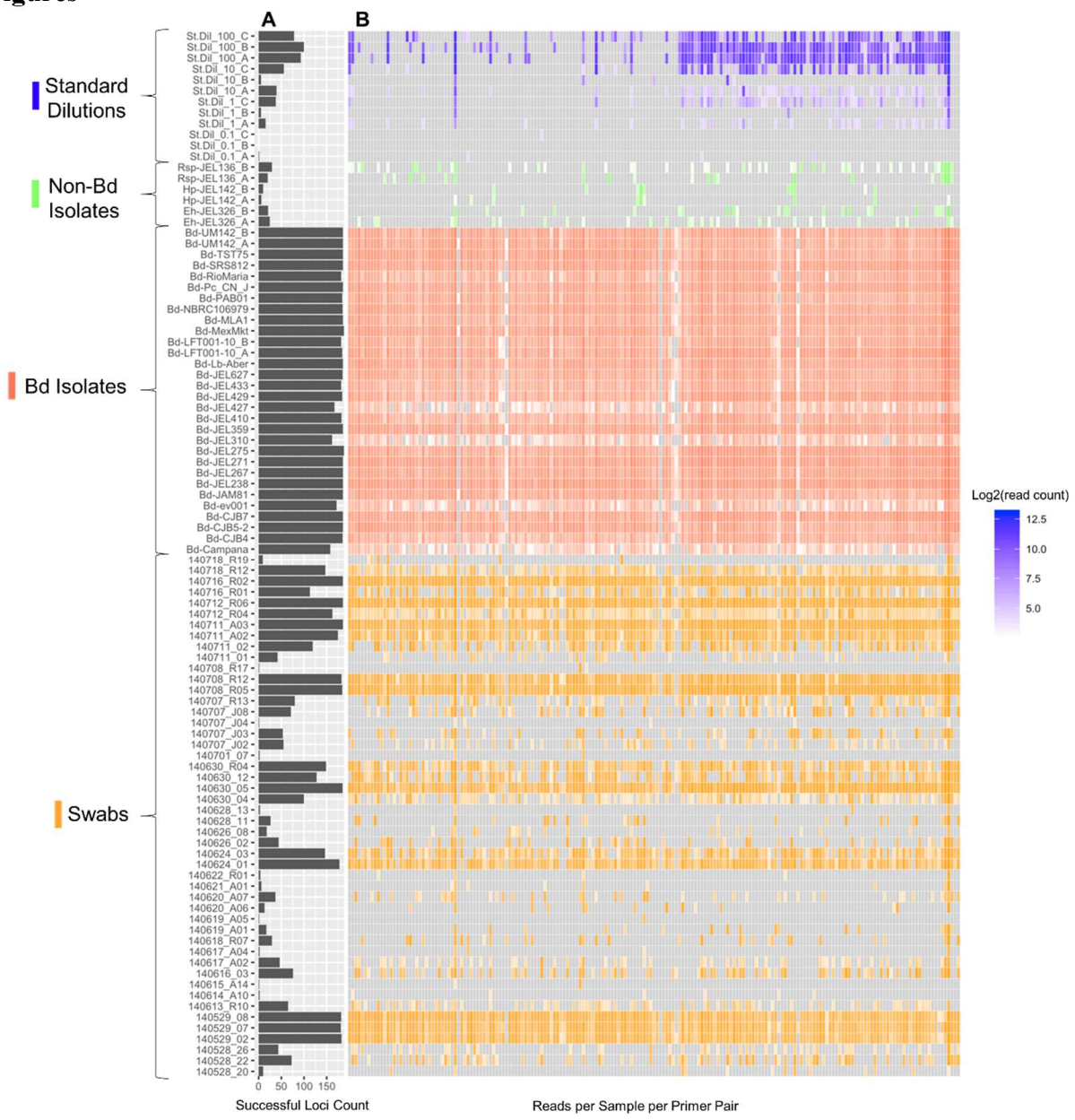

Figure 1: Sample performance. Samples names are given as row labels. (A) Barplot showing the number of successful loci recovered per sample (192 possible). (B) Heatmap showing the log2 count of reads per sample and loci (192 possible loci from left-to-right on the x-axis). Samples that are in the standard dilution series are in blue, Non-Bd pure culture samples in green, Bd pure culture in red, and swab samples in orange. The intensity of the color represents the number of reads per sample/locus with more intense color representing more reads associated with that sample/locus pair. Unsuccessful amplification for a sample/locus pair shown in grey.

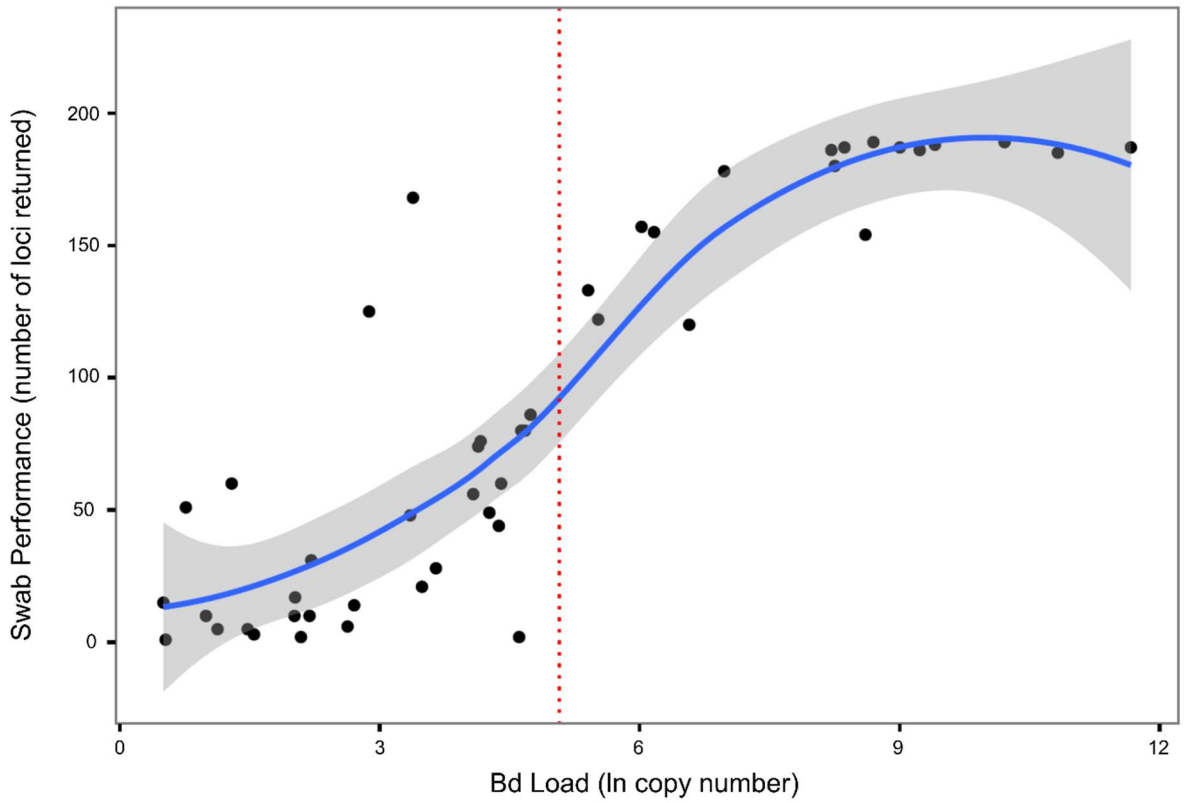

Figure 2: Scatterplot of swab performance compared to swab quality. The local regression (blue curve) and 95% confidence interval for best fit of points (grey curve) are shown. The red dotted line indicates the separation between the higher-performing and lower-performing samples at 5.073 ln Bd copy number (159.5 Bd DNA copies).

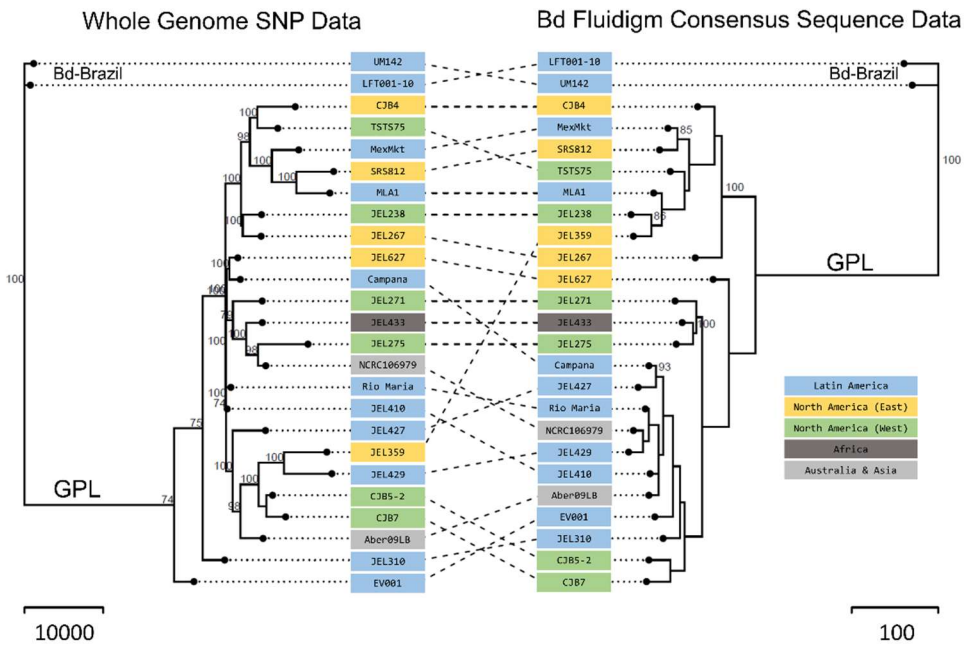

Figure 3: Comparison of Bd Fluidigm sequence data and whole genome data. Comparison of maximum parsimony phylogenies with 100 bootstrap replicates for 25 Bd isolates created using whole genome SNP data (left) and consensus sequences obtained using the Bd Fluidigm Access Array assay (right). The geographic origin of each isolate is indicated by color. Only isolates for which whole genome data were available were included in this analysis (see S2 Table).

Chapter 2: Cryptic diversity of a widespread global pathogen reveals new threats for amphibian conservation

Abstract

Biodiversity loss is one major outcome of human-mediated ecosystem disturbance. One way that humans have triggered wildlife declines is by transporting disease-causing agents to remote areas of the world. Amphibians have been hit particularly hard by disease due in part to a globally distributed pathogenic chytrid fungus (*Batrachochytrium dendrobatidis*, *Bd*). Prior research has revealed important insights into the biology and distribution of *Bd*, however there are still many outstanding questions in this system. Although we know that there are multiple divergent lineages of *Bd* that differ in pathogenicity, we know little about how these lineages are distributed around the world and where lineages may be coming into contact. Here, we implement a novel genotyping method for a global set of *Bd* samples. This method is optimized to amplify and sequence degraded DNA from non-invasive skin swab samples. We describe a new lineage of *Bd*, which we call *Bd*ASIA3, that appears to be widespread in southeast Asia. This new lineage cooccurs with the global panzootic lineage (*Bd*GPL) in multiple localities. Additionally, we shed light on the global distribution of *Bd*GPL and highlight the expanded range of another lineage, *Bd*CAPE. Finally, we argue that more monitoring needs to take place where *Bd* lineages are coming into contact and where we know little about *Bd* lineage diversity. Monitoring need not use expensive or difficult field techniques but can use archived swab samples to further explore the history – and predict the future impacts – of this devastating pathogen.

Introduction

Emerging infectious diseases are increasingly recognized as a threat to both human and wildlife health (Daszak, Cunningham, & Hyatt, 2000; Fisher et al., 2012; Jones et al., 2008). One reason emerging infectious diseases are on the rise is the facilitated spread of pathogen propagules via globalized trade. With the aid of modern shipping, pathogens have been introduced to naïve remote areas (Fisher & Garner, 2007). These new introductions can have grave consequences, in some cases causing mass mortality in wildlife populations (e.g. Foley et al., 2011; Skerratt et al., 2007). Understanding the pathways for disease spread is critical to predicting and addressing disease outbreaks (Jones et al., 2008).

Amphibians have been hit particularly hard by emerging infectious disease in the last century. Hundreds of amphibian species have been impacted by the pathogenic chytrid fungus *Batrachochytrium dendrobatidis* (*Bd*) (Longcore, Pessier, & Nichols, 1999; Wake & Vredenburg, 2008). *Bd* invades the keratinized tissue of amphibians (skin in adults, mouthparts in tadpoles), disrupting critical skin functions such as the regulation of osmotic pressure and electrolyte balance (Voyles et al., 2009). The resulting disease – chytridiomycosis – can be deadly to susceptible amphibians once the pathogen reaches a critical infection load (Vredenburg, Knapp, Tunstall, & Briggs, 2010). However, some host species can maintain *Bd* infection without disease development (Briggs, Knapp, & Vredenburg, 2010; Reeder, Pessier, & Vredenburg, 2012). These tolerant species can be important reservoir vectors of *Bd*. For

example, the American bullfrog (*Rana catesbeiana*) is a highly-traded, *Bd*-tolerant species that has been implicated in spreading *Bd* throughout the Western US, Brazil, and Korea (O'Hanlon et al., 2018; Schloegel et al., 2010; Yap, Koo, Ambrose, & Vredenburg, 2018).

Molecular studies have played an important role in illuminating the evolutionary history of *Bd*, patterns of spatial and temporal spread, and pathogen genetic diversity (e.g. Farrer et al., 2011; Jenkinson et al., 2016; Rosenblum et al., 2013). There are currently four documented major *Bd* lineages based on the most recent whole genome phylogeny (O'Hanlon et al., 2018). First the 'global panzootic lineage', *Bd*GPL, is globally distributed and associated with most mass mortalities in wild amphibian populations (Farrer et al., 2011). Second, *Bd*CAPE was first described from an isolate collected in Cape Province, South Africa and has since been found in Cameroon, Mallorca, and the United Kingdom (Farrer et al., 2011; O'Hanlon et al., 2018). Third, *Bd*ASIA1 was recently described from eight isolates collected in South Korea but also includes the previously-named *Bd*CH lineage collected in Switzerland (O'Hanlon et al., 2018). Fourth, *Bd*Brazil/ASIA2 was first described from samples collected in Brazil (Schloegel et al., 2012) and renamed to include the clade previously known as *Bd*Korea after whole genome sequencing revealed their close relationship (O'Hanlon et al., 2018). The observed phylogenetic relationship among the four currently described *Bd* lineages suggests that the earliest diverging lineage is *Bd*ASIA1, and the most recent is *Bd*GPL (O'Hanlon et al., 2018).

In addition to the four major lineages, some hybridization between lineages has been reported. Schloegel et al. (2012) documented the first evidence of sexual recombination in *Bd*, a finding later supported by whole genome sequencing (Rosenblum et al., 2013). Alarmingly, one of the recombinant lineages studied (an F1 hybrid of *Bd*GPL and *Bd*Brazil) was found to be more virulent than either parental lineage when tested against a native Brazilian host (Greenspan et al., 2018). Thus, the spread and recombination of different *Bd* lineages can lead to unpredictable and potentially dangerous outcomes. Therefore, documenting the spatial distribution of *Bd* genotypes is a high priority for amphibian conservation.

Recent genetic and genomic studies have provided unprecedented insight into the evolutionary history of *Bd*. However, a comprehensive understanding of historical and contemporary patterns of *Bd* diversity and spread has been limited by the lack of robust *Bd* genotype data in many areas of the world. One key limitation in using molecular tools to study *Bd* has been the need for pure cultures, which yield high quality and quantity DNA and have been required for whole-genome sequencing. However, the process of isolating and maintaining live *Bd* cultures is time-consuming and challenging, particularly in remote areas. In contrast, skin-swab samples are plentiful because they are easy to collect and are part of a standardized protocol to detect the presence of *Bd* via qPCR (Boyle, Boyle, Olsen, Morgan, & Hyatt, 2004). Swab samples provide ample DNA for sensitive PCR techniques but often do not have enough high-quality DNA for whole genome sequencing. Some studies have attempted to address this problem by sequencing small, hypervariable loci present in high copy number – specifically the ribosomal intragenic spacer (ITS-1) region. However, phylogenetic inferences made from this region produce relationships that are highly discordant with those inferred from high-coverage, whole genome sequencing (O'Hanlon et al., 2018). These challenges have resulted in a large gap

in knowledge between our robust understanding of *Bd* presence and prevalence in many parts of the world and our patchy knowledge of genetic variation and lineage distributions.

Thus, many critical questions remain in the *Bd*-amphibian system. First, are there additional undiscovered *Bd* lineages present in wild amphibian populations? Second, what is the current distribution of known *Bd* lineages in unsampled or under-sampled areas of the world? Third, where are divergent *Bd* lineages coming into contact? Answering these questions would provide a truly global understanding of the threat *Bd* poses to amphibians around the world and identify geographic centers of high conservation urgency. Here, we employ a novel microfluidic PCR genotyping method targeting almost 200 loci across the *Bd* genome from swab samples (Byrne et al., 2017). With this technique we can now leverage a global library of amphibian skin swabs that have never been genotyped. Our analysis provides a deeper understanding of the diversity and distribution of *Bd* globally and highlights cryptic variation in this pathogen around the world.

Methods

Fluidigm Sequencing

We genotyped *Bd* samples using a custom assay (see Byrne et al., 2017). Briefly, this assay uses the Fluidigm Access Array platform to perform microfluidic multiplex PCR on 191 regions of the *Bd* genome and one locus specific to the closely related *Batrachochytrium salamandrivorans* ITS rRNA. Each target locus is 150-200 base pairs long and the targets are distributed across 16 nuclear chromosomes and the mitochondrial genome of *Bd*. Targets were chosen based on their power to discriminate between major Bd clades as delineated in O'Hanlon et al. (2018). Extracted DNA from swab samples was first cleaned using an isopropanol precipitation protocol and preamplified in two separate PCR reactions, each containing 96 primer pairs at a concentration of 500nM. For each preamplification PCR reaction we used the FastStart High Fidelity PCR System (Roche) at the following concentrations: 1x FastStart High Fidelity Reaction Buffer with $MgCl_2$, 4.5mM $MgCl_2$, 5% DMSO, 200µM PCR Grade Nucleotide Mix, 0.1 U/µl FastStart High Fidelity Enzyme Blend. Preamplified products were treated with 4µl ExoSAP-it (Affymetrix Inc.) and incubated for 15min at 30˚C and 15min at 80˚C. Treated products were diluted 1:5 in PCR-grade water. The diluted products from each of the two preamplification reactions were then combined in equal proportions and used for downstream amplification and sequencing.

Each preamplified sample was loaded into the Fluidigm Access Array IFC during which barcodes are added. All samples were then pooled for sequencing on ¼ of an Illumina MiSeq lane using the 300bp paired-end kits at the University of Idaho IBEST Genomics Resources Core. We pre-processed all sequencing data as described in Byrne et al. 2017. First, we filtered reads by selecting sequence variants that were present in at least 5 reads and represented at least 5% of the total number of reads for that sample/locus. Next, we generated three different sequence types: consensus, ambiguities, and occurrence for each sample at each locus using the reduceamplicons R script (https://github.com/msettles/dbcAmplicons/blob/master/scripts/R/reduce_amplicons.R).

Consensus sequences are simply the most common sequence variant, ambiguities sequences use IUPAC ambiguity codes to code for multiple alleles, and occurrence sequences include a sequence for each unique variant.

Whole genome data

To compare sequence data from swabs to previously published whole genome data, we sought to generate comparable ambiguities sequences from raw genomic reads. First, we downloaded raw reads from the NCBI SRA (accession numbers in Dataset S1) and cleaned the reads using seqyclean v 1.9.9 (https://github.com/ibest/seqyclean). We aligned the paired reads to the reference genome JEL423 (Broad Institute v. 17-Jan-2007) using BWA MEM (Li & Durbin, 2009). Aligned reads were sorted using picard v.2.9.0 (http://broadinstitute.github.io/picard) and realigned around indels using the GATK (v.3.8.0) tools RealignerTargetCreator and IndelRealigner (McKenna et al., 2010). We then extracted all aligned reads within 3000bp of our target loci using samtools (v.1.8) and used Geneious (v.10.2.3, Kearse et al., 2012) to produce a consensus sequence with ambiguity codes at a threshold of 75% (meaning alleles had to be present in at least 25% of reads to be incorporated) and ignoring gaps. The threshold of 75% was determined by finding the lowest number of base pair differences between Fluidigm-sequenced isolates and comparable whole genome samples (see Table S1). We then used blastn (v.2.7.1) to find the exact coordinates for our target loci and extracted this sequence using bedtools (v.2.26.0). To compare the loci sequences produced using this method to those sequenced using the Fluidigm genotyping protocol, we compared samples for which we have both types of data (N=29, Table S1). We individually aligned all loci in R using MUSCLE (v.3.4.3; Edgar, 2004) and compared the concatenated pairwise alignment in Geneious to calculate similarity metrics (Table S2). We also produced a cophylogeny to demonstrate conserved topologies for the major lineages (Figure S7).

Phylogenetic Analyses

To account for variable levels of missing data in our dataset, we used two different phylogenetic approaches. First, to create a global phylogeny we applied strict missing data filters and concatenated all loci. Second, to allow for more samples to be included in geographically restricted regional analyses, we used a gene-tree to species-tree approach that is more robust to missing data.

Global Phylogeny

To create a phylogeny from the globally distributed sample set, we first applied data quality filters to both samples and loci. We selected samples that had at least 84 loci (no more than 50% missing data) and eliminated loci for which more than 66% of samples were missing data. We also trimmed loci that had >5 bp difference between the minimum and maximum sequence length to account for variation between whole genome and Fluidigm-generated sequence data, mostly driven by improper alignment around large indels. The final list of 172 loci were individually aligned using the MUSCLE package in R (v.3.4.3; Edgar, 2004) and concatenated. The concatenated alignments were visually checked for errors in Geneious (v.10.2.3, Kearse et al., 2012). We used the RAxML plugin (v.8.2.11; Stamatakis, 2014) in

Geneious using the rapid bootstrapping method for 100 bootstraps and the GTR substitution model and searched for best-scoring ML tree. We then used newick utils (v.1.6) to collapse all branch lengths with less than 50 bootstrap support.

Regional Phylogeny

For the regional analyses we used a gene-tree to species-tree method to create our consensus phylogeny. Since this method is more robust to missing data, we lowered our missing data threshold to allow all samples with at least 3 loci sequences. We also selected loci that had no more than 33% missing data for the selected samples and for which the difference between the maximum length and minimum length was no more than 5 base pairs. The final list of loci for each region were individually aligned using the MUSCLE package in R (v.3.4.3; Edgar, 2004) and alignments were visually checked for errors in Geneious (v.10.2.3, Kearse et al., 2012). Individual gene-trees were estimated using the RAxML plugin (v.8.2.11; Stamatakis, 2014) in Geneious using the rapid bootstrapping method for 100 bootstraps and the GTR substitution model and searched for best-scoring ML tree. We then used newick utils (v.1.6) to collapse all branch lengths with less than 10 bootstrap support. Trees with collapsed branches were then input into Astral-III (v.5.6.2; Zhang, Rabiee, Sayyari, & Mirarab, 2018). Astral estimates an unrooted species tree given a set of unrooted gene trees using the multi-species coalescent model. We selected this method because it is robust to missing data and allows for some unresolved locus trees as initial input (Zhang et al., 2018).

Results

Global Bd Diversity

We used our swab genotyping assay to assign 222 new samples from 24 different countries to major *Bd* clades (see Dataset S1). The dataset includes 189 field-collected swabs, 18 museum swabs, and 15 pure *Bd* isolates collected between 1984 and 2017 (Dataset S1; SI Appendix, Fig. S2). The samples represent all continents where *Bd* occurs and were chosen to target areas of the world where genotype data is lacking and explore localities where lineages may be coming into contact. We first describe our findings at the global scale, integrating our dataset with 47 previously published *Bd* whole genomes (Farrer et al., 2011; O'Hanlon et al., 2018; Rosenblum et al., 2013), some of which we re-sequenced using our method (see SI Appendix, Table S1). Figure 1A shows the most current and complete global survey of *Bd* lineage distributions. Our global phylogeny (Figure 1B) recapitulates the structure of a recent whole genome phylogeny (O'Hanlon et al., 2018), with the addition of a newly-discovered *Bd* clade found only in Asia that we name *Bd*ASIA3. Below we highlight results from each of four regions of the world. The regional results are summarized in Figure 2, where we show a separate phylogeny for each region of the world.

Asia

Our most significant finding in Asia is a unique and divergent *Bd* lineage that we name *Bd*ASIA3 (Figure 2A). This lineage is clearly differentiated in the phylogenetic analyses and appears to be widespread in the Philippines, Indonesia, and parts of China. *Bd*ASIA3 co-occurs

with *Bd*GPL in all three countries. In the Philippines 56% (19/34) of samples harbored the *Bd*ASIA3 lineage and 41% (14/34) of samples had the *Bd*GPL lineage. In Java, Indonesia 62% (8/13) of samples were in the *Bd*ASIA3 lineage and 38% (5/13) were *Bd*GPL. In China 43% (3/7) samples were *Bd*ASIA3 and 57% (4/7) were *Bd*GPL. Thus, this previously undescribed *Bd* lineage appears to be relatively common in samples collected from various parts of Asia.

One additional sample from the Philippines had a unique genetic signature and could not be confidently assigned to a known *Bd* lineage (RMB10661). To assess whether this sample represents a mixed infection or a hybrid between two lineages, we plotted the average number of alleles per locus (Figure 3). RMB10661 has a similar degree of heterozygosity as the average for each of the major lineages, so it does not appear to be a hybrid or mixed sample. In addition, this sample was sister to the *Bd*ASIA3 clade in the phylogeny and has unique haplotypes at some loci. Therefore, this sample appears to be distinct from currently named lineages and possibly represents another undescribed, early branching lineage.

Europe

In Europe we report the presence of three major lineages: *Bd*GPL, *Bd*CAPE, and *Bd*ASIA1 (Figure 2B), reinforcing the key finding that multiple divergent *Bd* lineages are now commonly found at the regional scale. Of our newly-genotyped samples from Europe 90% (38/42) belong to *Bd*GPL and 10% (4/42) belong to the *Bd*CAPE lineage. The presence of *Bd*ASIA1 in Europe was documented in a prior study (Farrer et al., 2011). Remarkably, we found that 4 swabs collected from Bullfrogs (*R. catesbeiana*) in the Netherlands carried the *Bd*CAPE genotype. This expands the known range of *Bd*CAPE in Europe.

Africa

In Africa we found that the *Bd*CAPE lineage is ubiquitous in Cameroon, while *BdG*PL dominates nearby parts of West Africa and previously uncharacterized parts of Central Africa (Figure 2C). All 25 *Bd* samples collected from Cameroon are members of the *Bd*CAPE lineage, indicating *Bd*CAPE is the dominant, and perhaps exclusive *Bd* lineage in Cameroon. Additionally, we found additional support for previous studies documenting the presence of *Bd*GPL in Madagascar (Bletz et al., 2015) and provide the first report of *Bd*GPL in Burundi and Kenya. In Burundi 43% (3/7) samples were in the *Bd*GPL lineage and 57% (4/7) samples were of an undetermined lineage. To further understand why these ambiguous samples did not group with a major lineage, we plotted the average number of alleles sequenced per locus (Figure 3). We found that the ambiguous samples from Burundi had a significantly higher average allele per locus than *Bd*CAPE and *Bd*GPL samples (Mann-Whitney test, $p<0.01$). These samples were most similar in average number of alleles per locus to an experimental mixture of two divergent *Bd* strains so may be instances of coinfection or hybridization.

Americas

*Bd*GPL is the dominant lineage in the Americas (excluding Brazil where both *Bd*GPL and *Bd*ASIA2/Brazil are found), however we report the first instance of *Bd*CAPE in the western hemisphere (Figure 2D). We found that 11% (2/19) of *Bd* samples collected from Cusuco

National Park in Honduras in 2014 were *Bd*CAPE whereas 89% (17/19) of samples were *Bd*GPL. *Bd*CAPE may be newly introduced (or detected) in the Americas and occurs in very close proximity to *Bd*GPL in Honduras. All other newly genotyped samples from the Americas were members of the *Bd*GPL clade.

Discussion

Are there undiscovered Bd lineages in wild populations?

Our discovery of a new divergent lineage of *Bd* endemic to Asia (*Bd*ASIA3) supports the hypothesis that *Bd* originated in Asia and highlights our contention that substantial gaps remain in our understanding of the global genetic diversity in *Bd*. Recent whole genome studies have proposed an Asian origin for *Bd*, citing the genetic signatures of long-term endemism in the *Bd*ASIA1 lineage and noting the high lineage diversity in southeast Asia (O'Hanlon et al., 2018). Interestingly, our global phylogeny (Figure 1A) shows that the newly discovered *Bd*ASIA3 is now the earliest diverging named *Bd* lineage. In addition, *Bd*ASIA3 has the longest interior branch lengths of any described lineage, indicating that it may have persisted in isolation and/or that closely related lineages have not yet been found or have gone extinct. Furthermore, there are additional well-supported nodes within the *Bd*ASIA3 clade, indicating some within-clade genetic structure. This phylogenetic pattern is consistent with constant population size dynamics for this lineage (Grenfell et al., 2004) and supports the hypothesis that *Bd*ASIA3 is an endemic Southeast Asian lineage. In contrast, the *Bd*GPL clade shows long external branch lengths indicating periods of exponential growth – a pattern consistent with the documented global spread of this lineage. It is likely that additional *Bd* lineages remain to be discovered, which may further alter our understanding of *Bd*'s evolutionary history, including the time and place of its origin.

Another line of evidence suggesting that our current understanding of *Bd* genetic diversity is incomplete comes from samples that could not be confidently assigned to a known major *Bd* clade. For example, one sample (RMB10661 collected from the relatively pristine forests of Luzon Island in the Philippines), was collected in an area where both *Bd*GPL and *Bd*ASIA3 are present (Figure 2A) and was phylogenetically estimated to be sister to the *Bd*ASIA3 clade (Figure 1B; SI Appendix, Fig. S3). Our analyses indicate that this sample is not a mixed infection – nor a hybrid - of two different *Bd* lineages. Thus, RMB10661 may represent genetic diversity that is not yet present in our current library of *Bd* genotypes. In fact, this sample may come from yet another undescribed, early diverging Asian *Bd* lineage. However, we refrain from naming this lineage given that there is only one representative sample. It is possible that additional cryptic *Bd* diversity remains undocumented in isolated, unstudied amphibian populations around the world.

What is the current distribution of Bd lineages in previously understudied parts of the world?

Our study expands the understanding of *Bd* lineage distributions in many parts of the world where *Bd* diversity was previously uncharacterized. While we are not the first to report *Bd*CAPE in Cameroon (O'Hanlon et al., 2018), we increased the sample size for Cameroon *Bd* genotypes (Figure 2B). The ubiquity of *Bd*CAPE in Cameroon is unique – we do not currently know of any other country occupied only by this lineage. Another study reported the presence of *Bd*GPL and other unidentified lineages in Cameroon (Miller et al., 2018), but used the ribosomal

ITS region to genotype *Bd* which is not phylogenetically informative (O'Hanlon et al., 2018). Our findings point to either a long relationship of *Bd*CAPE in Cameroon, or a recent complete sweep. A previous study that did not include genotype data reported *Bd* in Cameroon dating back to 1933 (Soto-Azat, Clarke, Poynton, & Cunningham, 2010). Indeed, *Bd*CAPE may have originated in this area and spread to other parts of Africa, Europe, and now Central America or it may have recently invaded and spread in Cameroon as well. This highlights an important point: *Bd* lineages are often named for the areas where they were first discovered (i.e. *Bd*CAPE was first discovered in Cape Province, South Africa; Farrer et al., 2011), but these names may become misleading as we discover more about the history and distribution of each lineage. Some lineage names have been changed or combined as more sequence data becomes available (such as the joining of *Bd*Korea and *Bd*Brazil into *Bd*ASIA2/Brazil; O'Hanlon et al., 2018). We raise this point to recognize that lineage names can sometimes introduce biases that may arise from historical attachments to original lineage designations and to suggest that alternative lineage naming schemes (i.e. numeric) may be worth considering in this system.

In East Africa, our data reveal an interesting pattern in the newly sequenced region of Burundi. Here we also encountered samples we could not assign to a major *Bd* clade. However – unlike the ambiguous sample from Asia - the unassigned Burundi samples had an average number of alleles per locus that was similar to levels of allelic diversity found in experimental mixtures of two divergent *Bd* isolates (Figure 3). Thus, these ambiguous samples may be a coinfection (on single hosts) of different *Bd* lineages, or a possible hybrid – as they lie between the *Bd*CAPE and *Bd*GPL clades in the Africa phylogeny (SI Appendix, Fig. S5). However, they do not appear closely related to previously published *Bd*GPL/*Bd*CAPE hybrids (O'Hanlon et al., 2018). Thus, additional work will be needed to differentiate between coinfection versus hybridization and to test whether these samples represent a separate hybridization event between *Bd*GPL and *Bd*CAPE. Our ongoing work includes sequencing more samples from this region to test these alternative hypotheses (for example by comparing mitochondrial and nuclear loci and analyzing patterns of linkage disequilibrium between loci).

Where are divergent Bd lineages coming into contact?

As more data become available, they reveal that divergent *Bd* lineages are overlapping across fine spatial scales. Our study documents multiple instances where two different lineages coexist at the same time and place (e.g. sampled meters apart). For example, we find both *Bd*CAPE and *Bd*GPL in Honduras. While previous studies have documented *Bd* in this area and attributed amphibian declines to the pathogen (Kolby, Padgett-Flohr, & Field, 2010), this is the first documented instance of the *Bd*CAPE lineage in the Americas. This finding is alarming for a number of reasons. First, we know that *Bd* is capable of hybridizing across lineages as has been documented in multiple parts of the world (Jenkinson et al., 2016; O'Hanlon et al., 2018; Lisa M Schloegel et al., 2012). Second, hybrid lineages can sometimes be more virulent than parental lineages (Greenspan et al., 2018). Third, although some amphibian species may have developed resistance and/or tolerance to a particular *Bd* lineage, it remains unclear how they might respond to the introduction of a new lineage or exposure to a hybrid lineage (Lips, Diffendorfer, Mendelson III, & Sears, 2008; Voyles et al., 2018). Finally, although some amphibian host

communities are beginning to recover from *Bd* outbreaks (e.g. Knapp et al., 2016; Voyles et al., 2018), many populations are persisting only in small numbers, making them especially vulnerable to new disease outbreaks.

We also found co-occurrence of divergent *Bd* lineages in parts of Asia. For example, we found *Bd*GPL and *Bd*ASIA3 at almost every sampling locality in the Philippines. Our data indicates that these lineages have been coexisting in this region for at least seven years. The earliest samples (from Mindanao Island in 2005) and more recent samples (from the same island in 2012) had both *Bd*GPL and *Bd*ASIA3 present (Dataset S1). Previous studies found *Bd* to be widespread in the Philippines, but the genotype of these samples was unknown (Diesmos, Diesmos, Siler, Vredenburg, & Brown, 2012; Swei et al., 2011). Our findings are consistent with either a slow spread of *Bd*GPL through the Philippines or a longer, more stable coexistence of divergent lineages. In West Java, Indonesia we found similar evidence of lineage cooccurrence in high montane amphibian communities. However, we do not yet have time-series samples from this area so cannot make inferences concerning the timing of arrival of different lineages.

In Europe and Asia we see additional examples of *Bd* lineages co-occurring at small spatial scales, this time in populations of invasive bullfrogs (*R. catesbeiana*). In the Netherlands, some samples collected from *R. catesbeiana* had *Bd*CAPE and others had *Bd*GPL, despite being collected in the same year in close geographic proximity. In the Yunnan province of China, the single *R. catesbeiana* sampled was infected with *Bd*GPL while the native species from the same locality carried *Bd*ASIA3. These findings support other recent studies suggesting that invasive *R. catesbeiana* are contributing to the spread of *Bd* around the world (Schloegel et al., 2010; Schloegel et al., 2012). *Rana catesbeiana* are consumed as food by humans globally and are one of the most commonly traded amphibian species. Commercial farms that raise *R. catesbeiana* may create disease spillover in regions with high amphibian species richness, including Brazil and Asia (Schloegel et al., 2009). Thus, our study provides additional evidence that bullfrog trade should be a major concern as it creates potential pathways for short and long-distance *Bd* dispersal (O'Hanlon et al., 2018).

New Threats for Amphibian Conservation

Our dataset expands our understanding of how *Bd* lineages are distributed around the world; however, there remain unexplored frontiers in this system. First, there are many parts of the world where we know *Bd* exists, but it remains unclear which lineages are present. For example, *Bd* in Asia is widespread but exists at very low prevalence and often at low infection intensities (Swei et al., 2011). Moreover, one recent study found that the traditional qPCR assay for *Bd* (Boyle et al., 2004) may not accurately quantify endemic Asian *Bd* lineages because of variation at the rRNA ITS primer binding sites (Mutnale et al., 2018). This could lead not only to underreporting the presence of Asian *Bd* in wild populations but could also generate a sampling bias for studies like ours that select samples for genotyping based on positive qPCR results. If we exclude samples because they ostensibly have too little *Bd* DNA, it could skew our results in favor of reporting more *Bd*GPL genotypes. Therefore, our current estimates of *Bd* diversity may still be grossly underestimated, and there may be additional endemic chytrid lineages that remain undiscovered in Asia and other parts of the world. Additional *Bd* genotyping in under-sampled

areas will be critical for fully understanding the evolutionary relationships between *Bd* and amphibian hosts.

Second, we have yet to fully explore temporal variation in *Bd* genotypes to understand the timing of lineage arrival, turnover, and spread. Swabbing museum specimens to record the historic presence/absence of *Bd* over the last century has produced a rich library of DNA samples for which our genotyping method is ideal (e.g. Burrowes & De la Riva, 2017; Rodriguez, Becker, Pupin, Haddad, & Zamudio, 2014). Our current dataset includes 18 successfully genotyped museum swabs collected from around the world (Dataset S1; SI Appendix, Fig. S2), the oldest from a specimen collected in 1984 in Peru. By genotyping museum swabs we can test hypotheses for factors driving *Bd*-related declines. Understanding the dynamics of historical amphibian declines is key for predicting future risk.

Third, our data indicates that *Bd* lineages are continually spreading and are co-occurring in close proximity. Given that novel *Bd* lineages and hybrid lineages could be a threat to naïve populations (Greenspan et al., 2018), it is increasingly important that we continue to monitor *Bd* presence, prevalence, genetic diversity, and host health. In addition to monitoring, best practices for limiting *Bd* spread must be communicated not only to scientists but also to the public traveling to remote areas and commercial farms. Furthermore, steps should be taken to mitigate cross-continental lineage spread such as restrictions on amphibian imports and exports and mandatory testing and treatment protocols. These precautions could not only prevent new *Bd* outbreaks but could help curb the spread of many other plant and wildlife diseases.

Conclusions

Our study provides a new understanding of the cryptic variation in one of the deadliest wildlife pathogens ever documented. We can now better track pathways of disease spread in this system and link specific pathogen lineages to outcomes in wild populations. Our genotyping method, optimized for low quality DNA samples, can be further implemented across different sample types (e.g. museum specimen swabs, eDNA samples) to further understand the ecology and evolution of *Bd* and to inform management and mitigation strategies. Although *Bd* has a global distribution, individual lineages that vary in pathogenicity still occur in geographically-limited ranges. Thus, as *Bd* genotypes continue to expand their range, we need to consider broader actions that may be necessary to halt *Bd* lineage spread and secondary contact that could have grave consequences for amphibian hosts.

Acknowledgements

This work was co-authored by Vance T. Vredenburg, An Martel, Frank Pasmans, Rayna C. Bell, David C. Blackburn, Cheryl J. Briggs, Rafe M. Brown, Molly C. Bletz, Jaime Bosch, Alessandro Catenazzi, Mariel Familiar López, Raul Figueroa-Valenzuela, Sonia L. Ghose, Jef R. Jaeger, Andrea J. Jani, Miloslav Jirku, Roland A. Knapp, Antonio Muñoz, Daniel M. Portik, Corinne L. Richards-Zawacki, Heidi Rockney, Sean Rovito, Tariq Stark, Hasan Sulaeman, Nguyen Thien Tao, Jamie Voyles, Anthony W. Waddle, Zhiyong Yuan, and Erica Bree Rosenblum. We thank Obed Hernández-Gómez and Thomas Jenkinson for assisting with lab work and providing comments on the manuscript and Max Lambert and Andrew Rothstein for

comments on the manuscript. This work was supported by NSF IOS 1354241 to EBR; NSF DEB 1557190 to CJB, RAK, and EBR; NSF DEB 1551488 to JV, CLR-Z, and EBR and NSF GRFP to AQB. Sequencing done at the U. of Idaho IBEST Genomics Resources Core is supported by NIH COBRE Phase III grant P30GM103324. Sample collection was supported by grants from the NSF (DEB-1202609 to DCB, DEB-0743491, 0334952, 1418895, and 1654388 to RMB, Belmont Forum 1633948 to VTV), the Czech Science Foundation and Inst. of Parasitology (P506/10/2330 and RVO: 60077344 to MJ), the National Natural Science Foundation of China (31702008 to ZYY), and the Yunnan Applied Basic Research Project (2018FD047 to ZYY).

Data Accessibility

The data reported in this paper has been deposited in the National Center for Biotechnology Information Sequence Read Archive, https://www.ncbi.nlm.nih.gov/sra (Bioproject PRJNA555719).

References

Atkinson, C. T., & Samuel, M. D. (2010). Avian malaria *Plasmodium relictum* in native Hawaiian forest birds: epizootiology and demographic impacts on ʻapapane Himatione sanguinea. *Journal of Avian Biology*, *41*(4), 357–366.

Bletz, M. C., Rosa, G. M., Andreone, F., Courtois, E. A., Schmeller, D. S., Rabibisoa, N. H. C., … Crottini, A. (2015). Widespread presence of the pathogenic fungus *Batrachochytrium dendrobatidis* in wild amphibian communities in Madagascar. *Scientific Reports*, *5*, 8633.

Boyle, D. G., Boyle, D. B., Olsen, V., Morgan, J. A. T., & Hyatt, A. D. (2004). Rapid quantitative detection of chytridiomycosis (*Batrachochytrium dendrobatidis*) in amphibian samples using real-time Taqman PCR assay, *Diseases of Aquatic Organisms, 60*(2), 141–148.

Briggs, C. J., Knapp, R. A., & Vredenburg, V. T. (2010). Enzootic and epizootic dynamics of the chytrid fungal pathogen of amphibians. *Proceedings of the National Academy of Sciences of the United States of America*, *107*(21), 9695–9700.

Burrowes, P. A., & De la Riva, I. (2017). Unraveling the historical prevalence of the invasive chytrid fungus in the Bolivian Andes: implications in recent amphibian declines. *Biological Invasions*, *19*(6), 1781–1794.

Byrne, A. Q., Rothstein, A. P., Poorten, T. J., Erens, J., Settles, M. L., & Rosenblum, E. B. (2017). Unlocking the story in the swab: A new genotyping assay for the amphibian chytrid fungus *Batrachochytrium dendrobatidis*. *Molecular Ecology Resources*, *17*(6), 1283-1292.

Daszak, P., Cunningham, A. A., & Hyatt, A. D. (2000). Emerging Infectious Diseases of Wildlife-- Threats to Biodiversity and Human Health. *Science*, *287*(5452), 443–449.

Diesmos, M. L. D., Diesmos, A. C., Siler, C. D., Vredenburg, V. T., & Brown, R. M. (2012). Detecting the Distribution of the Chytrid Fungus in the Philippines. *FrogLog*, *104*, 48–49.

Edgar, R. C. (2004). MUSCLE: multiple sequence alignment with high accuracy and high throughput. *Nucleic Acids Research*, *32*(5), 1792–7.

Farrer, R. A., Weinert, L. A., Bielby, J., Garner, T. W. J., Balloux, F., Clare, F., … Fisher, M. C. (2011). Multiple emergences of genetically diverse amphibian-infecting chytrids include a globalized hypervirulent recombinant lineage. *Proceedings of the National Academy of Sciences* , *108*(46), 18732–18736.

Fisher, M. C., & Garner, T. W. J. (2007). The relationship between the emergence of Batrachochytrium dendrobatidis, the international trade in amphibians and introduced amphibian species. *Fungal Biology Reviews*, *21*(1), 2–9.

Fisher, M. C., Henk, D. A., Briggs, C. J., Brownstein, J. S., Madoff, L. C., McCraw, S. L., & Gurr, S. J. (2012). Emerging fungal threats to animal, plant and ecosystem health. *Nature*, *484*(7393), 186–194.

Foley, J., Clifford, D., Castle, K., Cryan, P., & Ostfeld, R. S. (2011). Investigating and managing the rapid emergence of white-nose syndrome, a novel, fatal, infectious disease of hibernating bats. *Conservation Biology*, *25*(2), 223–31.

Greenspan, S. E., Lambertini, C., Carvalho, T., James, T. Y., Toledo, L. F., Haddad, C. F. B., & Becker, C. G. (2018). Hybrids of amphibian chytrid show high virulence in native hosts. *Scientific Reports*, *8*(1), 9600.

Grenfell, B. T., Pybus, O. G., Gog, J. R., Wood, J. L. N., Daly, J. M., Mumford, J. A., & Holmes, E. C. (2004). Unifying the Epidemiological and Evolutionary Dynamics of Pathogens. *Science*, *303*(5656), 327 LP-332.

Jenkinson, T. S., Betancourt Román, C. M., Lambertini, C., Valencia-Aguilar, A., Rodriguez, D., Nunes-de-Almeida, C. H. L., … James, T. Y. (2016). Amphibian-killing chytrid in Brazil comprises both locally endemic and globally expanding populations. *Molecular Ecology*, *25*(13), 2978–96.

Jones, K. E., Patel, N. G., Levy, M. A., Storeygard, A., Balk, D., Gittleman, J. L., & Daszak, P. (2008). Global trends in emerging infectious diseases. *Nature*, *451*(7181), 990–993.

Kearse, M., Moir, R., Wilson, A., Stones-Havas, S., Cheung, M., Sturrock, S., … Drummond, A. (2012). Geneious Basic: An integrated and extendable desktop software platform for the organization and analysis of sequence data. *Bioinformatics*, *28*(12), 1647–1649.

Knapp, R. A., Fellers, G. M., Kleeman, P. M., Miller, D. A. W., Vredenburg, V. T., Rosenblum, E. B., & Briggs, C. J. (2016). Large-scale recovery of an endangered amphibian despite ongoing exposure to multiple stressors. *Proceedings of the National Academy of Sciences* , *113*(42), 11889–11894.

Kolby, J. E., Padgett-Flohr, G. E., & Field, R. (2010). Amphibian chytrid fungus Batrachochytrium dendrobatidis in Cusuco National Park, Honduras. *Diseases of Aquatic Organisms*, *92*(2–3), 245–251.

Li, H., & Durbin, R. (2009). Fast and accurate short read alignment with Burrows–Wheeler transform. *Bioinformatics*, *25*(14), 1754–1760.

Lips, K. R., Diffendorfer, J., Mendelson III, J. R., & Sears, M. W. (2008). Riding the Wave: Reconciling the Roles of Disease and Climate Change in Amphibian Declines. *PLoS Biol*, *6*(3), e72.

Longcore, J. E., Pessier, A. P., & Nichols, D. K. (1999). *Batrachochytrium Dendrobatidis* gen. et sp. nov., a Chytrid Pathogenic to Amphibians. *Mycologia*, *91*(2), 219–227.

McKenna, A., Hanna, M., Banks, E., Sivachenko, A., Cibulskis, K., Kernytsky, A., … DePristo, M. A. (2010). The Genome Analysis Toolkit: A MapReduce framework for analyzing next-generation DNA sequencing data. *Genome Research*, *20*(9), 1297–1303.

Miller, C. A., Tasse Taboue, G. C., Ekane, M. M. P., Robak, M., Sesink Clee, P. R., Richards-Zawacki, C., … Anthony, N. M. (2018). Distribution modeling and lineage diversity of the chytrid fungus *Batrachochytrium dendrobatidis* (Bd) in a central African amphibian hotspot. *PLOS ONE*, *13*(6), e0199288.

Mutnale, M. C., Anand, S., Eluvathingal, L. M., Roy, J. K., Reddy, G. S., & Vasudevan, K. (2018). Enzootic frog pathogen *Batrachochytrium dendrobatidis* in Asian tropics reveals high ITS haplotype diversity and low prevalence. *Scientific Reports*, *8*(1), 10125.

O'Hanlon, S. J., Rieux, A., Farrer, R. A., Rosa, G. M., Waldman, B., Bataille, A., … Fisher, M. C. (2018). Recent Asian origin of chytrid fungi causing global amphibian declines. *Science*, *360*(6389), 621 LP-627.

Reeder, N. M. M., Pessier, A. P., & Vredenburg, V. T. (2012). A reservoir species for the emerging amphibian pathogen *Batrachochytrium dendrobatidis* thrives in a landscape decimated by disease. *PLoS ONE*, *7*(3), 1–7.

Rodriguez, D., Becker, C. G., Pupin, N. C., Haddad, C. F. B., & Zamudio, K. R. (2014). Long-term endemism of two highly divergent lineages of the amphibian-killing fungus in the Atlantic Forest of Brazil. *Molecular Ecology*, *23*(4), 774–87.

Rosenblum, E. B., James, T. Y., Zamudio, K. R., Poorten, T. J., Ilut, D., Rodriguez, D., … Stajich, J. E. (2013). Complex history of the amphibian-killing chytrid fungus revealed with genome resequencing data. *Proceedings of the National Academy of Sciences of the USA*, *110*(23), 9385–90.

Schloegel, L. M., Ferreira, C. M., James, T. Y., Hipolito, M., Longcore, J. E., & Hyatt, A. D. (2010). The North American bullfrog as a reservoir for the spread of *Batrachochytrium dendrobatidis* in Brazil. *Animal Conservation*, *13*, 53–61.

Schloegel, L. M., Picco, A. M., Kilpatrick, A. M., Davies, A. J., Hyatt, A. D., & Daszak, P. (2009). Magnitude of the US trade in amphibians and presence of *Batrachochytrium dendrobatidis* and ranavirus infection in imported North American bullfrogs (*Rana catesbeiana*). *Biological Conservation*, *142*(7), 1420–1426.

Schloegel, L. M., Toledo, L. F., Longcore, J. E., Greenspan, S. E., Vieira, C. A., Lee, M., … James, T. Y. (2012). Novel, panzootic and hybrid genotypes of amphibian chytridiomycosis associated with the bullfrog trade. *Molecular Ecology*, *21*(21), 5162–5177.

Skerratt, L. F., Berger, L., Speare, R., Cashins, S., McDonald, K. R., Phillott, A. D., … Kenyon, N. (2007). Spread of Chytridiomycosis Has Caused the Rapid Global Decline and Extinction of Frogs. *EcoHealth*, *4*(2), 125–134.

Soto-Azat, C., Clarke, B. T., Poynton, J. C., & Cunningham, A. A. (2010). Widespread historical presence of *Batrachochytrium dendrobatidis* in African pipid frogs. *Diversity and*

Distributions, *16*(1), 126–131.

Stamatakis, A. (2014). RAxML version 8: a tool for phylogenetic analysis and post-analysis of large phylogenies. *Bioinformatics*, *30*(9), 1312–1313.

Swei, A., Rowley, J. J. L., Rödder, D., Diesmos, M. L. L., Diesmos, A. C., Briggs, C. J., … Vredenburg, V. T. (2011). Is Chytridiomycosis an Emerging Infectious Disease in Asia? *PLOS ONE*, *6*(8), e23179.

Voyles, J., Woodhams, D. C., Saenz, V., Byrne, A. Q., Perez, R., Rios-Sotelo, G., … Richards-Zawacki, C. L. (2018). Shifts in disease dynamics in a tropical amphibian assemblage are not due to pathogen attenuation. *Science*, *359*(6383), 1517 LP-1519.

Voyles, J., Young, S., Berger, L., Campbell, C., Voyles, W. F., & Dinudom, A. (2009). Pathogenesis of Chytridiomycosis, a Cause of Catastrophic Amphibian Declines. *Science*, *326*(5952), 582–585.

Vredenburg, V. T., Knapp, R. a, Tunstall, T. S., & Briggs, C. J. (2010). Dynamics of an emerging disease drive large-scale amphibian population extinctions. *Proceedings of the National Academy of Sciences of the United States of America*, *107*(21), 9689–9694.

Wake, D. B., & Vredenburg, V. T. (2008). Colloquium paper: are we in the midst of the sixth mass extinction? A view from the world of amphibians. *Proceedings of the National Academy of Sciences of the United States of America*, *105 Suppl 1*, 11466–73.

Yap, T. A., Koo, M. S., Ambrose, R. F., & Vredenburg, V. T. (2018). Introduced bullfrog facilitates pathogen invasion in the western United States. *PLOS ONE*, *13*(4), e0188384.

Zhang, C., Rabiee, M., Sayyari, E., & Mirarab, S. (2018). ASTRAL-III: polynomial time species tree reconstruction from partially resolved gene trees. *BMC Bioinformatics*, *19*(6), 153.

Figures

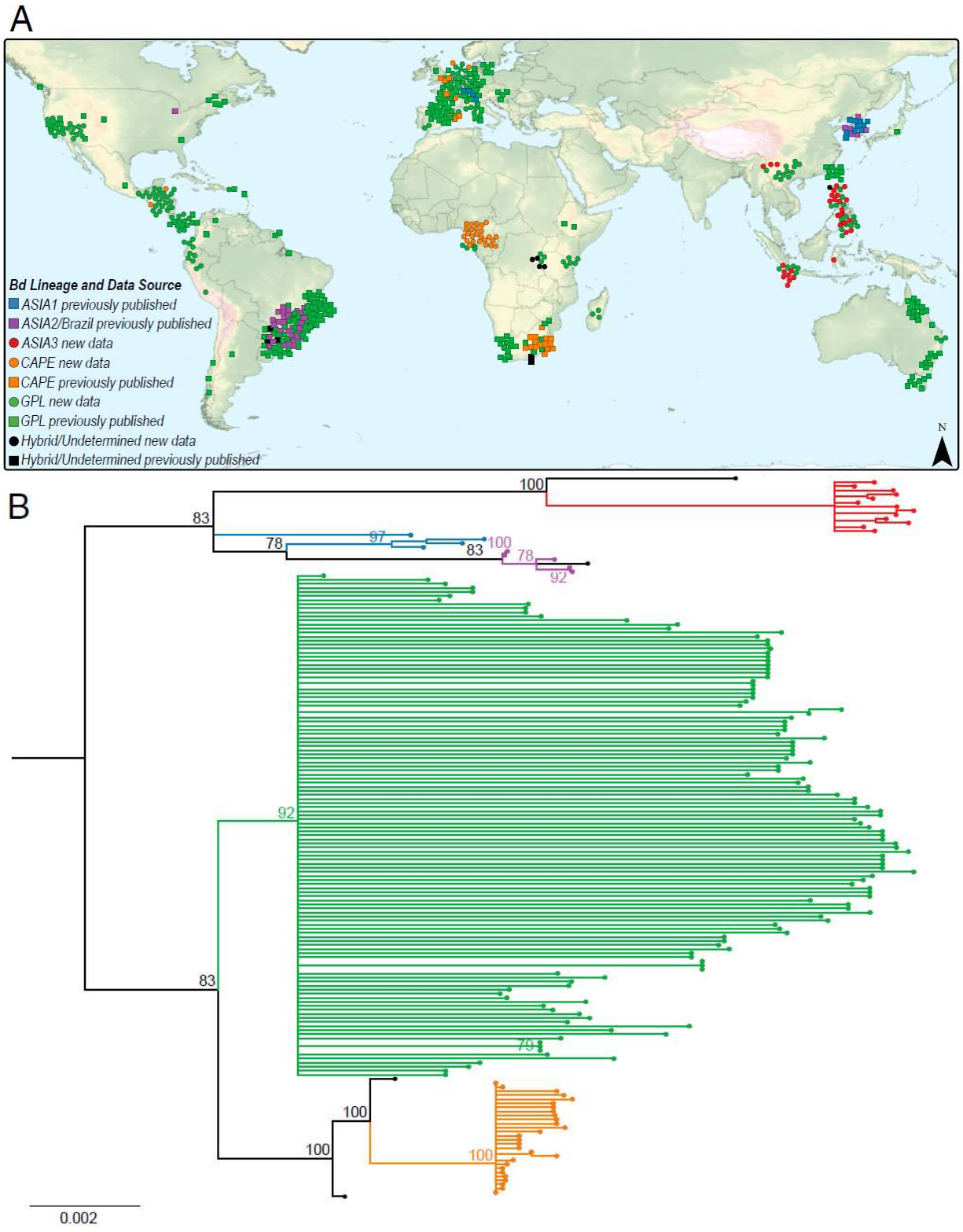
A
Bd Lineage and Data Source
ASIA1 previously published
ASIA2/Brazil previously published
ASIA3 new data
CAPE new data
CAPE previously published
GPL new data
GPL previously published
Hybrid/Undetermined new data
Hybrid/Undetermined previously published
N
B
100
83
78
97
83
100
78
92
92
83
79
100
100
100
0.002

Figure 1: A) Global map of *Bd* genotypes. Points within 100 meters are dispersed to decrease overlap and demonstrate sampling effort; therefore, map point locations are approximate. Colors indicate major *Bd* lineage, circles are newly genotyped samples (N=222) and squares are previously published *Bd* genotype data (N=334; data from 14-17, 27). **B)** Best scoring unrooted maximum likelihood tree estimated from 172 concatenated nuclear loci (23,651bp) and 100 bootstrap replicates performed in RAxML. Branches on phylogeny are colored by major *Bd* lineage. This tree includes newly sequenced samples with at least 84 loci (N=131) and whole genome data (N=47). Nodes with bootstrap support <50 have been collapsed and nodes >70 bootstrap support are labeled. Phylogeny with tip labels is available in the SI Appendix, Fig. S1.

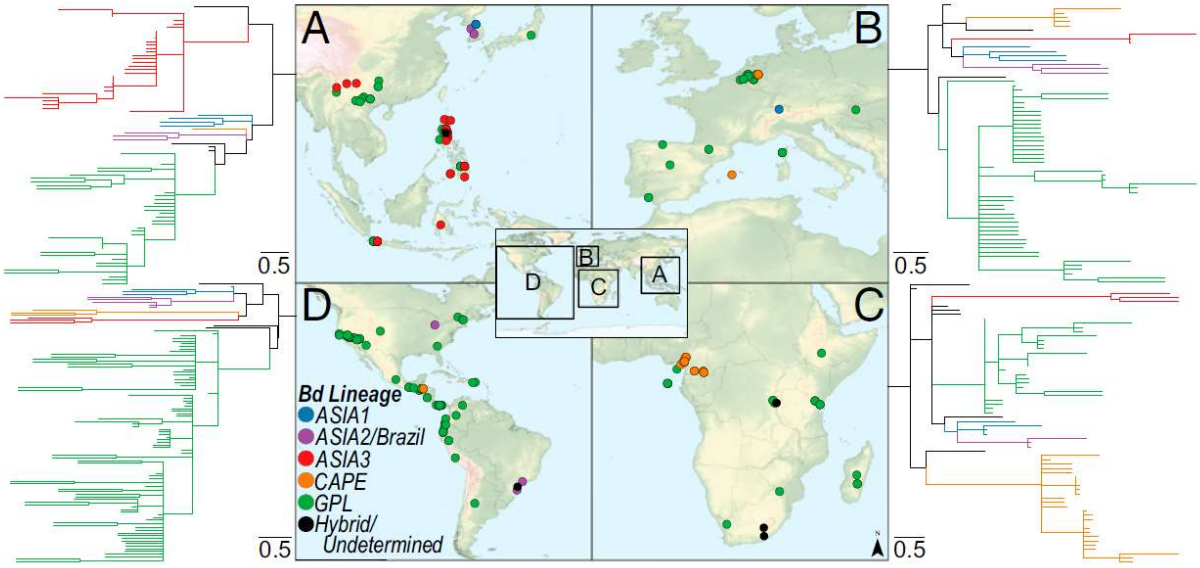

Figure 2: Maps and regional phylogenies showing *Bd* sampling locations and lineages in **A)** Asia (N=78) **B)** Europe (N=66) **C)** Africa (N=66) and **D)** the Americas (N=108). Points and clades colored as in Fig.1. Sample sets include representatives of each major clade in addition to all newly genotyped samples collected in that region. Overlapping points on the map are offset by 1° longitude for display purposes. Phylogenies are species tree consensus topologies calculated in Astral (v.5.6.2) from Maximum Likelihood gene trees, individually estimated in RAxML for each locus. Full size versions of the phylogenies with tip and node labels are available in the SI Appendix, Figures S3-6.

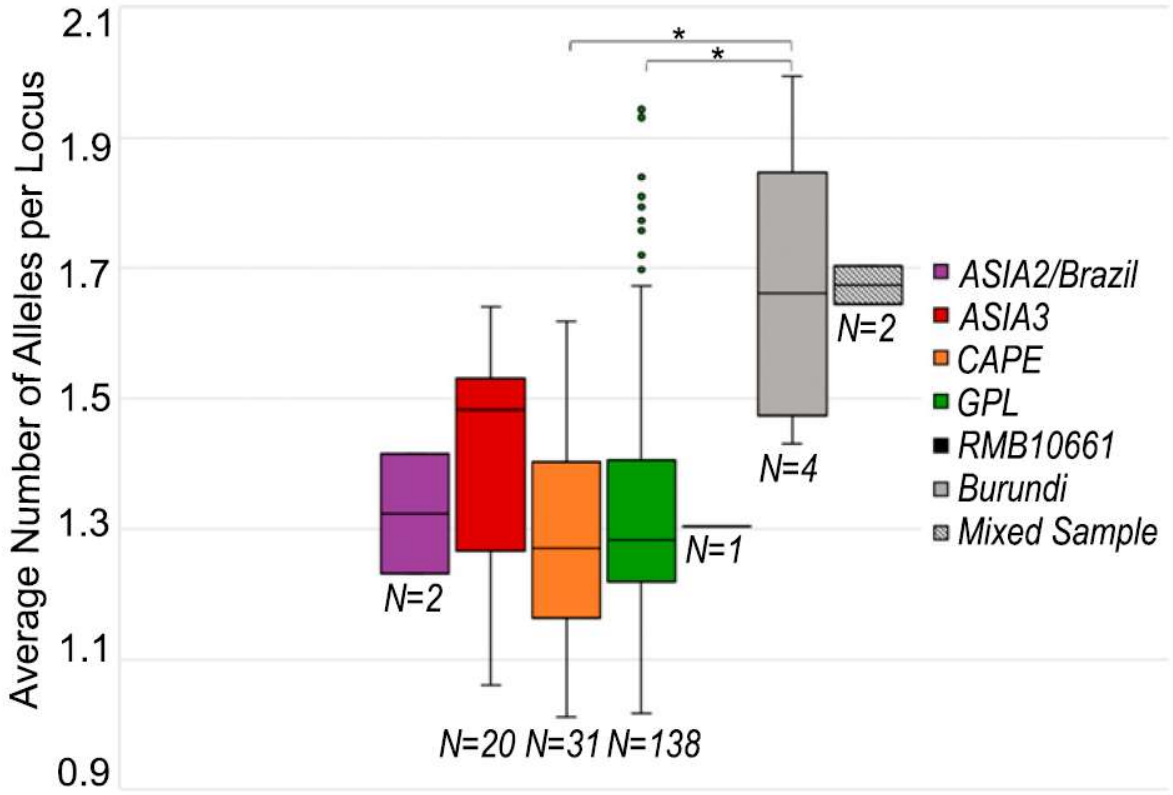

Figure 3: Average number of alleles for each major Bd lineage and ambiguous samples sequenced via the Fluidigm Access Array method. The mixed sample represents an experimental mixture of BdGPL and BdBrazil/ASIA2 isolates. The * indicates a significant difference between the Burundi samples and the BdGPL/BdCAPE lineages (Mann-Whitney 2-tail test $p<0.01$).

Chapter 3: Whole exome sequencing identifies the potential for genetic rescue in iconic and critically endangered Panamanian harlequin frogs

Abstract

Avoiding extinction in a rapidly changing environment often relies on a species' ability to quickly adapt in the face of extreme selective pressures. In Panamá, two closely related harlequin frog species (*Atelopus varius* and *Atelopus zeteki*) are threatened with extinction due to the fungal pathogen *Batrachochytrium dendrobatidis* (*Bd*). Once thought to be extirpated from Panamá, *A. varius* have recently been rediscovered in multiple localities across their historic range, however *A. zeteki* are possibly extinct in the wild. By leveraging a unique collection of 190 *Atelopus* tissue samples collected before and after the *Bd* outbreak in Panama, we describe the genetics of persistence for these species on the brink of extinction. We sequenced the transcriptome and developed an exome-capture assay to sequence the coding regions of the *Atelopus* genome. Using these genetic data, we evaluate the population genetic structure of historic *A. varius* and *A. zeteki* populations, describe changes in genetic diversity over time, assess the relationship between contemporary and historic individuals, and test the hypothesis that some *A. varius* populations have rapidly evolved to resist or tolerate *Bd* infection. We found a significant decrease in genetic diversity in contemporary (compared to historic) *A. varius* populations. We did not find strong evidence of directional allele frequency change or selection for *Bd* resistance genes, but we uncovered a set of candidate genes that warrant further study. Additionally, we found preliminary evidence of recent migration and gene flow in one of the largest persisting *A. varius* populations in Panamá, suggesting the potential for genetic rescue in this system. Finally, we propose that previous conservation units should be modified, as clear genetic breaks do not exist beyond the local, population level. Our analyses lay the groundwork for genetically informed conservation and advance our understanding of how imperiled species might be rescued from extinction.

Introduction

Extinction is a pressing threat for many species on Earth. A myriad of stressors – including climate change, habitat destruction, invasive species, and infectious disease – drive reductions in population sizes and decrease connectivity, often leading small populations towards an "extinction vortex" (Gilpin & Soule, 1986). This vortex is caused in part by the vulnerability of small populations to environmental and demographic stochasticity (Shaffer, 1981). In addition, erosion of genetic diversity also plays a key role in this process. Inbreeding depression, which leads to a loss of genetic diversity and an increase in the expression of deleterious genetic variants, is a significant contributor to extinction risk in small, isolated populations (Frankham, 2005). Problems associated with inbreeding depression can also apply to *ex-situ* captive breeding efforts, where small founding populations are brought into captivity and inbred, decreasing the chances of successful reintroductions in the future (Hedrick & Garcia-Dorado, 2016). Therefore, understanding the genetics of population declines is critical to understanding extinction risk and making informed conservation decisions.

In addition to providing key insights into population declines, genetic and genomic techniques can also help reveal mechanisms underlying persistence and recovery of natural

populations. There are a few non-mutually exclusive processes by which natural populations may be rescued from extinction. First, demographic rescue refers to the simple addition of individuals to a population via immigration and the subsequent boost in population size which can prevent extinction (Brown & Kodric-Brown, 1977). Second, genetic rescue refers to the positive effect of increased gene flow in small, threatened populations – over and above what can be attributed to the demographic effect of adding migrants (Ingvarsson, 2001). The positive effects of genetic rescue are the product of a reduction of genetic load (high frequency of deleterious genetic variants), and the high fitness of hybrid individuals (Tallmon, Luikart, & Waples, 2004). Third, evolutionary rescue occurs when populations undergo rapid adaptive evolution via natural selection (Gomulkiewicz & Holt, 1995; Gonzalez, Ronce, Ferriere, & Hochberg, 2013). The probability of evolutionary rescue as a means of population recovery is highest for populations with large initial sizes, low levels of initial maladaptation to particular environmental conditions, and high levels of standing genetic variation (Carlson, Cunningham, & Westley, 2014). In practice, little is known about which of these mechanisms contribute to recoveries of species on the brink of extinction.

One clade that has suffered particularly alarming declines is the neotropical harlequin frogs (genus *Atelopus*), due in large part to the devastating amphibian chytrid fungus *Batrachochytrium dendrobatidis* (*Bd*) (La Marca et al., 2005; Longcore, Pessier, & Nichols, 1999). It is estimated that 81% of *Atelopus* species have declined and only 12% have stable populations (La Marca et al., 2005). Despite early evidence suggesting a dire outcome, some *Atelopus* species have been rediscovered in small populations that persist within their historic range in Costa Rica (González-Maya et al., 2013), Venezuela (Rodríguez-Contreras, Señaris, Lampo, & Rivero, 2008), Ecuador (Barrio-Amorós et al., 2020; Tapia, Coloma, Pazmiño-Otamendi, & Peñafiel, 2017), and Panamá (Perez et al., 2014; Voyles et al., 2018). However, these populations are often small and isolated, in some cases show evidence of low recruitment (González-Maya, Gómez-Hoyos, Cruz-Lizano, & Schipper, 2018), and thus may still be at high risk of extinction. Persistent populations offer a unique opportunity to investigate mechanisms of host resistance or tolerance to *Bd* infection and disease development in this severely imperiled amphibian clade.

One intriguing case-study of rapid decline and persistence is the critically endangered *Atelopus varius* in Panamá (Voyles et al., 2018). This species, along with the closely-related Panamanian Golden Frog (*Atelopus zeteki*), declined precipitously after *Bd* swept through Panamá in the early 2000's (Crawford, Lips, & Bermingham, 2010). These two species, which together form a monophyletic clade (Richards & Knowles, 2007) have garnered significant interest and funding to mitigate population losses, owing in part to their charismatic appearance, historic ubiquity, and cultural significance in Panamá (Poole, 2008). Conservation interventions have included forming robust captive colonies in Panamá and in zoos across the United States (Gagliardo et al., 2008). While captive populations of *A. zeteki* and *A. varius* are considered secure (Lewis et al., 2019), a recent reintroduction attempt was not successful in re-establishing wild populations of *A. varius* (Panamá Amphibian Rescue and Conservation Project 2018).

Integrating studies of persistent wild populations into captive management decisions could be key to improving future ex-situ conservation efforts.

Previous research suggests that host-specific processes might be responsible for persistence of *Atelopus* in Panamá. Initial laboratory studies showed that *A. zeteki* is highly susceptible to *Bd* (Bustamante, Livo, & Carey, 2010). *Bd* infection intensity typically increases rapidly often leading to mortality (DiRenzo, Langhammer, Zamudio, & Lips, 2014), which may be due to *Bd*'s ability to suppress host immune defenses (Ellison, Savage, et al., 2014), a lack of protective microbial symbionts on host skin (Becker et al., 2015), and/or ineffectiveness of secreted antimicrobial peptides (Douglas C Woodhams, Voyles, Lips, Carey, & Rollins-Smith, 2006). Other studies have found that the virulence of *Bd* in Panamá has not changed since the pathogen's arrival, indicating that attenuating pathogen virulence is not driving host persistence (Voyles et al., 2018). Considering possible environmental mediators of persistence, studies have found that *A. varius* persist in many different microclimates (i.e. warmer lowlands and cooler highlands) (Perez et al., 2014), indicating that environmental refugia likely do not explain persistence in these species. Finally, there is evidence that persisting *A. varius* skin secretions are better at inhibiting *Bd* growth than secretions from *A. varius* brought into captivity before *Bd* arrival (Voyles et al., 2018). Given the lack of evidence indicating environmental or pathogen-mediated shifts predicting changes in survival, and noting preliminary evidence of increased host defenses against *Bd*, we use a genomic approach to investigate the hypothesis that changes in the amphibians themselves may underlie persistence.

In this study, we designed a genomic capture assay to sequence the expressed, functional regions of the *Atelopus* genome (Bi et al., 2012). With this exome capture assay, we sequenced *A. varius* and *A. zeteki* samples collected from across their historic range in Panamá and from the captive colonies at the Panamá Amphibian Rescue and Conservation Project (PARC). We also sequenced contemporary individuals from persisting populations. Our contemporary samples represent a significant re-survey effort of historic *A. varius/zeteki* sites across their entire historic range in Panama. Our captive samples represent all distinct *A. varius/zeteki* lineages currently in captivity in Panamá. Leveraging our paired time-series data we seek to 1) evaluate the population genetic structure of historic *A. varius* and *A. zeteki* in Panamá 2) compare the genetic diversity of historic, contemporary, and captive populations and 3) scan the coding regions of the *A. varius* genome to search for genetic variants linked to persistence in the face of ongoing disease threats. Together, addressing these objectives will advance our understanding of what demographic and/or adaptive processes contribute to host persistence and facilitate data-driven conservation efforts.

Methods

Sample collection

Our study included 190 total samples, with 130 historical (2001-2004), 39 contemporary (2012-2016), 17 captive, and 4 Costa Rican *Atelopus* samples. We collected historical samples before the *Bd* outbreak in Panamá as described in Richards and Knowles 2007 (ANAM permit SE/A-46-03, SEX/A-90-03, SE/A-6-04 and SEX/A-30-04, CITES permit 03US071994/9). For

contemporary samples, we conducted field surveys between 2012-2016 as described in Voyles et al 2018 (ANAM permit SE/AH-4-12, SE/AH-1-13, SE/AH-3-13, SE/A-42-14, SE/AH-2-14, SC/A-34-15, SC/AO-4-16, SE/AH-4-17). Briefly, we conducted visual encounter surveys during both the dry season (December-January) and wet season (May-July) at stream sites that were previously known to have *A. varius* or *A. zeteki* populations. We conducted surveys on 200m stream transects where 2-3 observers walked the length of the transect slowly searching for amphibians. We captured *A. varius* adults with a pair of fresh gloves and collected skin swabs for *Bd* detection and a toe clip sample for genetic analysis. We collected DNA samples from captive individuals via buccal swab at the El Valle Amphibian Conservation Center (EVACC). Finally, we sourced four DNA samples from the Museum of Vertebrate Zoology frozen tissue collection: MVZ149729: *Atelopus varius* collected in Costa Rica 1976, MVZ149734: *Atelopus senex* collected in Costa Rica 1976, MVZ223270: *Atelopus chiriquiensis* collected in Costa Rica 1990, MVZ223280: *Atelopus varius* collected in Costa Rica 1990.

qPCR for Bd

To test for the presence of *Bd* in contemporary *A. varius* samples, skin swabs were also collected. Genomic DNA was extracted from skin swabs using Qiagen DNeasy Blood and Tissue kit following the manufacturer's protocol for animal tissue. We used a quantitative polymerase chain reaction (qPCR) assay to quantify *Bd* DNA following Boyle et al. (2004) (Boyle, Boyle, Olsen, Morgan, & Hyatt, 2004) and included an internal positive control (Hyatt et al., 2007) and bovine serum albumin (final concentration 400ng/µL, (Garland, Baker, Phillott, & Skerratt, 2010)) in each reaction well. Each qPCR run included positive and negative controls and a seven-fold dilution series of plasmid-based *Bd* standards (Pisces Molecular, Boulder CO). We ran each extract in triplicate. Samples that exhibited >0 DNA copies were considered positive. Finally, we converted average *Bd* DNA copy number per 5µL reaction volume to whole-swab loads.

Exome capture design

Genomes for the focal species were not available a priori, so we sequenced transcriptomes to design our capture assay. To maximize transcript discovery we extracted RNA from three captive-bred *Atelopus varius* at varying stages of *Bd* infection (uninfected, early infected, late infected) using four different tissue types (liver, spleen, dorsal skin, ventral skin). All animals were euthanized by rapid decapitation followed by double pithing in accordance with the Tulane University IACUC protocol 0453. RNA was extracted using a Trizol protocol (Rio, Ares, Hannon, & Nilsen, 2010) with some minor modifications. First, we homogenized the tissue using 2.8mm ceramic beads and 500µl of Trizol with MoBio PowerLyzer at the recommended setting for animal tissues. We then transferred the homogenized tissue and Trizol to a Heavy Phase-Lock Gel tube and incubated for 5 minutes at room temperature. We added 200µl chloroform, incubated for 3 minutes, and spun at 12,000xG for 20 minutes at 4˚C. We removed the supernatant and added 0.5µl of 20mg/ml glycogen and inverted 10x. We then performed an isopropanol precipitation resuspended the RNA pellet in 50µl RNAse-free water, and treated samples Turbo DNAase (Ambion). RNA was quantified using Qubit and quality was assessed using the Agilent bioanalyzer. All RNA extractions had a RIN score of at least 7. For

library preparation we sent samples to IBEST Genomics Resources Core at the University of Idaho, where they performed an Apollo Poly mRNA select and Illumina strand RNA library prep. Samples were then sequenced at the QB3 Vincent J. Coates Genomics Sequencing Laboratory at UC Berkeley on one lane of an Illumina HiSeq 4000 using the 150 paired end read kit.

Next, we combined our sequence data to create a single assembled transcriptome for probe design. First, we cleaned reads following (Bi et al., 2012) and (Singhal, 2013) and assembled reads using TRINITY (Grabherr et al., 2011). We then selected the longest transcript per TRINITY gene and annotated them with *Nanorana parkeri*, *Xenopus tropicalis* and *Anolis carolinensis* protein reference using BLASTX (Altschul et al., 1997) and EXONERATE (Slater & Birney, 2005). Fragmented transcripts that hit to the same reference protein were joined by Ns according to their relative BLAST hit positions. The resulting transcripts were then combined to remove redundancies via Cd-hit-est (Li & Godzik, 2006) and CAP3 (Huang & Madan, 1999). We defined coding sequences (cds) of each annotated transcript using EXONERATE and specified these regions in a bed format. The pipelines used for transcriptome data processing and annotation are available at https://github.com/CGRL-QB3-UCBerkeley/DenovoTranscriptome.

Finally, we used our annotated transcriptome to design capture probes to later sequence all coding regions (exome) from our target samples. We used this approach to 1) reduce the amount of sequencing necessary while still broadly sampling functionally relevant genomic regions and 2) improve our ability to sequence low quality and/or quantity DNA samples (i.e. old tissues and buccal swabs). To design our assay, we used a custom Nimblegen SeqCap EZ Developer Library (Roche Nimblegen Inc.). We tiled capture probes across the cds of each transcript and masked using both self and *Nanorana parkeri* genome frequency (max number of matches = 2). The resulting probe set covered 99.6% of the annotated transcripts for a total target size of 19.4Mb from 24,863 targets.

Sample library prep, capture and sequencing

We selected a set of 190 historic, contemporary, and captive *A. varius* and *A. zeteki* samples to sequence using our exome capture targeted assay. Samples included multiple tissue types (toe clips, liver, tadpoles) and buccal swabs. Before DNA extraction, toe clips and tadpoles were stored in DESS buffer at room temperature, liver was stored in DMSO at -80˚C, and buccal swabs were stored in 95% ethanol at -20˚C. Liver, toes, and tadpoles were first rinsed with DNA-grade water and then homogenized using 2.8mm ceramic beads and the MoBio PowerLyzer. Buccal swabs were dried at 37˚C until all ethanol was evaporated. After initial sample prep, we followed the standard manufacturers protocol for the Qiagen DNeasy Blood and Tissue kit with the addition of an RNase A treatment before adding Buffer AL and ethanol. Samples were eluted in 200µl DNA-grade water and DNA concentration was measured using Qubit.

To prepare DNA samples for probe hybridization we used the KAPA Hyper Prep kit (Kapa Biosystems, Wilmington, MA) for genomic library preparation. First, we sheared genomic DNA on a Diagenode Bioruptor to an average fragment size of 350bp. We used 1.1µg of DNA

for sonication, unless the extraction yielded less than 1.1µg, then the entire extraction was used (min = 24.5ng). Sheared DNA was then cleaned using Kapa Pure Beads with a volumetric ratio of 1x. Cleaned DNA was prepped following the Kapa Hyper Prep protocol. 5µl of 15µM Illumina TruSeq Dual matched adapters were used in the ligation step. Post ligation we performed a 0.8X bead cleanup and resuspended adapter-ligated DNA in 20µl of 10mM Tris-HCl pH 8.0-8.5. Samples were then PCR amplified based on the initial amount of DNA (ranging from 2 cycles to 12 cycles of amplification) with a target of 1µg of DNA per sample post amplification. Post-amplification we cleaned samples again using a 1X bead-based cleanup and subsequently size selected using a 0.6-0.8 double sided size selection. Samples were resuspended in 50µl DNA-grade water. Sample quality was then assessed on an Agilent bioanalyzer and DNA concentration was measured using a Qubit. Equal amounts of DNA for each sample was then pooled into 12 pools, each with 16 samples.

Finally, to select only the targeted regions and wash away all other DNA fragments, we hybridized our DNA to capture probes. Target capture was performed following the Roche SeqCap EZ Library SR protocol at the Functional Genomics Laboratory (FGL), a QB3-Berkeley Core Research Facility at UC Berkeley. At the FGL, the biotinylated probes were hybridized to 12 separate 1µg pools, using SeqCap EZ Developer Reagent in place of COT1 Human DNA and universal blocking oligos provided by IDT (Xgen Universal Blockers-TS Mix), at 47 degrees for up to 72 hours. The hybridized samples were captured on streptavidin beads, and 14 cycles of post-capture PCR amplification was performed to enrich for target library fragments. Samples were then transferred to the Vincent J. Coates Genomic Sequencing Laboratory, a partner QB3-Berkeley Core Research Facility, quantified using Kapa Biosystems Universal Master Mix Illumina Quant qPCR reagents, pooled equimolar, and sequenced using 4 lanes of an Illumina HiSeq4000 paired-end 150 sequencing chemistry with dual 8-bp indexes. Sample data was then demultiplexed into fastq file format using Illumina bcl2fastq software version 2.19.

Exome capture data processing

After sequencing, reads from all 190 samples were individually cleaned and aligned to prepare for downstream analyses. First, we processed the data using seqCapture (https://github.com/CGRL-QB3-UCBerkeley/seqCapture). We filtered raw reads using Trimmomatic (Bolger, Lohse, & Usadel, 2014) and cutadapt (Martin, 2011) to trim adapter contaminations and low quality reads. We removed exact PCR duplicates using Super-Deduper (https://github.com/dstreett/Super-Deduper) and overlapping paired reads were merged using Flash (Magoč & Salzberg, 2011). We then selected 8 representative libraries with the most amount of data and assembled each using Spades (Bankevich et al., 2012) with multiple kmer sizes (21, 33, 55, 77, 99 and 127). For each individual assembly, we used Blastn (Altschul et al., 1997) (evalue cutoff = 1e-20, similarity cutoff = 80%) to compare the assembled contigs against the original annotated transcripts used for probe design and extracted the set of contigs associated with targets. We used Cd-hit-est (Li & Godzik, 2006) and Cap3 (Huang & Madan, 1999) to cluster and merge all raw assemblies into reduced, less-redundant assemblies. We then combined the assemblies for the 8 individuals by a similar methodology. We generated a final exome reference sequence where all non-redundant and discrete contigs (exons and their

flanking sequences) that were derived from the same target were joined with Ns based on their relative blast hit positions to the reference. We aligned cleaned sequence data from each individual library to this reference using Novoalign (http://www.novocraft.com/products/novoalign/) and only kept reads that mapped uniquely to the reference. We used Picard (http://broadinstitute.github.io/picard/) to add read groups and GATK v.3.8 (McKenna et al. 2010) to perform re-alignment. We then used SAMTools/bcftools (Li et al. 2009) to generate a raw VCF that contains all potential variable and invariable sites. These data in the VCF were then filtered using a custom filtering program, SNPcleaner (https://github.com/tplinderoth/ngsQC/tree/master/snpCleaner) by following the protocol specified in Bi et al. (2013). We only considered sites in which at least 70% of the individuals had at least 3X coverage. We also filtered sites showing an excess of heterozygosity using a one-tailed exact test with a P-value of 0.00001. After these filters, 34.8Mb sites from 14985 genes (exons and flanking) were used in downstream population genetic analyses.

Population genetic structure analysis

First, to characterize variation and clustering in our ingroup samples (N=186), we generated a PCA. We used ANGSD (v.0.919) (Korneliussen, Albrechtsen, & Nielsen, 2014) to call genotype likelihoods and produce a beagle file using sites that passed filters described above. We then used pcangsd (v.0.9) (Meisner & Albrechtsen, 2018) to generate a covariance matrix. We calculated eigenvalues and eigenvectors of the covariance matrix and plotted the first two eigen vectors in R (v.3.4.3). To compare genetic clustering patterns in populations with contemporary and historic samples, we repeated this process to create a PCA with only *A. varius* samples. Finally, to compare the relationship of Panamanian samples to samples from Costa Rica, we created a PCA with all samples sequenced in this study (N=190).

To test for genetic clusters, we used NGSadmix as implemented in ANGSD (Skotte, Korneliussen, & Albrechtsen, 2013). First, we used ANGSD to calculate genotype likelihoods using the -doGlf 2 flag and generated a beagle file. We did this separately for all ingroup samples and for all El Copé West samples (N=44). We also re-ran the analysis for El Copé West using the dataset with relatives trimmed (N=31). For all samples, we ran NGSadmix for all values of K from 1-13 ten times, and for El Copé West we ran all values of K from 1-6 ten times. We then compared the likelihood values for each run using CLUMPAK and calculated the most likely K using the ΔK method (Evanno et al., 2005).

To further understand the genetic relationship of individual samples, we calculated pairwise genetic distance using NGSdist v.1.0.2 (Vieira, Lassalle, Korneliussen, & Fumagalli, 2016). First, we calculated genotype likelihoods for all samples (N=190) using ANGSD -doGlf 8. We then calculated genetic distance using a subset of 1,422,762 sites. We repeated this calculation 100 times by randomly sampling with replacement blocks of 1000 SNPs for bootstrap support values. We used FastME v.2.1.5 (Lefort, Desper, & Gascuel, 2015) to calculate a neighbor joining tree from the original distance matrix with bootstrap support values. We collapsed all nodes with <70 bootstrap support. To compare genetic distance to geographic distance we calculated pairwise geographic distance and plotted this vs. genetic distance in R. We ran a Mantel test to assess statistical significance of the relationship between geographic and genetic distance. We also calculated a Mantel corellogram using the Ecodist package (v.2.0.1) in

R to compare the relationship of genetic and geographic distance across equally-spaced geographic bins (Goslee & Urban, 2007).

To quantify genetic distinctiveness between populations we calculated F_{ST} using ANGSD. First, we calculated the unfolded site frequency spectrum for each population separately and then calculated the joint site frequency spectrum for each comparison. We then calculated the global estimate for F_{ST} between populations in ANGSD using the "realSFS fst stats" function. We report the weighted F_{ST} value (Weir & Cockerham, 1984).

To test for, and take into account the effect of isolation by distance on population clustering, we used clustering algorithm called conStruct that models both continuous and discrete population structure (Bradburd et al., 2018). To reduce computation times and even sampling among populations, we trimmed our sample set to a maximum of 5 individuals per sampling locality per time period (excluding El Copé West where we trimmed highly-related individuals but allowed more than 5 individuals in the contemporary group). The final sample set included 117 individuals. We then randomly selected one SNP per contig for each of the samples (N=14,950 SNPs) and ran construct in R (v.3.4.3) using spatial and nonspatial models for K=1 to 5 with 5 replicates run for 10,000 iterations. We used the x.valdiation function in ConStruct to compare layer contributions and cross-validate the models.

Genetic diversity and effective population size

To calculate within-population measures of genetic diversity, we first calculated the folded site frequency spectrum for both populations as a whole and for individuals. We then calculated average heterozygosity, average per-site Watterson's theta (θ_W), and average per-site pi (π) for each population and time period using the filtered set of ~34 million SNPs.

We calculated effective populations size (Ne) using several methods. First, we used the program NeEstimator (v2.1) to calculate the Ne for each population using the linkage disequilibrium method (Do et al., 2014). We prepared an input file in Genepop format using a single randomly selected SNP per contig with no missing data (N=14,950 SNPs) and excluded singleton alleles. We only report Ne for populations with at least 10 samples. Next, we used a sibship analysis as implemented in COLONY2 (Jones & Wang, 2010) to determine Ne of each subpopulation (across time and space). This analysis considers how many full and half sib dyads are present within a population to estimate the current effective size (Wang, 2009). To reduce computation time we selected a block of 2000 SNPs, each from a separate contig, for each of the populations tested. We then ran COLONY2 using a polygamous mating system with inbreeding and a genotyping error rate of 0.0001. We used the full likelihood method with medium likelihood precision and medium run length. We did not specify male or female individuals *a priori* given these data are missing for many of our samples and we assumed random mating.

Scans for selection

To reduce relatedness as a confounding factor, we trimmed highly related individuals from our dataset before performing our selection tests. To do this, we calculated pairwise relatedness between all ingroup individuals using ngsRelate v.1 (Korneliussen & Moltke, 2015).

To generate the input for ngsRelate, we first used ANGSD to call genotype likelihoods (GL -3). We then used Ngsrelate to generate values for k0, k1, and k2. We calculated the coancestry coefficient (θ) between all individuals using the formula θ=k1 / 4 + k2 / 2 where k1 and k2 are the maximum likelihood estimates of the relatedness coefficient. We then used these coancestry coefficients to trim our dataset for downstream selection analyses, removing one or more of a group of individuals that are highly related (θ > 0.25 or putative siblings/parent-offspring). We trimmed 7 individuals from the Santa Fe historic population and 13 individuals from the El Copé West contemporary population by randomly selecting one individual from each related group to remain in the sample set.

To search the *A. varius* exome for genetic variants that may be under selection in contemporary populations, we conducted three different time-stratified selection analyses across two different comparisons. Our comparisons include one broad analysis of shared signatures of selections across all *A. varius* (Historic: N = 79, Contemporary: N = 26) and one local comparison focused on the largest single contemporary population from El Copé West (Historic: N = 14, Contemporary: N = 17). Both datasets had close relatives removed as described above. The first analysis we used to identify putative genes under selection was an association test as implemented in ANGSD (-doasso 1). First, we coded historic individuals as control (0) and contemporary individuals as case (1). For each comparison we calculated the Likelihood Ratio for each allele (LR) and compared these values to a chi-square distribution with df = 1 to get corresponding p-values. We also calculated per site F_{ST} and sliding window F_{ST} analyses to identify potential variants under selection. First, we calculated the unfolded site frequency spectrum for each trimmed population of interest using the reference fasta as the ancestral state. We then calculated the joint SFS for each comparison and used the realSFS function in ANGSD to calculate the per site F_{ST}, and sliding window F_{ST} (window = 5000bp, step = 1000bp). Negative values for F_{ST} were treated as $F_{ST} = 0$. For *A. varius* we compared 34,850,890 SNPs. For El Copé West we compared 34,851,023 SNPs. To assess the significance of outlier SNPs we randomly permuted samples across historic/contemporary groups, breaking the phenotype-genotype connection. We then plotted this null distribution of F_{ST} values against the true F_{ST} values calculated for each comparison (S3 Fig). This comparison tests the null hypothesis that $F_{ST} = 0$ for all SNPs, however it does not distinguish between drift and selection as mechanisms driving $F_{ST} > 0$.

To evaluate the potential function relevance of outlier SNPs, we selected the top 50 outlier SNPs from each method. We created a list of all unique contigs where these SNPs occurred for each comparison. To test for overrepresentation of shared biological functions within these lists, we used Blast2GO (v.5.2.5)(Götz et al., 2008). First, we annotated the reference set of combined genes and flanking regions using NCBI blastx and EMBL-EBI InterPro (Mitchell et al., 2014). We then used Blast2GO to run a Fisher's exact test for enrichment of specific biological processes, molecular functions, or cellular components in the set of candidate genes compared to the background set of all annotated genes (N = 14,930). We used an FDR filter at a significance level of 0.01.

Results

Our study presents the first genome-scale sequence dataset for the critically endangered *A. varius* and *A zeteki* of Panamá. Our transcriptome-based capture array resulted in 34.8 million

SNPs from 14,985 exons and flanking regions. Using our assay, we successfully sequenced genomic DNA from samples of varying DNA quality and/or quantity including minimally invasive buccal swabs, miniscule toe clips stored at room temperature for nearly two decades, and frozen museum tissues. Input DNA ranged from 25ng to 1577ng (mean = 673ng). Average coverage across filtered SNPs ranged from 5x to 31x (mean=13x) for our samples. Thus, we have high confidence in our SNP dataset and the inferences reported here.

In addition to millions of SNPs, our sequence dataset includes a robust sample of *A. varius/zeteki* across time points (before and after *Bd* introduction) throughout their range in Panama (2012-2016). We collected all contemporary samples from *A. varius* populations; we did not encounter *A. zeteki* during our contemporary surveys. While we collected contemporary samples from five distinct localities, a high percentage (77%, 30/39) of these came from a single locality – El Copé West. Furthermore, of the contemporary samples over half were juveniles (62%, 24/39), most of which were encountered at El Copé West in 2014. The prevalence of *Bd* in contemporary *A. varius* samples (25.6%, 10/39) matches the prevalence previously reported from the larger amphibian community in Panama (Voyles et al., 2018). Mean *Bd* infection intensity across contemporary samples was highly variable, ranging from 0.06 - 98,556 *Bd* DNA copies per swab. Only one individual (an adult encountered in Santa Fe in 2016) had an infection intensity higher than previously reported lethal pathogen loads for *A. zeteki* (DiRenzo et al., 2014). In summary, this dataset is a unique and thorough sampling of these two critically endangered species before and after a devastating disease outbreak.

Population genetic structure

The genetic structure of *A. varius* and *A. zeteki* in Panamá indicates a pattern of isolation by distance (IBD) (S1 Fig). We found a significant linear relationship between geographic and genetic distance (Mantel r = 0.599 p = 0.0001, S1 Fig A). Furthermore, the Mantel corellogram shows decreasing genetic relatedness over larger distances and reveals the tightest correlation between geographic and genetic distance between pairs within 20km of each other (S1 Fig B). The PCA of genetic variation clearly separates individual populations into their respective sampling localities (Fig 1 A,B). Based on the PCA and original sampling locality, we grouped *Atelopus* into eight distinct genetic groups. Of these eight groups, six were historically described as *A. varius* populations and two were described as *A. zeteki*. We found that average pairwise weighted F_{ST} between the two populations of *A. zeteki* was greater than the F_{ST} between some populations of *A. varius* and *A. zeteki* (Fig 1A). Furthermore, our NGSadmix plot showing K = 2 (best K as determined using the ΔK method (Evanno, Regnaut, & Goudet, 2005)) indicates that each genetic cluster is not restricted to either of the two species (Fig 1C). Rather, there is a gradual change in admixture proportions as you go from East to West, with *A. zeteki* representing one genotype and the Santa Fe population of *A. varius* representing the other extreme. All other *A. varius/zeteki* samples show admixture from both groups (Fig 2C).

To account for the effect of IBD in our cluster analysis, we ran conStruct, which explicitly models genetic covariance across space while calculating admixture proportions (Bradburd, Coop, & Ralph, 2018). This method considers different "layers" from which an individual can draw admixture from. First, by looking at the relative contributions of additional

layers, we found that layers beyond K = 2 contributed little admixture to each sample (S2 Fig B). Furthermore, we found that the spatial model had higher predictive power across all values of K from 1 to 5 (S2 Fig A). These findings indicate that IBD is strong in the dataset and that K = 2 best explains our data. By comparing the spatial and non-spatial structure plots (S2 Fig C), we see that at K = 2 admixture patterns between spatial and non-spatial models are similar. Furthermore, at higher values of K for both spatial and non-spatial models, there are rarely instances of clear population level separation or structuring in this dataset.

Genetic diversity and Ne

Genetic diversity and heterozygosity are variable within each historic population. The least genetically diverse population is *A. zeteki* from El Valle South. This population had the highest average relatedness (Fig 3A) and lowest heterozygosity (Fig 3B). The next highest average relatedness is in the Santa Fe population of *A. varius* (Fig 3). These two populations represent the extremes of the sampled range for this study (Fig 2A). In general, there is a pattern of decreasing heterozygosity as you move from West to East for these species (Fig 2B), revealing that heterozygosity was quite low for the putatively extinct in the wild *A. zeteki*.

We found a marked decrease in genetic diversity in the group of all contemporary *A. varius* compared to historic *A. varius* (Table 1). There was a 27% decrease in θ_W, and a 5% decrease in π over this time period. This pattern holds true when considering the individual cases of El Copé West ($\Delta\theta_W$ = -12%, $\Delta\pi$ = -11%), Caribbean ($\Delta\theta_W$ = -13%, $\Delta\pi$ = -6%) and Santa Fe ($\Delta\theta_W$ = -18%, $\Delta\pi$ = -3%). Genetic diversity is also lower in the captive populations of *A. zeteki/varius* as compared to their original source populations (Table 1). The small difference in heterozygosity between all contemporary and historic *A. varius* was not significant (Mann-Whitney U-test p = 0.58). However, there was a significant decrease in heterozygosity in El Copé West in contemporary vs. historic samples (ΔHe = -16%, Mann-Whitney U-test p < 0.0001, Fig 3B).

Effective population size is low for all contemporary populations. Considering all *A. varius*, Ne decreased by 48% from the historic to the contemporary time period based on the LD analysis (Ne historic = 69, Ne contemporary = 36). The sibship analysis estimated a more severe decrease of 66%. Historically, El Copé East had the highest Ne of 1,650. All other historic populations had very low Ne, especially the inbred populations of *A. zeteki* in El Valle South (Ne = 13) and *A. varius* from Santa Fe (Ne = 15).

Local patterns of genetic diversity and structure

Our data reveals that the single locality with the most contemporary samples, El Copé West, has a unique genetic relationship between the historic and contemporary individuals (Fig 3). All contemporary samples sequenced from other localities are genetically indistinguishable from the historic population sampled at that locality (Fig 3A). In contrast, at El Copé West, contemporary individuals are much more genetically variable than their historic counterparts (Fig 3A). Based on the NGSadmix and CLUMPAK analysis, we found that the most likely K = 3 for this population. From the admixture analysis, we see that the contemporary samples include three distinct genetic clusters, two of which are minimally represented in the historic sample set

(Fig 3B). Contemporary individuals from El Copé West also show more admixture than those from the historic group. Seven samples from the contemporary group show at least 25% admixture from two different genetic groups, while none of the historic samples do. Additionally, within the contemporary samples from El Copé West, we found evidence of successful breeding and maturation to ~6 months for at least two separate clutches (based on relatedness analysis). However, none of the 19 juveniles found in 2014 were encountered again in subsequent surveys. Overall, the contemporary samples from El Copé West revealed a unique genetic relationship to historic samples from the same locality, a pattern which was not found at other localities with contemporary individuals.

Tests for survival-associated genes

With the goal of generating a list of potential candidate genes for future studies, we leveraged our paired time series data to look for SNPs associated with persisting individuals in this system. By combining candidate SNPs from genes discovered via association test, F_{ST} outlier test, and F_{ST} sliding window analysis, we created a list of 61 unique genes for the comparison of all historic and contemporary *A. varius* (Table 2) and 76 unique genes for the comparison of historic and contemporary individuals from El Copé West (Table 3). Here, unique genes are defined as the contig containing the outlier SNP or SNPs from our assembled reference its associated annotation. Allele frequency changes between contemporary and historic populations for the list of 61 genes in the *A. varius* comparison ranged from 17 - 45%. For the 76 outlier genes in the El Copé West comparison allele frequency changes ranged from 38 - 58%. While this list was created from highly associated SNPs, none are statistically significant after correcting for multiple tests – see qqPlots showing results from association tests (Fig 4A) and plots of per-site F_{ST} vs permutation-generated null F_{ST} distributions (S3 Fig). We compared these lists to find overlap between the El Copé West and *A. varius* comparisons (Fig 4B) and found 5 genes included in both lists. We found no enrichment for specific biological processes, molecular functions, or cellular components in the set of combined genes or any of the separate candidate gene lists after using a Fisher's Exact Test with FDR correction for multiple tests (α=0.05). We manually identified potential candidate genes in each list that may be related to *Bd*-specific biological processes. We present these in Table 2,3 and discuss their functions further below.

Although we did not find strong evidence for selection on particular genetic pathways, our data provide important candidate loci for continued study. Beginning with the local comparison in El Copé West (Table 3), we identified several associated SNPs in immune-related genes – one SNP in a Toll like receptor 4 (TLR4) gene and another in a gene for a properdin factor in the complement system. Two genes with the strongest signal of association in this comparison were laminin subunit alpha-5 (7 associated SNPs) and fumarylacetoacetate hydrolase domain-containing protein 2 (FAHD2, 4 associated SNPs). In the larger *A. varius* comparison (that included all contemporary and historic *A. varius* populations), we found several highly associated genes of interest (Table 2). First, we found another associated SNP in a Toll like receptor gene (TLR1). Additionally, one gene that had a very strong signal of association (5 highly-associated SNPs and 19 outlier F_{ST} sliding windows for a total of 28,000 bp) was a lysosomal-trafficking regulator gene (LYST). We also document a highly-associated SNP in an

interferon-induced 35 kDa protein. Finally, two SNPS in a T-lymphoma invasion and metastasis-inducing protein 1 gene were also present in our list of associated SNPs for the *A. varius* comparison. Five genes were outliers in both the local El Copé West analysis and the larger comparison of all *A. varius* (Fig 4): transmembrane protein 131 (TMEM131), bis(5'-adenosyl)-triphosphatase (ENPP4), transcription cofactor vestigial-like protein 4 (VGLL4), zinc finger protein 518B (ZNF518B), and lysine-specific histone demethylase 1B (KDM1B). Below we discuss these genes in more detail and relate our findings to previous studies on molecular mechanisms of *Bd* resistance in amphibians.

Discussion

By comparing historic and contemporary genome-wide variation in two endangered *Atelopus* species, we document sharp and dramatic decreases in genetic diversity and effective population size following *Bd*-related declines. Moreover, we identify demographic and adaptive processes that may contribute to persistence. Overall, our genetic data can serve to inform conservation decisions for natural and captive populations of these flagship species, investigate genetic mechanisms of persistence after rapid population declines, and identify specific genes associated with *Atelopus* persistence that can spur future research and conservation efforts.

Identifying relevant conservation units

Atelopus varius and *A. zeteki* have traditionally been separated into two species and managed as five distinct evolutionarily significant units (ESUs) (Richards & Knowles, 2007; Zippel et al., 2007). These ESUs also inform how these species are managed in captivity – frogs are only bred within their designated ESU (Estrada et al., 2014). However, the genetic analysis used to support the ESU designations was limited to two mitochondrial markers, which alone were not sufficient to delineate the ESUs. The ESUs were delineated based on both genetic and phenotypic data (Richards & Knowles, 2007), although phenotypes for these species are highly variable across short geographic distances (J. M. Savage, 1972). Therefore, our genome-wide dataset can serve to clarify the relationships among populations of these species. Many of the historic samples sequenced in the Richards and Knowles 2007 study (Richards & Knowles, 2007) were re-sequenced for this study, giving us high power to test the original ESU hypothesis.

Our data do not support the delineation of *A. varius* and *A. zeteki* into five distinct ESUs and calls into question the original species boundary. We show that distance between source populations is highly correlated with genetic distance. Rather than distinct genetic breaks between populations, these species show a continuous increase in genetic distance with increasing geographic distance (S1 Fig). To account for IBD in our genetic cluster analysis, we ran the program conStruct, which explicitly accounts for the decay in relatedness between samples due to distance (Bradburd et al., 2018). Our conStruct results show that for both spatial and non-spatial models from K = 2 to K = 5 there are few instances of clearly defined genetic layers that are exclusive to a certain population or group of populations (S2 Fig). Most historic ESUs correspond to specific populations identified in our PCA analysis (ESUs 1,2,3,5). However, other ESUs group genetically distinct populations together (ESU 4). In our study, we see that individuals on the extremes of the range (i.e. *A. zeteki* from El Valle and *A. varius* form

Santa Fe) are genetically distinct from one another, but all other populations show a pattern of isolation by distance. Drawing species boundaries in the case of continuous genetic differentiation is a common and long-standing challenge in conservation (Moritz, 1994) and further work that puts the variation in Panamanian harlequin frogs in a broader geographic and taxonomic context is needed.

For now, our data indicate that *A. varius* and *A. zeteki* from Central Panamá may be best managed according to their source population, as most individuals from a single locality cluster closely with other individuals captured at that locality (Fig 2A). Genetic clustering based on geography, and management as such, aligns with the natural history of these species – *A. varius* are considered territorial and exhibit high site fidelity (Crump, 1986, 1988). However, limitations in the genetic diversity of captive populations may mean that animals need to be bred across populations. Given the high levels of admixture between most nearby populations in the wild, we suggest that geographic proximity be considered a good proxy for relatedness in this species. Breeding across populations that are geographically and genetically proximate, even if they are currently considered different species, may be necessary. For example, we found that the two populations of *A. zeteki* (El Valle North and El Valle South) are more diverged from each other than the El Valle North population is from El Copé East *A. varius* or *A. varius* from the Caribbean. Furthermore, the current captive population of *A. zeteki* in Panamá was collected from El Valle North and there are only four founders currently alive or represented in this collection (Panama Amphibian Rescue and Conservation Project, 2019). Therefore, integrating new understandings of the genetic relationships between populations of these species will be critical for captive management going forward.

Furthermore, our findings from the distance-based phylogenetic analyses and PCA that include Costa Rican samples support our conclusions that geographic distance is the best predictor of *Atelopus* genetic relatedness and indicate some taxonomic confusion for the *Atelopus* of western Panamá and Costa Rica. We found that geographic distance was a better predictor of genetic distance, not only for our focal species, but also for the four Costa Rican samples. For example, one *A. varius* collected in 1976 from western Costa Rica (MVZ149729) is less diverged from an *A. senex* sample collected in the same year approximately 80 km away (MVZ149734) than from another *A. varius* collected in 1990 (MVZ223280) that was ~250km away in Eastern Costa Rica. Meanwhile, our fourth Costa Rican sample, which was *A. chiriquiensis* also collected in 1990 in Eastern Costa Rica (MVZ223270), lies between the two *A. varius* outgroup samples in the phylogeny (S4 Fig). These findings are recapitulated in a PCA that includes the Costa Rican samples (S5 Fig). This supports our finding that proximity is a good predictor of genetic divergence in *Atelopus* and indicates that a broader molecular reanalysis of *Atelopus* from Central America is needed.

Preliminary evidence of genetic rescue

"Rescue", or the reversal in population trajectory for species on the brink of extinction, can be driven by several different underlying processes. Demographic rescue – or simply the increase in number of individuals – may boost population sizes but could leave a species vulnerable to persistent threats (Hufbauer et al., 2015). Genetic rescue, on the other hand,

involves an increase in genetic diversity in a population and could potentially facilitate evolutionary rescue if increased adaptive variation is introduced (Whiteley, Fitzpatrick, Funk, & Tallmon, 2015). Here, we see evidence of demographic rescue and preliminary signs of genetic rescue in one population. Additional research will be needed to assess whether these processes lead to evolutionary rescue.

Our strongest evidence for demographic and/or genetic rescue comes from El Copé West – the single population where we found 77% of our contemporary individuals. This contemporary population harbors individuals from three distinct genetic groups (Fig 4B) and genotypes in this population are much more variable than any other population of *A. varius* (Fig 4A). Some of the contemporary individuals have unique genotypes that are minimally represented in the historic sample group, indicating they may be recent migrants and could be contributing to demographic rescue. Furthermore, we see more individuals with high levels of admixture between different genetic groups in the contemporary samples (Fig 4B). However, contemporary individuals in this population do not show an increase in overall heterozygosity, possibly due to low heterozygosity in mated pairs and high overall relatedness in this group. We recognize that this finding represents a narrow spatial and temporal snapshot of population genetic dynamics in this system. However, El Copé West was the source of 77% of contemporary samples for this study, suggesting that it is a critical example to consider. More work is needed to continue sampling in this area to determine if admixed individuals truly have higher fitness in this environment. By comparing population outcomes from El Copé West to other surviving populations with non-admixed persisting populations, we can learn more about the potential for genetic rescue to spur recovery in this species.

Given preliminary evidence of genetic rescue in El Copé West, and our finding that strict boundaries separating nearby genetic groups are generally lacking in this system, we argue that assisted gene flow may be an important management strategy. Conservation interventions to increase genetic diversity such as breeding between populations may be especially important. A recent reintroduction attempt of ~500 *A. varius* individuals reared at PARC and released to the wild yielded no survivors (25). A growing number of studies indicate that genetic diversity is important for *Bd* resistance. One study found that heterozygosity at major histocompatibility complex (MHC) genes was significantly associated with survival in Lowland Leopard Frogs (*Rana yavapaiensis*) experimentally infected with *Bd* (A. E. Savage & Zamudio, 2011). Another recent study of Australian alpine tree frogs (*Litoria verreauxii alpina*) found that individuals with greater genome-wide heterozygosity had a reduced probability of *Bd* infection in the wild (Banks et al., 2019). Future reintroductions for *A. varius* and *A. zeteki* must consider new approaches, such as induced genetic rescue, to address persistent threats and maladapted captive colonies. Otherwise, we risk maintaining captive *A. varius* and *A. zeteki* populations without a clear path forward for successful reintroduction and reestablishment.

Candidate genes for future study

The role of the immune system in the host-*Bd* relationship varies widely among amphibian species. For example, transcriptomic studies have found that some susceptible species show robust, potentially over-reactive immune responses (Ellison, Savage, et al., 2014), while

others have suppressed or undetectable immune responses (Ellison, Tunstall, Direnzo, Hughey, & Eria, 2014; Rosenblum, Poorten, Settles, & Murdoch, 2012). Other studies have shown that *Bd* inhibits lymphocytes, indicating that it actively suppresses host acquired immunity (Fites et al., 2013). In our study we found several immune-related genes associated with contemporary survivors. First, we document associated SNPs in two toll-like receptor genes (TLR1, TLR4). TLR genes are known to recognize fungal pathogens and are essential to the innate immune response (Brightbill et al., 1999; Kaisho & Akira, 2003). Other studies have linked TLR genes to recognizing and responding to *Bd* (Ellison, Savage, et al., 2014; Kosch et al., 2019; O'Hanlon et al., 2018; Richmond, Savage, Zamudio, & Rosenblum, 2009; D. C. Woodhams et al., 2007). Another related gene in our candidate list was a lysosomal-trafficking regulator gene (LYST) which showed a strong signal of association (5 SNPs, 28kbp F_{ST} sliding window). These genes traffic molecules across cell membranes and are regulators of TLR gene functions (Westphal et al., 2016). In humans, mutations in LYST genes lead to a severe immunodeficiency and can lead to persistent skin infections (Westphal et al., 2016), making this target an intriguing candidate for future studies.

Furthermore, we found a highly associated SNP in a properdin gene related to the complement system. The vertebrate complement system is important in responding to fungal pathogens (Kozel, 1996) and properdin is a positive regulator of the alternative pathway in the complement system (Pillemer et al., 1954). Activating the complement system via properdin may be important for avoiding immunosuppression strategies employed by *Bd* (Ellison, Savage, et al., 2014). Other immune-related genes identified in our study were an interferon-induced 35 kDa protein and interferon-induced transmembrane protein 3. Rosenblum et al. 2008 (Rosenblum et al., 2008) showed a shared up-regulation of interferon related genes in response to *Bd* infection in a *Rana* and distantly-related *Silurana* species. Additionally, Ellison et al. (2014) (Ellison, Savage, et al., 2014) showed an increase in interferon related gene expression in *A. zeteki* infected with *Bd*. Interferons boost immune system processes and therefore may be involved in *Bd* response in these *A. varius* populations. Finally, two SNPS in a T-lymphoma invasion and metastasis-inducing protein gene identified in this analysis was also downregulated in the spleen of *A. zeteki* during *Bd* infection (Ellison, Savage, et al., 2014).

Two intriguing immune-related genes were shared across both the local (only El Copé West) and global (all *A. varius*) comparisons. First, transmembrane protein 131 (TMEM131) is an important regulator of thymocyte proliferation, which are cells responsible for the production of T lymphocytes (Maharzi et al., 2013). Another study of a persistent frog species (*Litoria dayi*) also identified a transmembrane protein gene as under strong selection from *Bd* (McKnight et al., 2020). Second, bis(5'-adenosyl)-triphosphatase (ENPP4) is a gene known for its role in facilitating immune response and is involved in "hydrolase activity" (GO:0016787). This GO term was over-expressed in *A. zeteki* that survived *Bd* infection in a previous study (Ellison, Savage, et al., 2014). Other studies have shown ENPP4 was up-regulated in snails exposed to bacterial molecular patterns (Zhang, Loker, & Sullivan, 2016), and in newts during lens regeneration (Sousounis et al., 2014).

Beyond the immune system, other studies have found that genes associated with maintaining skin integrity and countering *Bd* pathogenesis may also be key to surviving *Bd.* Skin integrity is key because *Bd* pathogenesis leading to host death is linked to disruption of skin functions (Voyles et al., 2009). Here we found that two laminin genes (laminin subunit alpha-5 and laminin subunit beta-1) were associated with *Bd* survival. Laminin is a major component of epithelial basement membranes (Spenlé, Simon-Assmann, Orend, & Miner, 2013) and could be important for maintaining skin integrity during *Bd* invasion. Finally, FAHD2, the gene with the most highly associated SNP in this global *A. varius* comparison, is linked to "hydrolase activity" (GO:0016787) as discussed above.

The presence of previously studied, immunologically relevant genes in our candidate list supports previous work showing that immune system processes are important for *Bd* tolerance or resistance in these species (Ellison, Savage, et al., 2014). We propose that toll-like receptor genes, and others that interact with this immune pathway such as LYST, may be key players in mounting an effective immune response to *Bd*. Furthermore, we find more evidence that genes linked to hydrolase activity could be important for *Atelopus* exposed to *Bd*. More work is needed to further understand the relationship of these candidate genes with long-term fitness outcomes, including more longitudinal genomic studies of other persisting *Atelopus* species.

Conclusions

Some natural, relic populations persist despite catastrophic declines and ongoing threats. Studying natural populations of threatened species can provide a window into population processes that may also be important for successful conservation. Here, we shed light on the population genetic structure of *A. varius* and *A. zeteki* in Panamá following dramatic declines from disease. Our data reveals that the species boundary separating *A. varius* and *A. zeteki* is not well-supported. We show that geography and distance predict genetic structure of *A. varius* and *A. zeteki* populations, indicating that populations should be managed according to their proximity with other populations, using our characterization of genetic distinctiveness as a guide. We report an intriguing and unique signature of genotypic diversity and recent admixture in one population, indicating genetic rescue may be viable option for conservation interventions in this system. Finally, recognizing the limited sample size of our contemporary dataset, we generated a list of candidate genes that may be associated with *Bd* survival to be considered in future studies. This study offers a new molecular toolkit for studying *Atelopus*, a clade that has suffered massive declines throughout the neotropics, and a model for disentangling the processes that could contribute to species returning from the brink of extinction.

Acknowledgements

This work is coauthored by C. Richards-Zawacki, J. Voyles, K. Bi, R. Ibañez, and E.B. Rosenblum. We thank H. Ross, E. Griffith, K. Zippel, L. Zippel, R. Perez, A. Estrada, J. Morgan, K. Terrell, G. Rios-Sotelo, G. Rosa, K. Charles, A. Levorse, and the Cruz family for help in the field. We thank K. Lundy, S. McDevitt, and L. Smith for help in the lab and T. Linderoth and G. Bradburd for help with data analysis. Funding for this project was provided by Disney Worldwide Conservation Fund and the National Science Foundation (grants IOS-1660311 to CLRZ, DEB-1457694 to EBR, CLRZ and JV, GRFP to AQB).

Data Accessibility

Sequence data used in this study is available via NCBI SRA (Bioproject PRJNA634906).

References

Altschul, S. F., Madden, T. L., Schäffer, A. A., Zhang, J., Zhang, Z., Miller, W., & Lipman, D. J. (1997). Gapped BLAST and PSI-BLAST: a new generation of protein database search programs. *Nucleic Acids Research*, *25*(17), 3389–3402.

Bankevich, A., Nurk, S., Antipov, D., Gurevich, A. A., Dvorkin, M., Kulikov, A. S., … Prjibelski, A. D. (2012). SPAdes: a new genome assembly algorithm and its applications to single-cell sequencing. *Journal of Computational Biology*, *19*(5), 455–477.

Banks, S. C., Scheele, B. C., Macris, A., Hunter, D., Jack, C., & Fraser, C. I. (2019). Chytrid fungus infection in alpine tree frogs is associated with individual heterozygosity and population isolation but not population-genetic diversity. *Frontiers of Biogeography*, *12.1*, e43875.

Barrio-Amorós, C. L., Costales, M., Vieira, J., Osterman, E., Kaiser, H., & Arteaga, A. (2020). Back from extinction: rediscovery of the harlequin toad *Atelopus mindoensis* Peters, 1973 in Ecuador. *Herpetology Notes*, *13*, 325–328.

Becker, M. H., Walke, J. B., Cikanek, S., Savage, A. E., Mattheus, N., Santiago, C. N., … Becker, M. H. (2015). Composition of symbiotic bacteria predicts survival in Panamanian golden frogs infected with a lethal fungus. *Proceedings of the Royal Society B: Biological Sciences, 282*(1805), 20142881.

Bi, K., Vanderpool, D., Singhal, S., Linderoth, T., Moritz, C., & Good, J. M. (2012). Transcriptome-based exon capture enables highly cost-effective comparative genomic data collection at moderate evolutionary scales. *BMC Genomics*, *13*(1), 403.

Bolger, A. M., Lohse, M., & Usadel, B. (2014). Trimmomatic: a flexible trimmer for Illumina sequence data. *Bioinformatics*, *30*(15), 2114–2120.

Boyle, D. G., Boyle, D. B., Olsen, V., Morgan, J. A. T., & Hyatt, A. D. (2004). Rapid quantitative detection of chytridiomycosis (*Batrachochytrium dendrobatidis*) in amphibian samples using real-time Taqman PCR assay, *Diseases of Aquatic Organisms, 60*(2), 141–148.

Bradburd, G. S., Coop, G. M., & Ralph, P. L. (2018). Inferring Continuous and Discrete Population Genetic Structure Across Space. *Genetics*, *210*(1), 33 LP-52.

Brightbill, H. D., Libraty, D. H., Krutzik, S. R., Yang, R.-B., Belisle, J. T., Bleharski, J. R., … Smale, S. T. (1999). Host defense mechanisms triggered by microbial lipoproteins through toll-like receptors. *Science*, *285*(5428), 732–736.

Brown, J. H., & Kodric-Brown, A. (1977). Turnover Rates in Insular Biogeography: Effect of Immigration on Extinction. *Ecology*, *58*(2), 445–449.

Bustamante, H. M., Livo, L. J., & Carey, C. (2010). Effects of temperature and hydric environment on survival of the Panamanian Golden Frog infected with a pathogenic chytrid

fungus. *Integrative Zoology*, *5*(2), 143–153.

Carlson, S. M., Cunningham, C. J., & Westley, P. A. H. (2014). Evolutionary rescue in a changing world. *Trends in Ecology and Evolution*, *29*(9), 521-530.

Crawford, A. J., Lips, K. R., & Bermingham, E. (2010). Epidemic disease decimates amphibian abundance, species diversity, and evolutionary history in the highlands of central Panama. *Proceedings of the National Academy of Sciences*, *107*(31), 13777–13782.

Crump, M. L. (1986). Homing and Site Fidelity in a Neotropical Frog, *Atelopus varius* (Bufonidae). *Copeia*, *1986*(2), 438–444.

Crump, M. L. (1988). Aggression in harlequin frogs: male-male competition and a possible conflict of interest between the sexes. *Animal Behaviour*, *36*(4), 1064–1077.

DiRenzo, G. V., Langhammer, P. F., Zamudio, K. R., & Lips, K. R. (2014). Fungal infection intensity and zoospore output of *Atelopus zeteki*, a potential acute chytrid supershedder. *PLoS ONE*, *9*(3).

Do, C., Waples, R. S., Peel, D., Macbeth, G. M., Tillett, B. J., & Ovenden, J. R. (2014). NeEstimator v2: re-implementation of software for the estimation of contemporary effective population size (Ne) from genetic data. *Molecular Ecology Resources*, *14*(1), 209–214.

Ellison, A. R., Savage, A. E., DiRenzo, G. V, Langhammer, P., Lips, K. R., & Zamudio, K. R. (2014). Fighting a Losing Battle: Vigorous Immune Response Countered by Pathogen Suppression of Host Defenses in the Chytridiomycosis-Susceptible Frog *Atelopus zeteki*. *G3: Genes, Genomes, Genetics*, *4*, 1275–1289.

Ellison, A. R., Tunstall, T., Direnzo, G. V, Hughey, M. C., & Eria, A. (2014). More than skin deep : functional genomic basis for resistance to amphibian. *Genome biology and evolution*, *7*(1), 286-298.

Estrada, A., Gratwicke, B., Benedetti, A., Dellatogna, G., Garrelle, D., Griffith, E., … Miller, P. (2014). The Golden Frogs of Panama (*Atelopus zeteki, A. varius*): A Conservation Planning Workshop: Final Report, 1–102.

Evanno, G., Regnaut, S., & Goudet, J. (2005). Detecting the number of clusters of individuals using the software STRUCTURE: a simulation study. *Molecular Ecology*, *14*(8), 2611–2620.

Fites, S., Ramsey, J., Holden, W., Collier, S., Sutherland, D. M., Reinert, L. ., … Rollins-Smith, L. (2013). The invasive chytrid fungus of amphibians paralyzes lymphocyte responses. *Science*, *342*(6156), 366–369.

Frankham, R. (2005). Genetics and extinction. *Biological Conservation*, *126*(2), 131–140.

Gagliardo, R., Crump, P., Griffith, E., Mendelson, J., Ross, H., & Zippel, K. (2008). The principles of rapid response for amphibian conservation, using the programmes in Panama as an example. *International Zoo Yearbook*, *42*(1), 125–135.

Garland, S., Baker, A., Phillott, A. D., & Skerratt, L. F. (2010). BSA reduces inhibition in a TaqMan® assay for the detection of *Batrachochytrium dendrobatidis*. *Diseases of Aquatic*

Organisms, *92*(2–3), 113–116.

Gilpin, M. E., & Soule, M. E. (1986). Minimum viable populations: processes of species extinction. *Conservation Biology: The Science of Scarcity and Diversity. Sinauer Associates, Sunderland, Massachusetts*, 19–34.

Gomulkiewicz, R., & Holt, R. D. (1995). When does evolution by natural selection prevent extinction? *Evolution*, *49*(1), 201–207.

González-Maya, J. F., Escobedo-Galván, A. H., Wyatt, S. a., Schipper, J., Belant, J. L., Fischer, A., … Corrales, D. (2013). Renewing hope: the rediscovery of *Atelopus varius* in Costa Rica. *Amphibia-Reptilia*, *34*, 573–578.

González-Maya, J. F., Gómez-Hoyos, D. A., Cruz-Lizano, I., & Schipper, J. (2018). From hope to alert: demography of a remnant population of the Critically Endangered *Atelopus varius* from Costa Rica. *Studies on Neotropical Fauna and Environment*, *53*(3), 194–200.

Gonzalez, A., Ronce, O., Ferriere, R., & Hochberg, M. E. (2013). Evolutionary rescue: An emerging focus at the intersection between ecology and evolution. *Philosophical Transactions of the Royal Society B: Biological Sciences*, *368*(1610).

Goslee, S. C., & Urban, D. L. (2007). The ecodist package for dissimilarity-based analysis of ecological data. *Journal of Statistical Software*, *22*(7), 1–19.

Götz, S., García-Gómez, J. M., Terol, J., Williams, T. D., Nagaraj, S. H., Nueda, M. J., … Conesa, A. (2008). High-throughput functional annotation and data mining with the Blast2GO suite. *Nucleic Acids Research*, *36*(10), 3420–3435.

Grabherr, M. G., Haas, B. J., Yassour, M., Levin, J. Z., Thompson, D. A., Amit, I., … Regev, A. (2011). Full-length transcriptome assembly from RNA-Seq data without a reference genome. *Nature Biotechnology*, *29*(7), 644–652.

Hedrick, P. W., & Garcia-Dorado, A. (2016). Understanding Inbreeding Depression, Purging, and Genetic Rescue. *Trends in Ecology & Evolution*, *31*(12), 940–952.

Huang, X., & Madan, A. (1999). CAP3: A DNA Sequence Assembly Program. *Genome Research* , *9*(9), 868–877.

Hufbauer, R. A., Szűcs, M., Kasyon, E., Youngberg, C., Koontz, M. J., Richards, C., … Melbourne, B. A. (2015). Three types of rescue can avert extinction in a changing environment. *Proceedings of the National Academy of Sciences*, *112*(33), 10557 LP-10562.

Hyatt, A. D., Boyle, D. G., Olsen, V., Boyle, D. B., Berger, L., Obendorf, D., … Gleason, F. (2007). Diagnostic assays and sampling protocols for the detection of *Batrachochytrium dendrobatidis*. *Diseases of Aquatic Organisms*, *73*(3), 175–192.

Ingvarsson, P. K. (2001, February 1). Restoration of genetic variation lost - The genetic rescue hypothesis. *Trends in Ecology and Evolution*. *16*(2), 62-63.

Jones, O. R., & Wang, J. (2010). COLONY: a program for parentage and sibship inference from multilocus genotype data. *Molecular Ecology Resources*, *10*(3), 551–555.

Kaisho, T., & Akira, S. (2003). Regulation of dendritic cell function through Toll-like receptors.

Current Molecular Medicine, *3*(8), 759–771.

Korneliussen, T. S., Albrechtsen, A., & Nielsen, R. (2014). ANGSD: Analysis of Next Generation Sequencing Data. *BMC Bioinformatics*, *15*(1).

Korneliussen, T. S., & Moltke, I. (2015). NgsRelate: a software tool for estimating pairwise relatedness from next-generation sequencing data. *Bioinformatics*, *31*(24), 4009–4011.

Kosch, T. A., Silva, C. N. S., Brannelly, L. A., Roberts, A. A., Lau, Q., Marantelli, G., … Skerratt, L. F. (2019). Genetic potential for disease resistance in critically endangered amphibians decimated by chytridiomycosis. *Animal Conservation*, *22*(3), 238–250.

Kozel, T. R. (1996). Activation of the complement system by pathogenic fungi. *Clinical Microbiology Reviews*, *9*(1), 34 LP-46.

La Marca, E., Lips, K. R., Lötters, S., Puschendorf, R., Ibáñez, R., Rueda-Almonacid, J. V., … Young, B. E. (2005). Catastrophic population declines and extinctions in neotropical harlequin frogs (*Bufonidae: Atelopus*). *Biotropica: The Journal of Biology and Conservation, 37*(2), 190-201.

Lefort, V., Desper, R., & Gascuel, O. (2015). FastME 2.0: A Comprehensive, Accurate, and Fast Distance-Based Phylogeny Inference Program. *Molecular Biology and Evolution*, *32*(10), 2798–2800.

Lewis, C. H. R., Richards-Zawacki, C. L., Ibáñez, R., Luedtke, J., Voyles, J., Houser, P., & Gratwicke, B. (2019). Conserving Panamanian harlequin frogs by integrating captive-breeding and research programs. *Biological Conservation*, *236*, 180–187.

Li, W., & Godzik, A. (2006). Cd-hit: a fast program for clustering and comparing large sets of protein or nucleotide sequences. *Bioinformatics*, *22*(13), 1658–1659.

Longcore, J. E., Pessier, A. P., & Nichols, D. K. (1999). *Batrachochytrium Dendrobatidis* gen. et sp. nov., a Chytrid Pathogenic to Amphibians. *Mycologia*, *91*(2), 219–227.

Magoč, T., & Salzberg, S. L. (2011). FLASH: fast length adjustment of short reads to improve genome assemblies. *Bioinformatics*, *27*(21), 2957–2963.

Maharzi, N., Parietti, V., Nelson, E., Denti, S., Robledo-Sarmiento, M., Setterblad, N., … Canque, B. (2013). Identification of TMEM131L as a Novel Regulator of Thymocyte Proliferation in Humans. *The Journal of Immunology*, *190*(12), 6187 LP-6197.

Martin, M. (2011). Cutadapt removes adapter sequences from high-throughput sequencing reads. *EMBnet. journal, 17*(1), 10-12.

McKnight, D. T., Carr, L. J., Bower, D. S., Schwarzkopf, L., Alford, R. A., & Zenger, K. R. (2020). Infection dynamics, dispersal, and adaptation: understanding the lack of recovery in a remnant frog population following a disease outbreak. *Heredity*, 1-14.

Meisner, J., & Albrechtsen, A. (2018). Inferring Population Structure and Admixture Proportions in Low-Depth NGS Data. *Genetics*, *210*(2), 719 LP-731.

Mitchell, A., Chang, H.-Y., Daugherty, L., Fraser, M., Hunter, S., Lopez, R., … Finn, R. D. (2014). The InterPro protein families database: the classification resource after 15 years.

Nucleic Acids Research, *43*(D1), D213–D221.

Moritz, C. (1994). Defining "evolutionarily significant units" for conservation. *Trends in Ecology & Evolution*, *9*(10), 373–375.

O'Hanlon, S. J., Rieux, A., Farrer, R. A., Rosa, G. M., Waldman, B., Bataille, A., … Fisher, M. C. (2018). Recent Asian origin of chytrid fungi causing global amphibian declines. *Science*, *360*(6389), 621 LP-627.

Panama Amphibian Rescue and Conservation Project. (2018). *2018 Annual Report*. Retrieved from https://parcplace.org/wp-content/uploads/2019/01/PARC-2018-FINAL.pdf

Panama Amphibian Rescue and Conservation Project. (2019). *2019 Annual Report*. Retrieved from https://parcplace.org/wp-content/uploads/2020/02/2019-Anual-Report.pdf

Perez, R., Richards-zawacki, C. L., Krohn, A. R., Robak, M., Griffith, E. J., Ross, H., … Voyles, J. (2014). Short Communication Field surveys in Western Panama indicate populations of Atelopus varius frogs are persisting in regions where *Batrachochytrium dendrobatidis* is now enzootic, *Amphibian & Reptile Conservation*, *8*(2), 30–35.

Pillemer, L., Blum, L., Lepow, I. H., Ross, O. A., Todd, E. W., & Wardlaw, A. C. (1954). The Properdin System and Immunity: I. Demonstration and Isolation of a New Serum Protein, Properdin, and Its Role in Immune Phenomena. *Science*, *120*(3112), 279–285.

Poole, V. (2008). Project golden frog. *Endangered Species Update*, *25*(1), S7–S7.

Richards, C. L., & Knowles, L. L. (2007). Tests of phenotypic and genetic concordance and their application to the conservation of Panamanian golden frogs (*Anura, Bufonidae*). *Molecular Ecology*, *16*(15), 3119–3133.

Richmond, J. Q., Savage, A. E., Zamudio, K. R., & Rosenblum, E. B. (2009). Toward Immunogenetic Studies of Amphibian Chytridiomycosis: Linking Innate and Acquired Immunity. *BioScience*, *59*(4), 311–320.

Rio, D. C., Ares, M., Hannon, G. J., & Nilsen, T. W. (2010). Purification of RNA using TRIzol (TRI reagent). *Cold Spring Harbor Protocols*, *2010*(6), pdb-prot5439.

Rodríguez-Contreras, A., Señaris, J. C., Lampo, M., & Rivero, R. (2008). Rediscovery of *Atelopus cruciger* (Anura: Bufonidae): current status in the Cordillera de La Costa, Venezuela. *Oryx*, *42*(2), 301–304.

Rosenblum, E. B., Poorten, T. J., Settles, M., & Murdoch, G. K. (2012). Only skin deep: Shared genetic response to the deadly chytrid fungus in susceptible frog species. *Molecular Ecology*, *21*(13), 3110–3120.

Rosenblum, E. B., Stajich, J. E., Maddox, N., & Eisen, M. B. (2008). Global gene expression profiles for life stages of the deadly amphibian pathogen Batrachochytrium dendrobatidis. *Proceedings of the National Academy of Sciences of the United States of America*, *105*(44), 17034–17039.

Savage, A. E., & Zamudio, K. R. (2011). MHC genotypes associate with resistance to a frog-killing fungus. *Proceedings of the National Academy of Sciences of the United States of*

America, *108*(40), 16705–16710.

Savage, J. M. (1972). The Harlequin Frogs, Genus *Atelopus*, of Costa Rica and Western Panama. *Herpetologica*, *28*(2), 77–94.

Shaffer, M. L. (1981). Minimum population sizes for species conservation. *BioScience*, *31*(2), 131–134.

Singhal, S. (2013). De novo transcriptomic analyses for non-model organisms: an evaluation of methods across a multi-species data set. *Molecular Ecology Resources*, *13*(3), 403–416.

Skotte, L., Korneliussen, T. S., & Albrechtsen, A. (2013). Estimating individual admixture proportions from next generation sequencing data. *Genetics*, *195*(3), 693–702.

Slater, G. S. C., & Birney, E. (2005). Automated generation of heuristics for biological sequence comparison. *BMC Bioinformatics*, *6*(1), 31.

Sousounis, K., Bhavsar, R., Looso, M., Krüger, M., Beebe, J., Braun, T., & Tsonis, P. A. (2014). Molecular signatures that correlate with induction of lens regeneration in newts: lessons from proteomic analysis. *Human Genomics*, *8*(1), 22.

Spenlé, C., Simon-Assmann, P., Orend, G., & Miner, J. H. (2013). Laminin α5 guides tissue patterning and organogenesis. *Cell Adhesion & Migration*, *7*(1), 90–100.

Tallmon, D. A., Luikart, G., & Waples, R. S. (2004). The alluring simplicity and complex reality of genetic rescue. *Trends in Ecology and Evolution*. *19*(9), 489-496.

Tapia, E. E., Coloma, L. A., Pazmiño-Otamendi, G., & Peñafiel, N. (2017). Rediscovery of the nearly extinct longnose harlequin frog *Atelopus longirostris* (Bufonidae) in Junín, Imbabura, Ecuador. *Neotropical Biodiversity*, *3*(1), 157–167.

Vieira, F. G., Lassalle, F., Korneliussen, T. S., & Fumagalli, M. (2016). Improving the estimation of genetic distances from Next-Generation Sequencing data. *Biological Journal of the Linnean Society*, *117*(1), 139–149.

Voyles, J., Woodhams, D. C., Saenz, V., Byrne, A. Q., Perez, R., Rios-Sotelo, G., … Richards-Zawacki, C. L. (2018). Shifts in disease dynamics in a tropical amphibian assemblage are not due to pathogen attenuation. *Science*, *359*(6383), 1517 LP-1519.

Voyles, J., Young, S., Berger, L., Campbell, C., Voyles, W. F., & Dinudom, A. (2009). Pathogenesis of Chytridiomycosis, a Cause of Catastrophic Amphibian Declines. *Science*, *326*(5952), 582–585.

Wang, J. (2009). A new method for estimating effective population sizes from a single sample of multilocus genotypes. *Molecular Ecology*, *18*(10), 2148–2164.

Weir, B. S., & Cockerham, C. C. (1984). Estimating F-statistics for the analysis of population structure. *Evolution*, *38*(6), 1358–1370.

Westphal, A., Cheng, W., Yu, J., Grassl, G., Krautkrämer, M., Holst, O., … Lee, K.-H. (2016). Lysosomal trafficking regulator Lyst links membrane trafficking to toll-like receptor–mediated inflammatory responses. *Journal of Experimental Medicine*, *214*(1), 227–244.

Whiteley, A. R., Fitzpatrick, S. W., Funk, W. C., & Tallmon, D. A. (2015). Genetic rescue to the rescue. *Trends in Ecology and Evolution*, *30*(1), 42–49.

Woodhams, D. C., Ardipradja, K., Alford, R. A., Marantelli, G., Reinert, L. K., & Rollins-Smith, L. A. (2007). Resistance to chytridiomycosis varies among amphibian species and is correlated with skin peptide defenses. *Animal Conservation*, *10*(4), 409–417.

Woodhams, D. C., Voyles, J., Lips, K. R., Carey, C., & Rollins-Smith, L. A. (2006). Predicted disease susceptibility in a Panamanian amphibian assemblage based on skin peptide defenses. *Journal of Wildlife Diseases*, *42*(2), 207–218.

Zhang, S.-M., Loker, E. S., & Sullivan, J. T. (2016). Pathogen-associated molecular patterns activate expression of genes involved in cell proliferation, immunity and detoxification in the amebocyte-producing organ of the snail Biomphalaria glabrata. *Developmental & Comparative Immunology*, *56*, 25–36.

Zippel, K. C., Ibáñez, R., Lindquist, E. D., Richards, C. L., Jaramillo, C. A., & Griffith, E. J. (2007). Implicaciones en la conservación de las ranas doradas de Panamá, asociadas con su revisión taxonómica. *Herpetologicos*. 1:29–39.

Figures

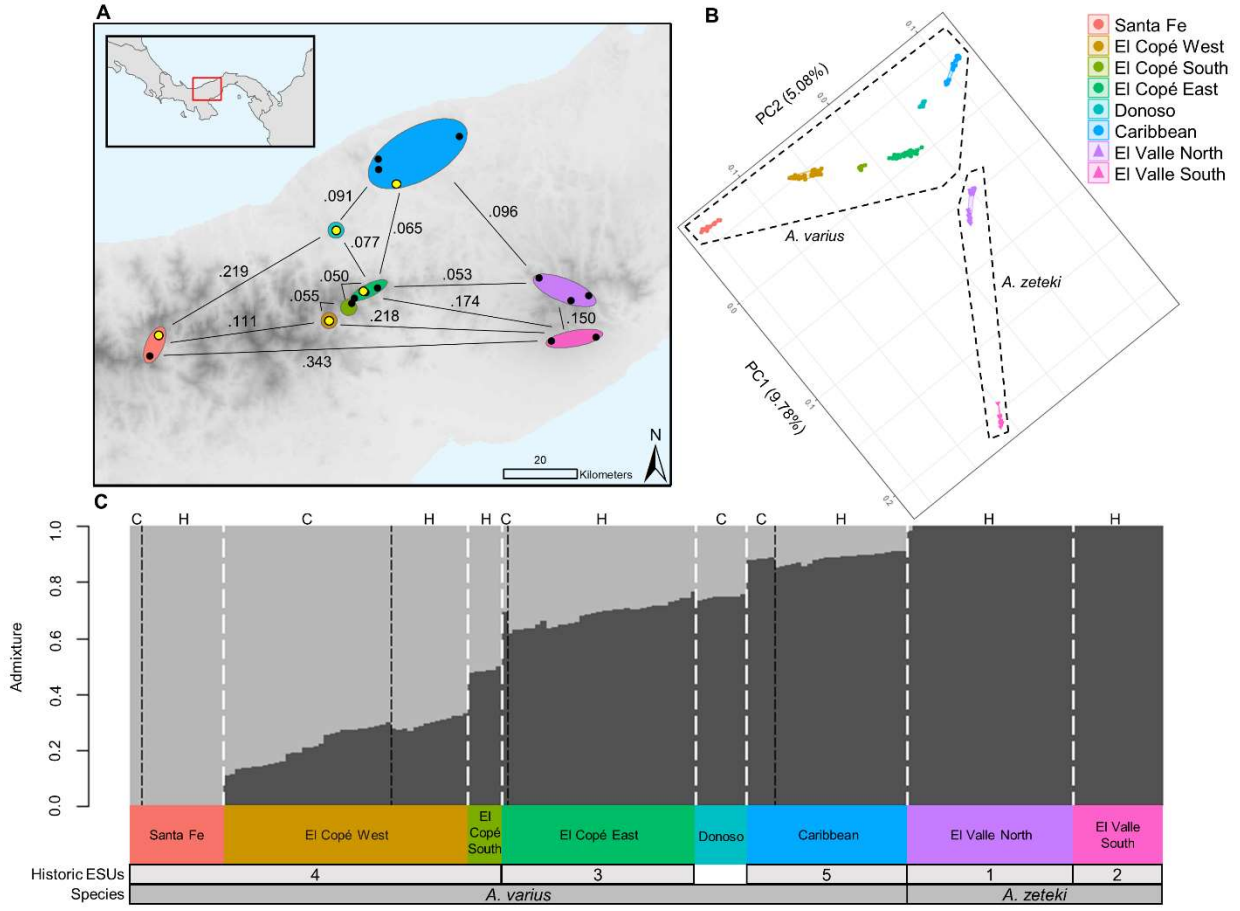

Fig 1: Geographic and genetic distribution of 186 *A. varius* and *A. zeteki* samples showing a close match between sampling locality and location on genetic PC space. (A) Map of sampling localities with pairwise weighted F_{ST} values between adjacent populations. Individual sampling locations are marked with dots and populations indicated with colored ovals. Black dots indicate no contemporary surviving *A. varius*/*zeteki* and yellow dots indicate localities where contemporary *A. varius* were captured. (B) PCA from genetic covariance matrix. Samples separated into 8 major clusters that correspond to geographic location of capture. Localities colored as in map. PCA is rotated to correspond to map of source populations. Historic species groups are labeled and marked with a dashed polygon. (C) Admixture plot for K = 2. White dashed lines separate localities and black dashed lines within localities separate contemporary (left) and historic (right) individuals. Evolutionarily Significant Units (ESUs) and species designations from Richards and Knowles 2007 are listed below sampling localities.

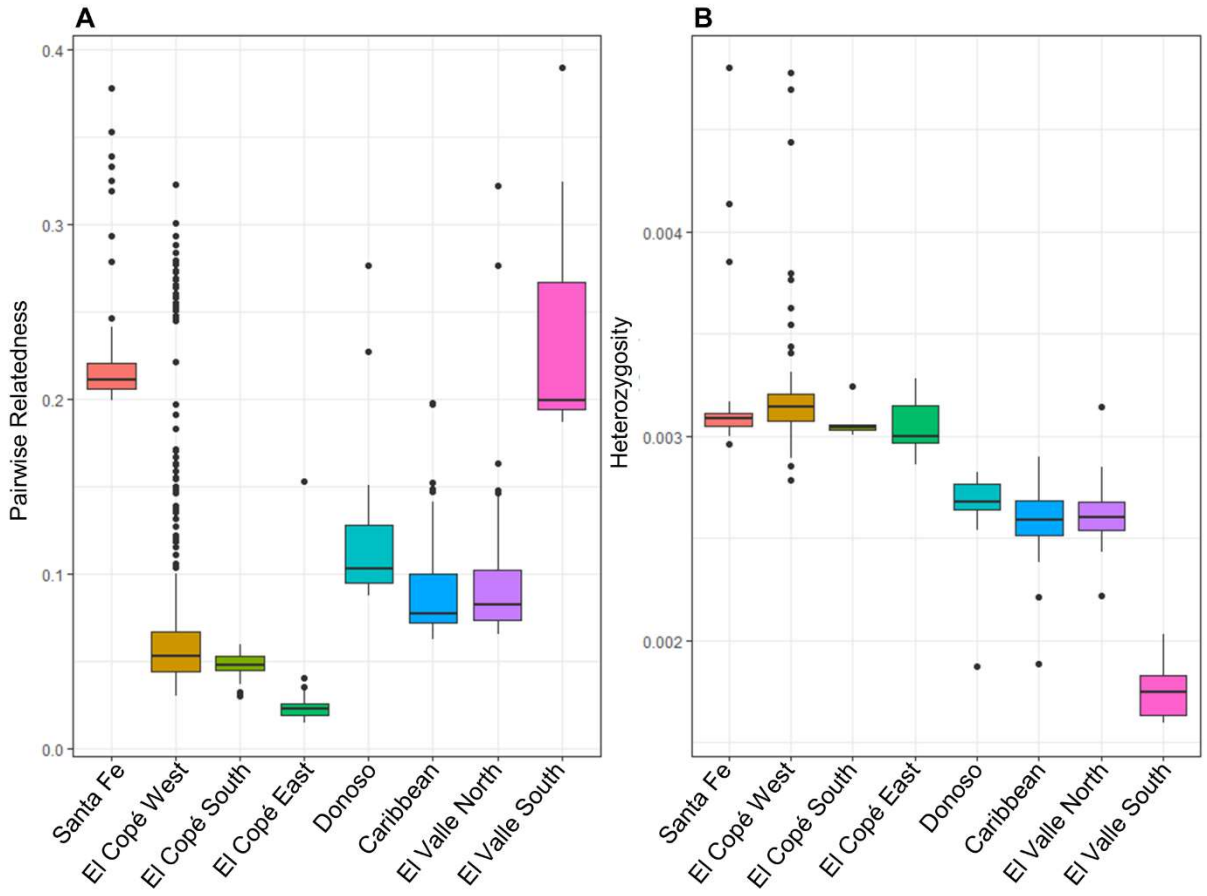

Fig 2: Boxplots showing high pairwise relatedness at the eastern and western-most localities and a decrease in heterozygosity from west to east. (A) Pairwise relatedness within each population, as measured using the coancestry coefficient (θ). θ was calculated using the formula $\theta = \frac{k1}{4} + \frac{k2}{2}$ where k1 and k2 are the maximum likelihood (ML) estimates of the relatedness coefficients. (B) Exome wide heterozygosity for individuals from each population. Populations colored as in Fig 1.

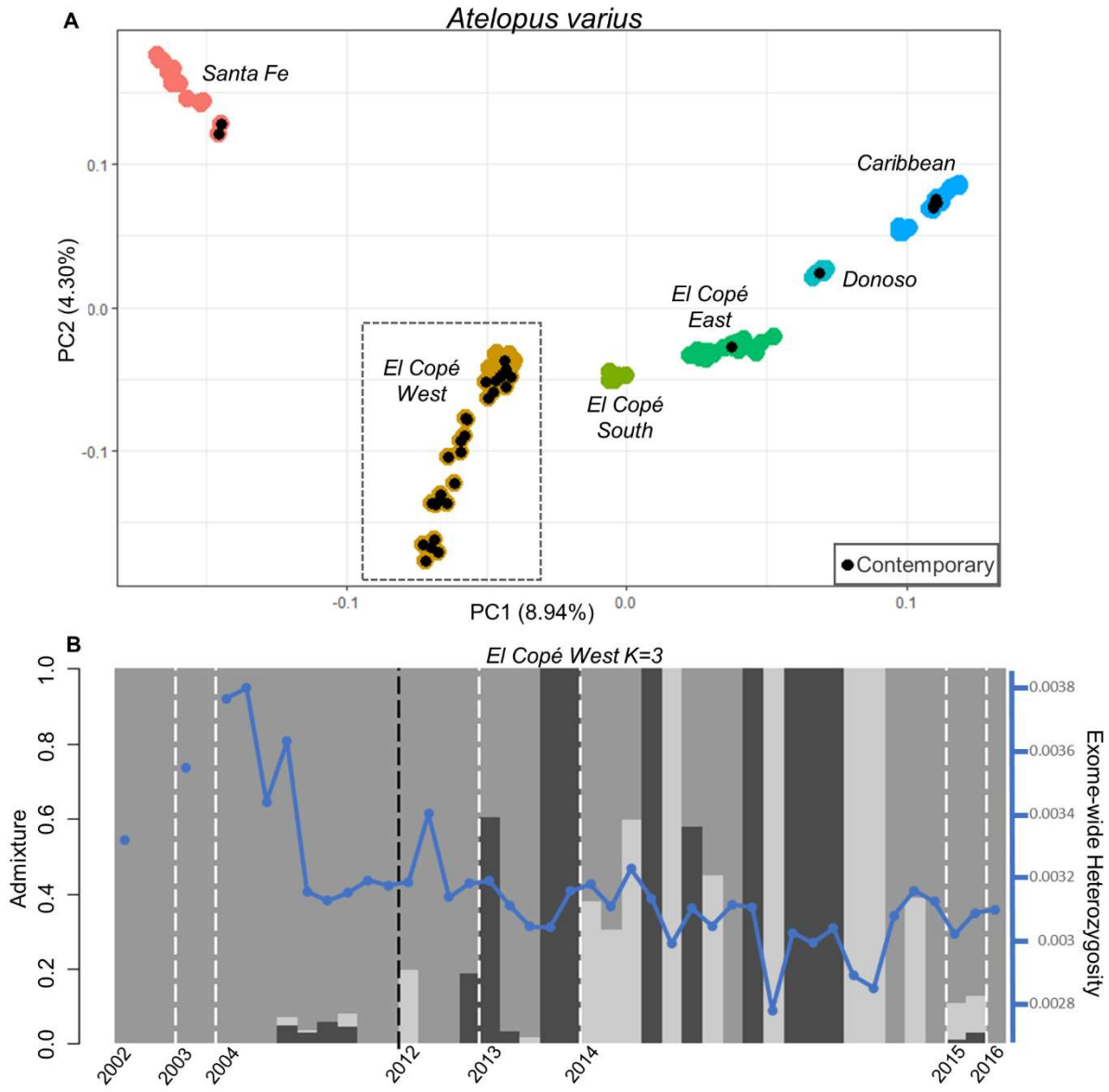

Fig 3: PCA and Admixture plots of *A. varius* samples reveal a unique genetic pattern at El Copé West. (A) PCA from genetic covariance matrix of historic (color only) and contemporary (black center) *A. varius* samples. (B) Admixture plot for all El Copé West samples showing the best K = 3. Samples are sorted based on date of collection and historic and contemporary samples are separated by a black dashed line. Exome-wide heterozygosity for each individual is shown in the blue dot plot.

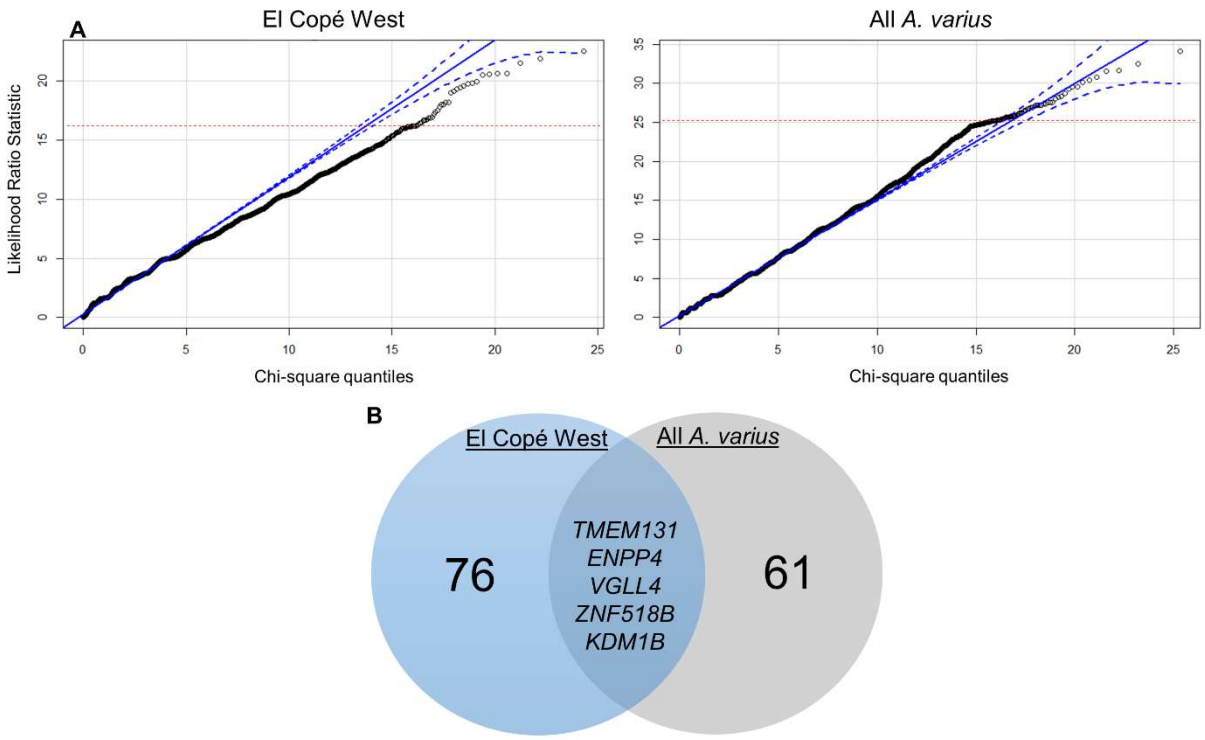

Fig 4: (A) Quantile-Quantile plots for El Copé West (left) and all *A. varius* (right). Points are the Likelihood Ratio Statistic for every SNP calculated by ANGSD -doAsso 1 and are chi-squared distributed with df=2. Blue lines represent a robust regression line with a 95% confidence interval as implemented in the qqPlot function in the car package (v.3.0.2) in R (v.3.4.3). Red dashed line indicates the value above which lie the top 50 most highly associated SNPs (El Copé West: LRT=16.00; FDR p-value=0.95, *A. varius*: LRT=25.49; FDR p-value=0.007). (B) Number of candidate genes for each comparison after combining list of top 50 genes from association test, F_{ST} outlier test, and F_{ST} sliding window test. Five shared genes found in both the global and local comparison are listed.

Tables

Table 1: Average per-site Watterson's theta (θ_W), average per-site pi (π), and average Heterozygosity for samples grouped by species and population. All are calculated using the folded site frequency spectrum. Average pairwise relatedness is calculated from relatedness coefficients. Ne are calculated in two different ways 1) using the LD method as implemented in NeEstimator (v2.1) - 95% CI are from Jackknifing across samples and 2) using a sibship analysis implemented in COLONY. * indicates significant difference between heterozygosity and average relatedness of historic and contemporary samples (Mann-Whitney U-test $p < 0.01$).

Population	θ_W	π	Ne - NeEstimator [95%CI]	Ne - COLONY [95%CI]	Avg. Heterozygosity	Avg. Relatedness	N
A. varius historic	.0062	.0032	69 [54,93]	121 [89,166]	.0031	.0215*	86
A. varius contemp.	.0045	.0031	36 [24,61]	41 [27,68]	.0030	.0490*	39
A. zeteki historic	.0032	.0025	43 [30,67]	54 [35,87]	.0023	.0894	44
El Copé West							
Historic	.0043	.0034	266 [113,inf]	[1,inf]	.0037*	.0610*	14
Contemporary	.0037	.0030	26 [16,50]	36 [22,65]	.0031*	.0730*	30
Santa Fe							
Historic	.0037	.0030	15 [8,41]	38 [20,97]	.0033	.2227	15
Contemporary	.0030	.0029			.0030	.2040	2
El Copé South							
Historic	.0034	.0030			.0031	.0472	6
El Copé East							
Historic	.0045	.0030	1650 [875,13559]	[1,inf]	.0031	.0213	27
Captive	.0034	.0029			.0030	.0276	7
Donoso							
Captive	.0027	.0026			.0027	.1179	8
Caribbean							
Historic	.0029	.0026	136 [98,218]	552 [209,inf]	.0026	.0878*	24
Contemporary	.0025	.0025			.0025	.1066*	5
El Valle North							
Historic	.0032	.0026	164 [94,559]	378 [176,inf]	.0026	.0876	28
Captive	.0025	.0025			.0026	.0939	2
El Valle South							

Historic	.0016	.0018	13 [9,18]	44 [21,136]	.0017	.2310	16

Table 2: Outlier contigs and associated annotations for global *A. varius* analysis. List of 61 genes associated with contemporary *A. varius*. * indicates contigs shared across El Copé West and *A. varius* analyses. Bold genes are discussed in the main text.

Contig Name	Annotation	Outlier Detection Method	N SNPs	N F_{ST} Windows	Allele Frequency Change
combined_Contig473	TPA: putative transposase	Fstwin	0	1	NA
combined_Contig708	Cytochrome P450 2K1	asso, Fst	1	0	0.17
combined_Contig726	probable alpha-ketoglutarate-dependent hypophosphite dioxygenase	Fst	1	0	0.19
combined_Contig963	adenylosuccinate synthetase isozyme 2	asso, Fstwin	1	2	0.44
combined_Contig1050	**toll-like receptor 1 (TLR1)**	Fst	1	0	0.19
combined_Contig1123	solute carrier family 2, facilitated glucose transporter member 11-like	Fst	1	0	0.32
combined_Contig1242	protein-lysine methyltransferase METTL21D	asso	1	0	0.20
combined_Contig1363	poly [ADP-ribose] polymerase 4-like	asso	1	0	0.40
combined_Contig1472	olfactory receptor 6N2-like	asso	1	0	0.40
combined_Contig1601	protein unc-93 homolog A-like	asso, Fst	2	0	0.42-0.43
combined_Contig2446	protein spinster homolog 1-like	asso	1	0	0.41
combined_Contig3340	VPS10 domain-containing receptor SorCS2	Fst	1	0	0.20
combined_Contig3424	replication protein A 14 kDa subunit	asso, Fst	1	0	0.43
combined_Contig3518	**interferon-induced 35 kDa protein**	asso, Fst	1	0	0.25
combined_Contig3827	neuropeptide Y receptor type 1-like	Fst	1	0	0.25
combined_Contig4454	sodium/potassium/calcium exchanger 2 isoform X1	asso	1	0	0.40
combined_Contig4938	ribonuclease T2 L homeolog isoform X1	Fstwin	0	1	NA
combined_Contig4941	kynurenine 3-monooxygenase	Fstwin	0	3	NA
combined_Contig4943	**lysosomal-trafficking regulator (LYST)**	asso, Fstwin	5	19	0.40-0.45
combined_Contig5063*	**transmembrane protein 131-like (TMEM131)***	asso, Fst	1	0	0.21
combined_Contig5390	coiled-coil domain-containing protein 22	Fst	1	0	0.19
combined_Contig5608*	Zinc finger protein 518B-like (ZNF518B)*	asso, Fst	1	0	0.35
combined_Contig5975	centrosomal protein of 170 kDa-like isoform X1	asso	1	0	0.43
combined_Contig6021*	lysine-specific histone demethylase 1B isoform X1 (KDM1B)*	asso, Fst	1	0	0.42
combined_Contig6469	zinc finger protein 638	asso, Fst	1	0	0.26
combined_Contig6941	PREDICTED: uncharacterized protein LOC108790942	asso, Fstwin	1	1	0.40
combined_Contig6942	nuclear pore complex protein Nup133	asso, Fstwin	1	4	0.45
combined_Contig7024	**T-lymphoma invasion and metastasis-inducing protein 1 isoform X1**	asso, Fst	2	0	0.36-0.37
combined_Contig7123	titin-like isoform X32	asso, Fst	5	0	0.30-0.31
combined_Contig7251	LOC548985 protein	asso	2	0	0.30

combined_Contig7495	protein disulfide-isomerase-like protein of the testis	Fst	1	0	0.30
combined_Contig7505	promethin-A isoform X1	Fst	1	0	0.23
combined_Contig7677	**interferon-induced transmembrane protein 3-like**	Fst	1	0	0.32
combined_Contig8245	neuron navigator 1	Fst	1	0	0.40
combined_Contig8274	A disintegrin and metalloproteinase with thrombospondin motifs 13 (ADAMTS13)	Fst	1	0	0.28
combined_Contig8333	Histone chaperone ASF1A	asso, Fst	3	0	0.32-0.35
combined_Contig8554	general transcription factor 3C polypeptide 5	asso, Fst	1	0	0.28
combined_Contig8659	carnitine o-palmitoyltransferase muscle isoform isoform 1	asso, Fst	1	0	0.18
combined_Contig9310	spectrin alpha chain, non-erythrocytic 1	asso	1	0	0.40
combined_Contig9344	transmembrane protein 223 isoform X1	Fst	1	0	0.25
combined_Contig9477	misshapen-like kinase 1 isoform X2	asso, Fst	1	0	0.26
combined_Contig9605	phosphofurin acidic cluster sorting protein 1-like	Fst	1	0	0.30
combined_Contig9813	myotubularin-related protein 6	Fst	1	0	0.22
combined_Contig10055*	**bis(5'-adenosyl)-triphosphatase (ENPP4)***	asso, Fst	1	0	0.34
combined_Contig10067	aminoacyl tRNA synthase complex-interacting multifunctional protein 2 isoform X2	asso	1	0	0.19
combined_Contig10096	eyes absent homolog 3	asso, Fst	1	0	0.30
combined_Contig11387	golgin subfamily B member 1-like	Fst	1	0	0.25
combined_Contig12499	transformation/transcription domain-associated protein	asso, Fst	1	0	0.21
combined_Contig12753	meteorin-like protein	asso	1	0	0.42
combined_Contig13296	protein arginine methyltransferase NDUFAF7, mitochondrial precursor	Fstwin	0	1	NA
combined_Contig13379	fumarate hydratase, mitochondrial	Fstwin	0	1	NA
combined_Contig13502	CCAAT/enhancer-binding protein zeta	asso, Fst, Fstwin	2	4	0.40-0.48
combined_Contig13521	TPA: putative transposase	asso, Fst, Fstwin	2	5	0.41-0.42
combined_Contig13561	TAF5-like RNA polymerase II p300/CBP-associated factor-associated factor 65 kDa subunit 5L	Fstwin	0	1	NA
combined_Contig13570	conserved oligomeric Golgi complex subunit 2	Fstwin	0	5	NA
combined_Contig13631	cytochrome c oxidase subunit 5B, mitochondrial-like	Fst	3	0	0.18-0.27
combined_Contig13777*	transcription cofactor vestigial-like protein 4 (VGLL4)*	Fst	1	0	0.31
combined_Contig13778	methenyltetrahydrofolate synthase domain-containing protein	Fst	1	0	0.28
combined_Contig14222	exocyst complex component 8	Fstwin	0	1	NA
combined_Contig14696	probable cytosolic iron-sulfur protein assembly protein ciao1	asso, Fst	2	0	0.24
combined_Contig15194	proteasome subunit beta type-2	Fst	1	0	0.32

Table 3: Outlier contigs and associated annotations for local El Copé West analysis. List of 76 genes associated with contemporary *A. varius* at El Copé West. * indicates contigs shared across El Copé West and *A. varius* analyses. Bold genes are discussed in the main text.

Contig Name	Annotation	Outlier Detection Method	N SNPs	N F_{ST} Windows	Allele Frequency Change
combined_Contig212	zinc finger protein 180 isoform X1	Fstwin	0	1	NA
combined_Contig1205	LOC100127334 protein	Fstwin	0	1	NA
combined_Contig1263	solute carrier family 22 member 7-like	Fstwin	0	1	NA
combined_Contig1417	uncharacterized methyltransferase-like C25B8.10	asso	1	0	0.33
combined_Contig2428	mdm2-binding protein	asso	1	0	0.32
combined_Contig2601	ethanolamine-phosphate cytidylyltransferase isoform X1	asso, Fst, Fstwin	1	1	0.39
combined_Contig2972	Capn1 protein	Fst, Fstwin	1	1	0.50
combined_Contig3007	oncostatin-M-specific receptor subunit beta	asso	1	0	0.37
combined_Contig3643	Hermansky-Pudlak syndrome 5 protein-like	asso, Fst	1	0	0.32
combined_Contig3740	phosphatidylinositol 4-phosphate 5-kinase type-1 beta isoform X2	asso	1	0	0.36
combined_Contig5063*	**transmembrane protein 131-like (TMEM131)***	asso, Fst	2	0	0.35 - 0.43
combined_Contig5369	serine/threonine-protein phosphatase 4 regulatory subunit 3	Fstwin	0	1	NA
combined_Contig5608*	zinc finger protein 518B-like (ZNF518B)*	Fstwin	0	1	NA
combined_Contig5933	probable global transcription activator SNF2L2 isoform X1	Fst, Fstwin	1	3	0.49
combined_Contig5977	adipocyte plasma membrane-associated protein-like	asso	1	0	0.39
combined_Contig6001	collagen alpha-1(XX) chain	asso, Fst	1	0	0.46
combined_Contig6019	nuclear pore complex protein Nup153	asso, Fst, Fstwin	1	8	0.52
combined_Contig6021*	lysine-specific histone demethylase 1B isoform X1 (KDM1B)*	asso, Fst	1	0	0.58
combined_Contig6146	mitochondrial ribosome-associated GTPase 2 isoform X1	Fst	1	0	0.44
combined_Contig6151	U4/U6 small nuclear ribonucleoprotein Prp3	asso, Fst, Fstwin	1	1	0.42
combined_Contig6295	**laminin subunit alpha-5**	asso, Fst	7	0	0.38 - 0.48
combined_Contig6623	Xemd1 protein	Fstwin	0	1	NA
combined_Contig6773	mitogen-activated protein kinase 4	Fst	1	0	0.43
combined_Contig7200	MGC78973 protein	Fst	1	0	0.48
combined_Contig7281	transmembrane and coiled-coil domain-containing protein 6-like	Fstwin	0	1	NA
combined_Contig7713	gastrula zinc finger protein XlCGF17.1-like	Fstwin	0	1	NA
combined_Contig8034	lipoyltransferase 1, mitochondrial	Fstwin	0	1	NA
combined_Contig8734	disco-interacting protein 2 homolog B	asso, Fst	1	0	0.42
combined_Contig8998	LOC733236 protein	asso, Fst	1	0	0.57
combined_Contig9237	E3 ubiquitin-protein ligase MYCBP2	Fstwin	0	2	NA
combined_Contig9468	striatin-interacting protein 2 isoform X2	asso	1	0	0.33
combined_Contig9792	hsp70-binding protein 1	asso, Fst	1	0	0.36
combined_Contig10016	PREDICTED: uncharacterized protein C18orf8 homolog	asso	1	0	0.39
combined_Contig10055*	**bis(5'-adenosyl)-triphosphatase (ENPP4)***	asso, Fstwin	1	1	0.33

	ectonucleotide pyrophosphatase/phosphodiesterase				0.51
combined_Contig10520	family member 1 ENPP1	asso, Fst	1	0	
combined_Contig10543	NXPE family member 4-like	asso, Fst	1	0	0.32
combined_Contig10696	charged multivesicular body protein 4b	asso	1	0	0.32
combined_Contig10697	AN1-type zinc finger protein 1 [Xenopus tropicalis]	asso, Fst	1	0	0.44
combined_Contig10810	unconventional myosin-IXb	asso, Fst, Fstwin	2	9	0.41 - 0.49
combined_Contig10900	monocarboxylate transporter 14	Fst	1	0	0.47
combined_Contig10917	cytochrome c oxidase assembly protein COX11, mitochondrial	asso, Fst	2	0	0.35 - 0.39
combined_Contig11234	cbp/p300-interacting transactivator 2	Fstwin	0	1	NA
combined_Contig11237	transmembrane protein 132A-like	asso	1	0	0.33
combined_Contig11288	**toll-like receptor 4 (TLR4)**	asso, Fst	1	0	0.32
combined_Contig11457	RNA demethylase ALKBH5	asso, Fst	1	0	0.43
combined_Contig11459	mitochondrial dynamics protein MID49	Fst	1	0	0.45
combined_Contig11470	**fumarylacetoacetate hydrolase domain-containing protein 2 isoform X1 (FAHD2)**	asso, Fst, Fstwin	4	1	0.41 - 0.47
combined_Contig11552	calpain-3 isoform X6	Fstwin	0	1	NA
combined_Contig11606	serine/threonine protein kinase	asso, Fst	1	0	0.32
combined_Contig11652	Novel Trtraspanin family protein	Fst	1	0	0.46
combined_Contig11762	phosphoglucomutase-like protein 5	asso, Fst	1	0	0.32
combined_Contig12056	A disintegrin and metalloproteinase with thrombospondin motifs 3	asso	2	0	0.36 - 0.39
combined_Contig12085	TPA: putative transposase	Fst	1	0	0.38
combined_Contig12325	DAZ associated protein 2	Fstwin	0	1	NA
combined_Contig12326	Small transmembrane and glycosylated protein homolog	Fstwin	0	1	NA
combined_Contig12730	transmembrane protein 205 isoform X1	asso, Fst	1	0	0.42
combined_Contig12815	regulator of nonsense transcripts 3B isoform X1	Fst, Fstwin	1	1	0.36
combined_Contig13139	integrin alpha-6 isoform X3	asso	1	0	0.33
combined_Contig13170	sortilin 1 S homeolog precursor	asso	1	0	0.35
combined_Contig13349	coiled-coil domain-containing protein 39	Fstwin	0	2	NA
combined_Contig13370	alpha-2-macroglobulin-like protein 1	asso	1	0	0.34
combined_Contig13456	protein Jade-3	Fstwin	0	1	NA
combined_Contig13463	attractin-like protein 1	asso, Fst	1	0	0.46
combined_Contig13467	calcium uniporter regulatory subunit MCUb, mitochondrial-like	Fstwin	0	1	NA
combined_Contig13491	RING finger protein 121	asso, Fst	1	0	0.43
combined_Contig13532	cytoplasmic polyadenylation element-binding protein 4 isoform X1	asso	1	0	NA
combined_Contig13694	ELAV-like protein 1	Fstwin	0	1	NA
combined_Contig13776	**properdin factor, complement**	asso	1	0	0.52
combined_Contig13777*	transcription cofactor vestigial-like protein 4 (VGLL4)*	Fstwin	0	1	NA
combined_Contig14016	islet cell autoantigen 1 isoform X1	asso, Fst	1	0	0.46
combined_Contig14195	LOC100037234 protein	Fstwin	0	1	NA
combined_Contig14434	eukaryotic translation initiation factor 4 gamma 1 isoform X1	Fst	2	0	0.46

combined_Contig14586	ADP-ribosyltransferase 5	Fstwin	0	1	NA
combined_Contig14622	solute carrier family 12 member 8 isoform X1	Fstwin	0	1	NA
combined_Contig14943	**laminin subunit beta-1-like**	asso	1	0	0.33
combined_Contig15350	C4SR protein	Fst	1	0	0.40

Conclusions

The development of high-throughput genomic sequencing techniques for non-model organisms has opened the door to widespread genetic monitoring and detailed explorations of rapid evolutionary change. Here, I describe the development and implementation of two new sequencing methodologies for conservation purposes. First, in Chapter 1 I describe a new multi-locus sequencing technique that harnesses the power of microfluidic multiplex PCR to generate sequence data from limited DNA input. Second, in Chapter 2 I provide an example of how this new technology can be used to reveal new insights into the global distribution of *Bd* lineages. In this chapter I describe a new lineage of *Bd* and discuss possible mechanisms of global *Bd* spread. Finally, in Chapter 3 I detail the development and implementation of a new exome capture assay that I used to sequence historic and contemporary frogs from Panama. Using this technology, I was able to scan the genomes of the critically endangered, *Bd*-susceptible *Atelopus varius* to both refine conservation units and identify genes associated with persisting individuals. Overall, in this dissertation I leverage the power of genetic and genomic sequencing technologies to reveal key insights into the dynamics between *Bd* and amphibian hosts. This work serves to advance our understanding of host-pathogen coevolutionary dynamics and inform amphibian conservation.

Appendices

Appendix for Chapter 1

S1 Table: List of primer pairs and amplicon location for each target locus.

Primer Name	F-Primer	R-Primer	Amp Size	Chr	Amp lower	Amp upper
AB1	GCATCGGGTGCATTATCTCT	TTGCAGAATTCCAACGTGTC	185	1	313988	314172
AB2	TTCCTGGTGTTGGGCTATTT	GATATGCTACCGTCGGCATT	172	1	359745	359916
AB3	GAAGACTCGAAGCCTTCTTCTG	TCAACCCTAGGTCAAAGAATCG	190	1	587513	587712
AB4	GTCAAATATCTGGCATCAATGG	GATGCGAGCAACACTCAAGA	152	1	602449	602600
AB5	ATGGTGTGCAAGTTCTGTCG	TCAGATGAGTTGCAGCGTCT	200	1	636488	636687
AB6	AGCGTGTGTGTCCTTTCTGA	GAAACAGGTTATGCGCGATT	177	1	704829	705005
AB7	TGCTGCTGCTGCTCTTATTG	AGAAATTGCAGGAAGGCAAG	196	1	726564	726759
AB8	TCCAAAGTCTACCGTCTGAGG	TGTGTGCGAGTCGAATTTCT	158	1	768568	768725
AB9	CTCGGTACTTGATCCCGAAA	CGGTGGTTGTCGTAGTGGTA	197	1	824753	824949
AB10	GCCGACCGAACTATCTGTTG	GGGCAGAGGCAGGTAAGAAT	161	1	1448993	1449153
AB11	CGGAAAGCCAATACCAACAA	CATTGCGCATTCTAATTGTCA	181	1	1603492	1603672
AB12	AAAGAATGGCGAGTTGATGG	TCGATGTGGACGACTGTGTT	154	1	1638140	1638293
AB13	ATGTGCACCTATGCGAGATG	GGCGCTTCAAATGAGGTTT	152	1	1734364	1734515
AB14	AAACGACGTGACTTGAAATGC	CGTGCTGGTAAGTCCAATCA	192	1	1836914	1837105
AB15	ATCTTGGCCATCAACAGTCC	CTTGGCCATCAACGACAAC	191	1	1892960	1893150
AB16	TTACCAAGCCTGTCGAGGAT	TGATAGGATGCTAGTGATTTC AGG	195	1	1920032	1920226
AB17	CGTTTCGATGGTTGTTCCTT	GTCTAGCGTATTTCTCAAGGG TTT	176	1	2000821	2000996
AB18	AATCGTATGTGTCATGTCAGGAA	TTTGATCGTATGCTGGCAGT	181	1	2429426	2429606
AB19	TCTGTTGCTGCCAACTCAAC	TGGATTTGAATGGAGGGTAAA	179	1	2444004	2444182
AB20	GATGCTTTACCCACATCAAGC	CGTCCAACTACAGGCGTAGG	161	1	2628163	2628323
AB22	TGACAAGTAGGTCTTTATGGTCTAGC	GGCTCCAGCTTTGTTGATTT	197	1	2766038	2766234
AB23	GAAGTGGTACTGATGGGCTGA	AAAGAACCACGGCAATCAAC	150	1	2884950	2885099
AB24	GCAAATGTATGATTTGGGTCAG	TTTATGGGTGGTTATTATTAAT GCAA	187	1	2886279	2886465
AB26	AATAAACCAAGATGGTGTGC	CGAAACTTTCTACCAGTTCAA	194	1	2892369	2892562
AB27	CTTGAATCAATAAAGCGAAA	CGGTAAATAATGGCTCAGAC	182	1	2893053	2893234
AB28	TGCTACCTTGATTGTTTGG	AAACAAGATGGCATAGAACC	197	1	2896019	2896215
AB29	CGTGGTGTCAGTTTGCTAGG	GGATGAATTTGATGATGACGAA	189	1	2896707	2896895
AB30	CTTCCCATCTTCAGCATCGT	AGAGCGCTTATTTCCGAAGA	150	1	2897432	2897581
AB31	GGGTTTAAAGTCTCTAGTCAAGTCGT	CACTCAACTTTGTCAAACACAC AC	159	1	2898398	2898556
AB32	GAGATGAAGCATTAGTATCCGCTAA	TGAAAGAATTAATAGCCATGATA AGC	200	1	2898847	2899046
AB33	TCACCAATATCTAGCCCTTC	AGGAGCAATTGGAGGTAATA	188	1	2899845	2900032
AB34	TTGCATCCTTGTGGTTATCG	ACACGGATCGTTGATGCTTT	154	1	2900522	2900675
AB35	GCGTCTCTGACTTGGTGGTT	TGGCATTCATCAGGTACCAA	184	1	2901038	2901221
AB36	CTCGCATCTTGACGGAAGTT	TGGTACACTGCCAATACTAAGCA	190	1	2902503	2902692
AB37	CCGAGTGTTTCACAGATGGA	GTTTATGCACTTACCATTCACGA	152	1	3088725	3088876

AB38	TCCATCCATGAGAACTGCTG	ACGGAGTTGTTCCTGCTTTG	169	1	3221820	3221988
AB39	ATTACTCTTGGTTCTTAATGCATCC	CGCTTCTTCCATTCGACATT	184	1	3228043	3228226
AB40	AACTGATGGAGACGTGACGA	CTGATCATGCCAACTGGATTT	177	1	3273912	3274088
AB41	GTGGTGAGCAAGGTGATGTG	CTCGAGAGCTCTGCTGATCC	181	1	3369353	3369533
AB42	TGTATGGCAATGCTGTTCAGT	ACCAAAGCACAATTTCTGCAC	150	1	3381012	3381161
AB43	AGTGCGTCACCAGGTTTAGC	CAAACTGTTGCAGCATCGAC	157	1	3471614	3471770
AB44	CGCCAACGTCTACTCATCTTT	ACAAGAGCTCCAATGCTTATGTT	191	1	3615380	3615570
AB45	CAGACGATGCTGATGACGAT	AAGGCAGATGCATTTGAAGC	163	1	4115429	4115591
AB46	GGATCGCATCAACCCTCTAA	GATGGAGGTGCATCTCGTG	155	1	4126735	4126889
AB47	CGTCGTGCTGATCTCTACTAGG	GTCTATCCTACGGTGATGGCTTA	198	1	4310166	4310363
AB48	TGATTGATATTGAGCAGGCTGT	TCGGCTTGAGCATCTACAAA	151	1	4336242	4336392
AB49	ACACATGGCAATCACCAAGA	TCACTCACCAATATGCTTGACA	170	2	55536	55705
AB50	GTTGCATCAAGGGTTTCGAT	GTCGTGGACCACTTTCTCCT	182	2	64938	65119
AB51	CCATTATGCACGACTGTTGC	TCGGAATAAACCAAGTGCAAA	199	2	208384	208582
AB52	TTGTAGGGTCGAGCAGTAGGA	CAAATCTTCCTGGCATGCTT	181	2	238016	238196
AB53	ACCGCACTAAACAAATGAGT	CCGCATAGCAATCACTTTA	195	2	354999	355193
AB54	CCGTACTTGGACACATGCAA	GCAACTGTCTTGAGCAAACG	151	2	369236	369386
AB55	GCAGATGGCTTGGTTGATTT	GCCGCTCAATTGTCTGGTA	186	2	500969	501154
AB56	AGCGCACTCCACAACTCTG	TGCGACTGTTTGAAATCGAG	187	2	686134	686320
AB57	CATTCCGCTTTGTTCGACTT	TCGGCCAATATCTGGTGAAT	174	2	832660	832833
AB58	GCTTGATCCGCTTCTGATGT	TCTGCTGTCCTTGATGCTTG	158	2	915369	915526
AB59	ACGATCACCGAGTTCAAGAGA	GGTGTGAATGCATTACGACTGT	197	2	925547	925743
AB60	TGTCCATGTTCTAATTCCCTTACA	AGCGACGAGGAAGAAGATTG	158	2	1338575	1338732
AB61	GCCAGACTCCGCTTAGCTC	AATAGCGGGTGTTGGTTCAC	161	2	1366229	1366389
AB62	CGCGTTCTAACCCAAGAAAG	CAGCTGTACTCGCCAATGAA	190	2	1603908	1604097
AB63	GTGCCGATTACAAACCACCT	CTCCCGGTTTGACTAGCACT	196	2	1806071	1806266
AB64	TCCAAACGCATTACCATCAA	GCGACACATGGACTGAGCTA	164	2	2055254	2055417
AB65	CAAACAATATCGAGCCCAATAAA	TCATTGTTTGAATGATTTGCATTA	191	3	48914	49104
AB66	ACAGCATTCATCAAGCCTAGC	AGAAGGAATGGATGGCAAGTT	183	3	170120	170302
AB67	ATTGCCAAGCGATGTTCAA	TAGCATCGCCTAACCCAAAC	199	3	221106	221304
AB68	CGTACATTCTTTGATGATTATATTGCT	CTTGAGTACCAGCGCAATCA	178	3	395887	396064
AB69	ATCGATCGTCCAAGAAATGG	GCAAGTGTAGCTCTGGGATGA	196	3	502521	502716
AB70	CAACTGTCGCATTCCTGAAA	AAAGCAATGGAAGCAAATGG	162	3	589816	589977
AB71	GCTGCACGCTGATACTCTTG	GCTTTGGGCCATGTCAAATA	176	3	681377	681552
AB72	ACAATGTCGAGGCAGGAAAT	GGCTCGAAACTCGTCAACTT	185	3	851429	851613
AB73	GCGCCAGCTATTTCTAATGC	AACTGGAGCTGCGATTGTCT	174	3	868998	869171
AB74	GGTTGCTCAGGATGCACAA	CAAACCCAAGACGGTACAGAA	200	3	973363	973562
AB75	TGGACACGATTCGTCGTATT	TTGGGTTCAAATGCTGTCAA	166	3	1086489	1086654
AB76	ATTCCTCCAATGCATCCAAC	AGCTGCAGACACGTCAAAGA	200	3	1157815	1158014
AB77	TACATCACCACCCTGGGTTT	GGCTGTTGCATATCGTCAAA	181	3	1250336	1250516
AB78	TGACTGGACCCATTTCTCAA	CGTAAGAGACGAGTTTGTCGTG	197	3	1695986	1696182

AB79	GGTGCACTTTCGATCCACTC	CAACACTTCATGTCGGGAAA	167	4	172424	172590
AB80	CTGATTGCTCTAGCCCAGTTG	CGATTCAGCTAGGCTTTGGA	150	4	275519	275668
AB81	TTTGGATTGGATGGAAAGAGA	ACAGGGAAACCAAAGTGCAT	194	4	307157	307350
AB82	ACTCTTCCAAGCGACCAATC	ACAGTTCGCGGAACATTTG	196	4	320583	320778
AB83	CCCAATTGTTTCATTCCTTCA	GGGTAAGTTGATCAATACGTCT AGC	195	4	877303	877497
AB84	GATGCGGTTGCTGCTCTAA	TGTTGACGGTGATGACATGAT	193	4	917289	917481
AB85	GCCAAAGGCATTCCAGAGTA	TAGTCCAAACGGCAGGAATC	152	4	1050099	1050250
AB86	ATTGCCTTCTTGTTGGTTGC	TTTGGTTTCCTCAACAACACTA TC	199	4	1269059	1269257
AB87	CTGATGCTGGATTGCAGAAA	GCTGAAACACACCAACTTTGAA	167	4	1517251	1517417
AB88	TCAACTGGCTTTGAGCACAC	CTTCAACTCCGTCACAACGA	191	4	1642004	1642194
AB89	AGGCAAATGTGGAATGGAAG	TTCTTGTTGCCATATCTTCAGC	184	4	1726777	1726960
AB90	ATGCTGCTGCAAATGTCATC	GGTCGTTCAGAGGTGGGTAA	161	5	88871	89031
AB91	CAGTTGGCATAGTGCATACGA	CATCATGGTGAAACCAACCA	185	5	119163	119347
AB92	TTGATTGTGCGAGCAAGATG	TGGAAGAACTCTCTCGCCATA	176	5	467911	468086
AB93	TGTTGATGGAGCACCAAGTC	AGCGTCATTCAACCGAGAAT	186	5	495631	495816
AB94	GAGTGCTATTTGCCGACGA	TCGACGCCATTTGACAATAA	178	5	604680	604857
AB95	ACCTCGTCCAAACCAACAAG	CGCGCTGATTAACCAAACTT	179	5	766354	766532
AB96	ACATCAACGTGCCAGACACT	GCAGTTGGAAGATGTGGTGA	160	5	801200	801359
AB97	TCTCAAGATACGAGCGAATGC	TCGAGCAGATCATTGTCGAT	193	5	964645	964837
AB98	GCATTCATCTTGGCTGCATA	GGCGAATGCATTGTTGACTA	169	5	1174087	1174255
AB99	TGGACACCGTTACGTTGAAA	TTCAAAGAAACCCAAACAACAA	186	5	1178930	1179115
AB100	CGGCACGATTGTATTTGGAT	CATTCATGGCTGGAACATTG	185	5	1190809	1190993
AB101	TTCAGAATGGTTTAGAGTGTGGAA	AGGGCTGCAACAACTGGAT	172	5	1217079	1217250
AB102	GGTGTCGAGGATGGTATGAAA	GTCCAGCCACCTATGCAAGT	175	5	1219000	1219174
AB103	CTGCGCAAGAACGACTACAC	TGGTTGACGATGCTCAAGTC	179	5	1231035	1231213
AB104	CTTGGCTGTCGATGCAGTTA	ATCATACCAGGCCATCAAGG	162	5	1388510	1388671
AB105	CCAGAAACTATTCGCCAACC	GAAACTCTCGGCACTCTTGC	195	5	1431283	1431477
AB106	CGCGTTCAAGACAACAAGAA	GCCAGTCTTGTGAATGATGG	192	5	1481521	1481712
AB107	ATGTTTGGAACGCCAATCTC	CAATGTCTTGGCCAGTTTGA	190	5	1493217	1493406
AB108	CGATGCAAATCATGACCATT	TGCTCTGCTTTCCATGAGTC	199	5	1581926	1582124
AB109	GGTCCACGATTGAGTTGTAT	AAAGGCACAATGTTCAGTAAA	196	5	1646312	1646507
AB110	AGAGAGGGCAGACAAACGAA	CGCCTATGGTGGCATTATTC	153	6	229967	230119
AB111	CTTGCAGTGTACTCCTGTTCAAA	CACGTAAAGTGGAGCACTGAAT	200	6	257353	257552
AB112	ATGACCAGACCATCAAAGC	GATGGCTCTCATCCAAGAC	200	6	262251	262450
AB113	ATTGTTGGGCCAATTGTGTT	TCGATTGAGTGAAGGCATGA	189	6	263967	264155
AB114	TTGATTGGCAGCACCATCT	CTCCCGAGTTCTATGGTGGA	192	6	268590	268781
AB115	AATGACCAAACACGATTAAAGATG	TGTGCAAATTCACTAAACCTCGT	182	6	269033	269214
AB116	CACCTCTGCTCTTGTGTCCA	CAGCCAATTCAGGACGATAAT	155	6	270225	270379
AB117	TTGCATTGTTCCACATGGTT	GCCAACGACTCCAATGTAAGA	190	6	270774	270963
AB118	ACGACGCTCAAATCGAGTCT	TTCGGGTAAACCAGCCAGT	189	6	275529	275717
AB119	GATCTCGGATACCTGCATCG	TTCGCTGATTTCTTCAAACG	174	6	672925	673098

AB120	TTTCTGGAGTGGCAAATGGT	AATGTGTACTCGATCCATCTCTGA	194	6	674851	675044
AB121	GAAGCACTGCCAGATTTCATT	TCAAGTGTGCTTGTGATCCTG	157	6	1499384	1499540
AB122	CATCATGGGTGTTCTCAACG	TGTGACTCGTTCAAGCTCGT	190	6	1501406	1501595
AB123	AGATGTGGGTGTTGTTGTCG	ACAAACTAGATGCACTGGAGGAT	196	6	1502583	1502778
AB124	TCCCAATTCCATTTACTGCTATC	TTCAATCAAGGCTCACGTTG	179	6	1505105	1505283
AB125	CTGCACAACAGGTCAGCCTA	GAGCTTGAGGTTTGATTGCTG	163	6	1506318	1506480
AB126	ATGCTGCTGCAGTCTCGTT	TTGATGTCGATGTCGATGCT	165	6	1514147	1514311
AB127	GCACCACCATAAGTATTTCC	GAAGGCTGCAATCAATATGT	169	6	1515289	1515457
AB128	AGTGATGCGGTTCAGGAAAT	CGTTTGGAGTGGCAGCTT	163	6	1524325	1524487
AB129	TCAAACAAACGTCCAAACAAA	CGAAACAGACAAAGGTCAGTACA	198	7	64092	64289
AB130	ACATATCCCAATTGCGAAGC	CGTTTAGGCGATCTTGGTGT	187	7	383319	383505
AB131	TCCTGTTCCACTTGCTCCTT	CCAAATCTACCAACACGCTATTC	163	7	384564	384726
AB132	GACGGTCTTGTAGTCCTCTCAAA	CAATCACTTACACGCCTTCG	169	7	657804	657972
AB133	GAGCGGGTTCTTTAATGTATCG	GGACAAATCTGGCCAATGTAA	152	8	339948	340099
AB134	CACAGCACTGGCAGTTGAAT	CTCAACACCAAAGCCTCGAC	157	8	400602	400758
AB135	AACTCGTGTCAAGCGTGTCTT	CACACCGGTTGAGGGTTTAG	178	8	412232	412409
AB136	GGATTCCTCCGTATTTCTTGG	TTAAAGCCAAGCATGTGCAA	160	8	689056	689215
AB137	CTGCGATTGGATGTGGTTTA	CAAGTGATCCACACGACACC	165	8	958034	958198
AB138	GACAAAGTGCCGAGTGTTTG	ACGTTGGCGATATCCCTTG	200	8	980090	980289
AB139	CAGGATCTGCCAGTTTCGAT	GGTGCTCCATAAAGTGACAGG	199	9	139438	139636
AB140	TTTCGTCAGTGGTCCAAACA	CTAACATGCCGATTGTGTCG	187	9	552522	552708
AB141	TAGTGCTCCATCTTGCGTGA	TGGAGCTTGTTCATCATACTGTG	185	9	612990	613174
AB142	TTCAATCGCTTCTGCAGTCTT	TGAGCAAGTCTGTTCAAGGTG	200	9	677185	677384
AB143	TTGCTTTGCTTTACAATCTTGC	GCAGCTGCAAGAGCTTTGTT	173	9	773255	773427
AB144	CGACTCTTGCAAAGTGCTCAT	GGAAGAATGTCGTTCATTCACA	180	9	985986	986165
AB145	TTCCTGCTGGAATTGAAAGC	TCGTCCTTCAGCAGTGACTTT	186	9	987059	987244
AB146	CAAGTGCCCACACATGGTAA	CCAGTTCCACACTCCGAAAT	167	10	272152	272318
AB147	CCAATCGGTGTCAAATAACTCA	GCAGTCCGTAACACCAAACA	197	10	317911	318107
AB148	GCAATTGTCTCGCGATAAGG	TGATAGCTCTCTTGAAACATCCAC	198	10	373573	373770
AB149	GCAGGTAGAAGGCAAGCAAT	CGGGAGCTATATATTTCCAGCA	184	10	594347	594530
AB150	GCTGAATTCCAACGTCCTGT	AGCCTTGTTGCCATCTTCAT	197	10	833756	833952
AB151	GTCTCGAACACAAGGGCATT	TTACCAACGAACCCAAATCC	180	11	161159	161338
AB152	ATGGAAACAGGTGGAGCAAG	TTCTGAACTGCAGCATCCAC	194	11	164571	164764
AB153	AACCAAGTTGTATGGGTCACG	CGTAATACCGATCAAACATGACA	176	11	461713	461888
AB154	ATGATGATGGGAGCAAGTCC	TTTGTTACATCAGGAGCAGCA	161	11	491869	492029
AB155	GACAAAATGGAAATCATTACATCG	TTTTGTTCCAAACACAATATCCA	150	11	826884	827033
AB156	TGACGGAACCAAAGACATGA	GCAGCTTGAAGTGCCTTGAT	193	11	901302	901494
AB157	CCCTTTCTATTGCATTTCACAA	TGTGACATTGTTGCTTGCTG	159	12	30400	30558
AB158	TGATGACAACCCATGGAACA	TCCAACATACTCCAGTCCAACA	180	12	31070	31249
AB159	ATCGAGCGTGAAATGACAAA	TCGAACCGATATGCAAGAAA	188	12	67618	67805
AB160	CCTCCCTTGTATGGCATTTG	GGATGCAGCCAAGTATCTCC	150	12	78035	78184

AB161	GCCAGCAAACTCAAACCACT	TGAGAATATTTGCTGGGCTGA	198	12	328929	329126
AB162	CGCATTCAGACACCACAGAT	GCATCAAATTGGCGAGAGTT	191	12	368538	368728
AB163	GACGTAAATCGTTCCACTTTCC	AGTCCATTTGGGATCGTCAC	158	12	384586	384743
AB164	AGAGCCTGAGCAGTGCAAAT	TTTCCTGCAAGGATGCTCTT	160	12	409728	409887
AB165	CGTCATGAGAAAGACCGAGAA	GACATCTCTGCCAAGGCTTC	169	12	710519	710687
AB166	AACCTGATTGATCATGGATGG	GCAACAATCCCTTTACCACTG	182	12	715087	715268
AB167	GCTGACCATATTTGCGGACT	TGTTGACGTTGCTTGTGGTT	172	12	728217	728388
AB168	ACAGTTGAACATGAAGCAGCA	GCAGCCTGTTGACAAGGAAT	193	13	213397	213589
AB169	CTTCCGACTCCAAGTACTACACC	TCAGTGGAGAATGCAGACTCTT	195	13	840442	840636
AB170	CCTGACTCCATCTCCGTCAT	AAACGCAGGCGATAGATTTG	183	14	343204	343386
AB171	TGACATTGCTTTATAGATGGCTTC	TTCTGAACCTCGCCATTCTT	171	14	430658	430828
AB172	TTTATTGTCGAAGTGTTGGTGAA	TTGAACCATTCTGTGGCCTA	195	14	648360	648554
AB173	AAAGCAGTTCCAGCCTTCAA	TACGAGAAGAGCCAGCCATT	195	14	730791	730985
AB174	TTGGAATGCACCATCTCTTG	TAGTCATGCCAGCCACTACG	163	14	746727	746889
AB175	CAGCTGTAAGCCAACACAGG	TCAAGGACTTTAGACAGTGCT CA	192	15	3611	3802
AB176	GTGCGCCAACAGAATGGTAT	AGACCAACAGGACCGAGAGA	171	15	25275	25445
AB177	GTCAATCGTGTTGGATGGTTT	AATACGCCTGGTCCTGACAT	165	15	73992	74156
AB178	GCAAGCATGAGTGGTTGAAA	TGATATGGTTGGGCGTAACA	182	15	117594	117775
AB179	TACGAACGAGGACAACACGA	ACGATCAAGCAGTTATTCTAC CAA	188	15	150736	150923
AB180	GCAAACACGCTCCGTTAAA	GCAGCTATGGACCACATTGA	195	15	228792	228986
AB181	ATAAGCCGCTGAAACAATGC	CGACTCGACAATCAGCAGAA	168	15	441460	441627
AB182	TGGCTTGCAAGATGATGGTA	CCAATGCCAAGATTCCTGTT	163	16	34185	34347
AB183	CAGCAGTATTGATACTCGAGGTATTTC	AGATGATGCGCGGTGTATTT	171	16	49473	49643
AB184	AATGGGACGAGTGACATATCG	TTGAGCATTGCACGCTTATC	165	16	123463	123627
AB185	TCACGGAATAGTTCATCGGTAA	ACAGTGCTGGTGCAGTCTTG	173	16	273708	273880
AB186	CATCCAGTTGATCCAAGCAA	GCGTTGACTCCAGCTACAGA	185	16	395396	395580
AB187	AGCAATGAGCAGACAATCTTACC	GAATCCCAAGGAACCCGTAT	172	16	451316	451487
AB188	CCCATATGACCTTCGGATTC	TTGATGAATATCTCCACCCTA TCA	163	Mt	26277	26439
AB189	AATTTCTGAGTTAACCTATCCATC	CCCAGAGGTCCTCATAGAAT	200	Mt	136154	136353
AB190	GATTCGCTTTAGCATAACCT	CTTGCTGCTCCAGGTAGTAT	155	Mt	155578	155732
AB191	TGAACGCACATTGCACTCTAC	CACTCATTATCTGCTCCATCTCC	172	BsaI ITS		
AB192	CAAATGGTTAGACACGGGATG	CCAACGAGTCATGTTGGAAA	195	5	208626	208820
AB193	TTAACACGCCAAACATCGAC	AATGGTCGATTTCACAACCAA	181	39	779	959
AB194	ATCACAATCGCGTACTAAATGG	TTGACACGTCAAACATCGACT	198	57	3252	3449

S2 Table: List of all samples included in the Bd Fluidigm Access Array. Pure cultures were diluted to a concentration of 2ng/µl and 1µl was used as the initial input for the assay. Associated Bd clade information is from whole genome data published in Rosenblum *et al.* 2013 or from unpublished whole genome data. Technical replicates were included for all non-Bd isolates and for two Bd isolates (LFT001-10 and UM142). 1ul of each extract was used as

the initial input for swab samples and the Bd DNA copy number associated with this volume is listed below.

Sample ID	Sample Type	Fungal Species	Amphibian Species Origin	Geographic Origin	Associated Bd Clade	Initial Bd input
Hp-JEL142_A	Pure Culture	*Homolaphlyctis polyrhiza*	NA	NA	NA	2ng
Hp-JEL142_B	Pure Culture	*Homolaphlyctis polyrhiza*	NA	NA	NA	2ng
Eh-JEL326_A	Pure Culture	*Entophlyctis helioformis*	NA	NA	NA	2ng
Eh-JEL326_B	Pure Culture	*Entophlyctis helioformis*	NA	NA	NA	2ng
Rsp-JEL136_A	Pure Culture	*Rhizophydium brooksianum*	NA	NA	NA	2ng
Rsp-JEL136_B	Pure Culture	*Rhizophydium brooksianum*	NA	NA	NA	2ng
Bd-LFT001-10_A	Pure Culture	*Batrachochytrium dendrobatidis*	*Hylodes ornatus*	Serra do Japí, Brazil	Bd-Brazil	2ng
Bd-LFT001-10_B	Pure Culture	*Batrachochytrium dendrobatidis*	*Hylodes ornatus*	Serra do Japí, Brazil	Bd-Brazil	2ng
Bd-JEL275	Pure Culture	*Batrachochytrium dendrobatidis*	*Anaxyrus boreas*	Clear Creek, CO, USA	GPL	2ng
Bd-JEL429	Pure Culture	*Batrachochytrium dendrobatidis*	*Rana catesbeiana*	Merida, Venezuela	GPL	2ng
Bd-JEL310	Pure Culture	*Batrachochytrium dendrobatidis*	*Smilisca phaeota*	Fortuna, Panama	GPL	2ng
Bd-CJB4	Pure Culture	*Batrachochytrium dendrobatidis*	*Rana muscosa/sierrae*	Yosemite National Park, CA, USA	GPL	2ng
Bd-CJB7	Pure Culture	*Batrachochytrium dendrobatidis*	*Rana muscosa/sierrae*	Kings Canyon National Park, CA , USA	GPL	2ng
Bd-MLA1	Pure Culture	*Batrachochytrium dendrobatidis*	*Hypsiboas cordobae*	Las Higueritas Natural Reserve, Argentina	GPL	2ng
Bd-Lb-Aber	Pure Culture	*Batrachochytrium dendrobatidis*	*Litoria booroolongensis*	Abercrombie River, Australia	GPL	2ng
Bd-MexMkt	Pure Culture	*Batrachochytrium dendrobatidis*	*Hyla eximia*	Mercado Emilio Carranza, Mexico City, Mexico	GPL	2ng
Bd-UM142_A	Pure Culture	*Batrachochytrium dendrobatidis*	*Rana catesbeiana*	Ypsilanti, MI, USA (market)	Bd-Brazil	2ng
Bd-UM142_B	Pure Culture	*Batrachochytrium dendrobatidis*	*Rana catesbeiana*	Ypsilanti, MI, USA (market)	Bd-Brazil	2ng
Bd-ev001	Pure Culture	*Batrachochytrium dendrobatidis*	*Rheobates palmatus*	Ubaque, Colombia	GPL	2ng
Bd-NBRC106979	Pure Culture	*Batrachochytrium dendrobatidis*	*Ceratophrys cranwelli*	Chuo-ku, Japan	GPL	2ng
Bd-SRS812	Pure Culture	*Batrachochytrium dendrobatidis*	*Rana catesbeiana*	Savanna River, SC, USA	GPL	2ng
Bd-TST75	Pure Culture	*Batrachochytrium dendrobatidis*	*Rana muscosa/sierrae*	Yosemite National Park, CA, USA	GPL	2ng
Bd-JEL238	Pure Culture	*Batrachochytrium dendrobatidis*	*Rana yavapaiensis*	Mesquite Wash, AZ, USA	GPL	2ng
Bd-JEL267	Pure Culture	*Batrachochytrium dendrobatidis*	*Rana catesbeiana*	Mont-Saint-Hilaire, Quebec, Canada	GPL	2ng
Bd-JEL271	Pure Culture	*Batrachochytrium dendrobatidis*	*Rana catesbeiana*	Point Reyes, CA, USA	GPL	2ng
Bd-JEL359	Pure Culture	*Batrachochytrium dendrobatidis*	*Rana clamitans*	Berlin, NH, USA	GPL	2ng

Bd-JEL427	Pure Culture	*Batrachochytrium dendrobatidis*	*Eleutherodactylus coqui*	El Yunque, Puerto Rico	GPL	2ng
Bd-Pc_CN_JLV	Pure Culture	*Batrachochytrium dendrobatidis*	*Pristimantis cruentus*	Cerro Negro, Panama	*No whole genome data available	2ng
Bd-JEL433	Pure Culture	*Batrachochytrium dendrobatidis*	*Xenopus laevis*	Namaqualand, South Africa	GPL	2ng
Bd-JEL627	Pure Culture	*Batrachochytrium dendrobatidis*	*Rana catesbeiana*	Bethel, ME, USA	GPL	2ng
Bd-CJB5-2	Pure Culture	*Batrachochytrium dendrobatidis*	*Rana muscosa/sierrae*	Sierra National Forest, CA, USA	GPL	2ng
Bd-PAB01	Pure Culture	*Batrachochytrium dendrobatidis*	*Eleutherodactylus coqui*	Maricao, Puerto Rico	*No whole genome data available	2ng
Bd-JAM81	Pure Culture	*Batrachochytrium dendrobatidis*	*Rana muscosa*	California, USA	*Not included in cophylogeny comparison	2ng
Bd-JEL410	Pure Culture	*Batrachochytrium dendrobatidis*	Information not available	El Copé, Panama	GPL (from unpublished whole genome data)	2ng
Bd-Campana	Pure Culture	*Batrachochytrium dendrobatidis*	*Hyalinobatrachium vireovittatum*	Altos de Campana, Panama	GPL (from unpublished whole genome data)	2ng
Bd-RioMaria	Pure Culture	*Batrachochytrium dendrobatidis*	*Pristimantis cruentus*	Rio Maria, Panama	GPL (from unpublished whole genome data)	2ng
140528_20	Swab Sample	*Batrachochytrium dendrobatidis*	*Espadarana prosoblepon*	Panama		1.66 copies
140528_22	Swab Sample	*Batrachochytrium dendrobatidis*	*Espadarana prosoblepon*	Panama		64.37 copies
140528_26	Swab Sample	*Batrachochytrium dendrobatidis*	*Agalychnis lemur*	Panama		2.15 copies
140529_02	Swab Sample	*Batrachochytrium dendrobatidis*	*Rana warszewitschii*	Panama		3684.6 copies
140529_07	Swab Sample	*Batrachochytrium dendrobatidis*	*Rana warszewitschii*	Panama		10215.33 copies
140529_08	Swab Sample	*Batrachochytrium dendrobatidis*	*Rana warszewitschii*	Panama		50278.04 copies
140613_R10	Swab Sample	*Batrachochytrium dendrobatidis*	*Silverstoneia flotator*	Panama		62.59 copies
140614_A10	Swab Sample	*Batrachochytrium dendrobatidis*	*Rhaebo haematiticus*	Panama		7.52 copies
140615_A14	Swab Sample	*Batrachochytrium dendrobatidis*	*Silverstoneia flotator*	Panama		100.4 copies
140616_03	Swab Sample	*Batrachochytrium dendrobatidis*	*Atelopus varius*	Panama		107.4 copies
140617_A02	Swab Sample	*Batrachochytrium dendrobatidis*	*Dendrobates minutus*	Panama		3.64 copies
140617_A04	Swab Sample	*Batrachochytrium dendrobatidis*	*Rana vaillanti*	Panama		4.38 copies
140618_R07	Swab Sample	*Batrachochytrium dendrobatidis*	*Pristimantis gaigei*	Panama		9.13 copies
140619_A01	Swab Sample	*Batrachochytrium dendrobatidis*	*Hyalinobatrachium colymbiphyllum*	Panama		7.57 copies
140619_A05	Swab Sample	*Batrachochytrium dendrobatidis*	*Allobates talamancae*	Panama		1.7 copies
140620_A06	Swab Sample	*Batrachochytrium dendrobatidis*	*Craugastor talamancae*	Panama		14.97 copies
140620_A07	Swab Sample	*Batrachochytrium dendrobatidis*	*Pristimantis museosus*	Panama		71.2 copies
140621_A01	Swab Sample	*Batrachochytrium dendrobatidis*	*Allobates talamancae*	Panama		8.94 copies

140622_R01	Swab Sample	*Batrachochytrium dendrobatidis*	*Atelopus varius*	Panama		3.09 copies
140624_01	Swab Sample	*Batrachochytrium dendrobatidis*	*Rana warszewitschii*	Panama		3832.79 copies
140624_03	Swab Sample	*Batrachochytrium dendrobatidis*	*Silverstoneia flotator*	Panama		476.37 copies
140626_02	Swab Sample	*Batrachochytrium dendrobatidis*	*Silverstoneia flotator*	Panama		28.59 copies
140626_08	Swab Sample	*Batrachochytrium dendrobatidis*	*Craugastor crassidigitus*	Panama		32.73 copies
140628_11	Swab Sample	*Batrachochytrium dendrobatidis*	*Rana warszewitschii*	Panama		38.45 copies
140628_13	Swab Sample	*Batrachochytrium dendrobatidis*	*Sachatamia albomaculata*	Panama		4.72 copies
140630_R04	Swab Sample	*Batrachochytrium dendrobatidis*	*Craugastor fitzingeri*	Panama		17.78 copies
140630_04	Swab Sample	*Batrachochytrium dendrobatidis*	*Rana warszewitschii*	Panama		8122.91 copies
140630_05	Swab Sample	*Batrachochytrium dendrobatidis*	*Rana warszewitschii*	Panama		222.53 copies
140630_12	Swab Sample	*Batrachochytrium dendrobatidis*	*Rana warszewitschii*	Panama		412.47 copies
140701_07	Swab Sample	*Batrachochytrium dendrobatidis*	*Colostethus panamensis*	Panama		8.1 copies
140707_J02	Swab Sample	*Batrachochytrium dendrobatidis*	*Espadarana prosoblepon*	Panama		81.58 copies
140707_J03	Swab Sample	*Batrachochytrium dendrobatidis*	*Espadarana prosoblepon*	Panama		59.09 copies
140707_J04	Swab Sample	*Batrachochytrium dendrobatidis*	*Espadarana prosoblepon*	Panama		13.87 copies
140707_J08	Swab Sample	*Batrachochytrium dendrobatidis*	unknown	Panama		102.92 copies
140707_R13	Swab Sample	*Batrachochytrium dendrobatidis*	*Hyloscirtus colymba*	Panama		114.53 copies
140708_R05	Swab Sample	*Batrachochytrium dendrobatidis*	*Rana warszewitschii*	Panama		116706.13 copies
140708_R12	Swab Sample	*Batrachochytrium dendrobatidis*	*Hyloscirtus colymba*	Panama		4283.28 copies
140708_R17	Swab Sample	*Batrachochytrium dendrobatidis*	*Sachatamia albomaculata*	Panama		91698.13 copies
140711_01	Swab Sample	*Batrachochytrium dendrobatidis*	*Smilisca phaeota*	Panama		79.44 copies
140711_02	Swab Sample	*Batrachochytrium dendrobatidis*	*Rana warszewitschii*	Panama		249.96 copies
140711_A02	Swab Sample	*Batrachochytrium dendrobatidis*	*Rana warszewitschii*	Panama		1069.82 copies
140711_A03	Swab Sample	*Batrachochytrium dendrobatidis*	*Rana warszewitschii*	Panama		12171.81 copies
140712_R04	Swab Sample	*Batrachochytrium dendrobatidis*	*Silverstoneia flotator*	Panama		29.52 copies
140712_R06	Swab Sample	*Batrachochytrium dendrobatidis*	*Sachatamia albomaculata*	Panama		5980.99 copies
140716_R01	Swab Sample	*Batrachochytrium dendrobatidis*	*Rana warszewitschii*	Panama		715.08 copies
140716_R02	Swab Sample	*Batrachochytrium dendrobatidis*	*Rana warszewitschii*	Panama		27155.08 copies
140718_R12	Swab Sample	*Batrachochytrium dendrobatidis*	*Rhaebo haematiticus*	Panama		5457.36 copies
140718_R19	Swab Sample	*Batrachochytrium dendrobatidis*	*Rhaebo haematiticus*	Panama		2.71 copies
St.Dil_100_A	Standard Dilution	*Batrachochytrium dendrobatidis*				100 copies
St.Dil_10_A	Standard Dilution	*Batrachochytrium dendrobatidis*				10 copies
St.Dil_1_A	Standard Dilution	*Batrachochytrium dendrobatidis*				1 copies
St.Dil_0.1_A	Standard Dilution	*Batrachochytrium dendrobatidis*				0.1 copies

St.Dil_100_B	Standard Dilution	*Batrachochytrium dendrobatidis*				100 copies
St.Dil_10_B	Standard Dilution	*Batrachochytrium dendrobatidis*				10 copies
St.Dil_1_B	Standard Dilution	*Batrachochytrium dendrobatidis*				1 copies
St.Dil_0.1_B	Standard Dilution	*Batrachochytrium dendrobatidis*				0.1 copies
St.Dil_100_C	Standard Dilution	*Batrachochytrium dendrobatidis*				100 copies
St.Dil_10_C	Standard Dilution	*Batrachochytrium dendrobatidis*				10 copies
St.Dil_1_C	Standard Dilution	*Batrachochytrium dendrobatidis*				1 copies
St.Dil_0.1_C	Standard Dilution	*Batrachochytrium dendrobatidis*				0.1 copies

S3 Table: Cost estimate for Bd Fluidigm Access Array vs whole genome sequencing for post-extraction samples. This comparison assumes that the cost of DNA extraction and post-sequencing analysis of samples are equal for each approach. All costs are based on prices for services and goods bought or rendered in 2016.

Bd Fluidigm Access Array			
Item	*Unit Cost*	*Samples per Unit*	*Per Sample Cost*
Fluidigm 48x48 well Singleplex Chip	$886.00	48	$18.46
Plate of amplicon primer/Illumina double barcoded adapters	$40.00	96	$0.42
Library Preparation and Quantification (qPCR, Fragment Analyzation, and Bead Size Selection)	$60.00	96	$0.63
MiSeq Sequencing v3 (600 cycles)	¼ lane at $682.25	100x coverage for 192 samples	$3.55
Pre-amplification reagents (Roche FastStart High Fidelity PCR kit and ExoSAP-IT)	$5838	2500	$2.34
Primers	$5760	5000	$1.15
		TOTAL PER SAMPLE COST:	**$26.55**
Whole Genome Sequencing			
Item	*Unit Cost*	*Samples per Unit*	*Per Sample Cost*
Illumina DNA Library Prep	$181.50	1	$181.50
MiSeq Sequencing v3 (600 cycles)	1 lane at $2,274.00	60x coverage for 6 samples	$379.00

		TOTAL PER SAMPLE COST:	**$560.50**

Appendix for Chapter 2

S1 Table: Whole genome data and associated NCBI SRA accession numbers for samples used to generate consensus loci sequences and compare whole genome loci sequences to sequenced amplicons.

Isolate Name	NCBI SRA accession number	Geographic Origin	Lineage	Reference	Fluidigm sequenced?
BdBE1	SRS2757215	Belgium	Bd-GPL	O'Hanlon et al. 2018 (2)	Y
BdBE2	SRS2757216	Belgium	Bd-GPL	O'Hanlon et al. 2018 (2)	Y
BdBE3	SRS2757203	Belgium	Bd-GPL	O'Hanlon et al. 2018 (2)	Y
BdBE4	SRS2757202	Belgium	Bd-GPL	O'Hanlon et al. 2018 (2)	Y
BdBE5	SRS2757217	Belgium	Bd-GPL	O'Hanlon et al. 2018 (2)	Y
BdBE6	SRS2757201	Belgium	Bd-GPL	O'Hanlon et al. 2018 (2)	Y
BdNL1	SRS2757200	Belgium	Bd-GPL	O'Hanlon et al. 2018 (2)	Y
Hung_2039	SRS2757169	Hungary	Bd-GPL	O'Hanlon et al. 2018 (2)	N
MC94	SRS2757147	South Africa	Bd-GPL	O'Hanlon et al. 2018 (2)	N
ETH4	SRS379476	Ethiopia	Bd-GPL	Farrer et al. 2013 (8)	N
0739	SRS2757206	Switzerland	Bd-CH	O'Hanlon et al. 2018 (2)	N
CCB1	SRS2757205	Spain	Bd-CAPE	O'Hanlon et al. 2018 (2)	N
SA-EC3	SRS2757071	South Africa	Bd-CAPE/Bd-GPL Hybrid	O'Hanlon et al. 2018 (2)	N
SA-EC5	SRS2757072	South Africa	Bd-CAPE/Bd-GPL Hybrid	O'Hanlon et al. 2018 (2)	N
CFFT061	SRS2757098	Brazil	Bd-ASIA2/Bd-Brazil	O'Hanlon et al. 2018 (2)	N
KB45	SRS2757137	South Korea	Bd-ASIA2/Bd-Brazil	O'Hanlon et al. 2018 (2)	N
KB108	SRS2757135	South Korea	Bd-ASIA2/Bd-Brazil	O'Hanlon et al. 2018 (2)	N
KB347	SRS2757075	South Korea	Bd-ASIA1	O'Hanlon et al. 2018 (2)	N
KBO_317	SRS2757076	South Korea	Bd-ASIA1	O'Hanlon et al. 2018 (2)	N
KRBOOR_323	SRS2757080	South Korea	Bd-ASIA1	O'Hanlon et al. 2018 (2)	N
UM142	SRR635210	Michigan, USA	Bd-ASIA2/Bd-Brazil	Rosenblum et al. 2013 (9)	Y
LbAber	SRR635200	Australia	Bd-GPL	Rosenblum et al. 2013 (9)	Y
TST75	SRR635208	California, USA	Bd-GPL	Rosenblum et al. 2013 (9)	Y
SRS812	SRR635207	South Carolina, USA	Bd-GPL	Rosenblum et al. 2013 (9)	Y
NBRC106979	SRR635206	Japan	Bd-GPL	Rosenblum et al. 2013 (9)	Y
MLA1	SRR635205	Argentina	Bd-GPL	Rosenblum et al. 2013 (9)	Y
MexMkt	SRR635204	Mexico	Bd-GPL	Rosenblum et al. 2013 (9)	Y
JEL627	SRR635199	Maine, USA	Bd-GPL	Rosenblum et al. 2013 (9)	Y
JEL433	SRR635198	South Africa	Bd-GPL	Rosenblum et al. 2013 (9)	Y
JEL429	SRR635201	Venezuela	Bd-GPL	Rosenblum et al. 2013 (9)	Y
JEL427	SRR635068	Puerto Rico	Bd-GPL	Rosenblum et al. 2013 (9)	Y

JEL359	SRR634983	New Hampshire, USA	Bd-GPL	Rosenblum et al. 2013 (9)	Y
JEL310	SRR634981	Panama	Bd-GPL	Rosenblum et al. 2013 (9)	Y
JEL275	SRR634978	Colorado, USA	Bd-GPL	Rosenblum et al. 2013 (9)	Y
JEL271	SRR634977	California, USA	Bd-GPL	Rosenblum et al. 2013 (9)	Y
JEL267	SRR634976	Quebec, Canada	Bd-GPL	Rosenblum et al. 2013 (9)	Y
JEL238	SRR634975	Arizona, USA	Bd-GPL	Rosenblum et al. 2013 (9)	Y
EV001	SRR634967	Colombia	Bd-GPL	Rosenblum et al. 2013 (9)	Y
CJB7	SRR634693	California, USA	Bd-GPL	Rosenblum et al. 2013 (9)	Y
CJB5-2	SRR634692	California, USA	Bd-GPL	Rosenblum et al. 2013 (9)	Y
CJB4	SRR632144	California, USA	Bd-GPL	Rosenblum et al. 2013 (9)	Y
LFT001-10	SRR635202	Brazil	Bd-ASIA2/Bd-Brazil	Rosenblum et al. 2013 (9)	Y
CLFT024-02	SRR634964	Brazil	Hybrid: Bd-ASIA2/Bd-Brazil & Bd-GPL	Rosenblum et al. 2013 (9)	N

S2 Table: Comparison of amplicon sequences derived from whole genome data and from sequencing via the Fluidigm Access Array. Whole genome amplicons are consensus sequences with IUPAC ambiguity codes using a threshold of 75%.

Isolate Name	Loci compared	# identical bases	# differences	% similarity	# SNP differences	# indel base differences
BdBE1	186	25,502	60	99.66	15	40
BdBE2	185	25,380	39	99.70	9	25
BdBE3	185	25,206	211	99.32	152	55
BdBE4	185	25,372	46	99.67	9	28
BdBE5	184	25,215	38	99.79	10	23
BdBE6	185	25,350	61	99.75	31	23
BdNL1	185	25,367	39	99.73	7	24
CJB4	183	24,996	90	99.58	11	60
CJB5-2	185	25,305	98	99.59	28	56
CJB7	184	25,160	83	99.59	18	52
EV001	172	23,540	38	99.81	15	17
JEL238	185	25,315	93	99.58	24	60
JEL267	185	25,326	81	99.58	13	60
JEL271	185	25,323	92	99.56	22	65
JEL275	185	25,325	90	99.61	14	70
JEL310	166	22,706	32	99.84	17	9
JEL359	185	25,310	97	99.57	25	60
JEL427	168	22,965	92	99.62	34	54
JEL429	183	25,020	68	99.69	12	52
JEL433	183	25,016	83	99.62	13	64
JEL627	184	25,164	87	99.53	15	62
LbAber	185	25,276	133	99.53	65	61
LFT001-10	182	24,815	138	99.41	67	68
MexMkt	186	25,473	77	99.65	10	61
MLA1	185	25,165	95	99.58	18	71
NBRC106979	185	25,327	73	99.69	19	47
SRS812	184	25,169	77	99.68	9	56
TST75	185	25,262	145	99.50	52	63
UM142	185	25,301	104	99.54	11	87

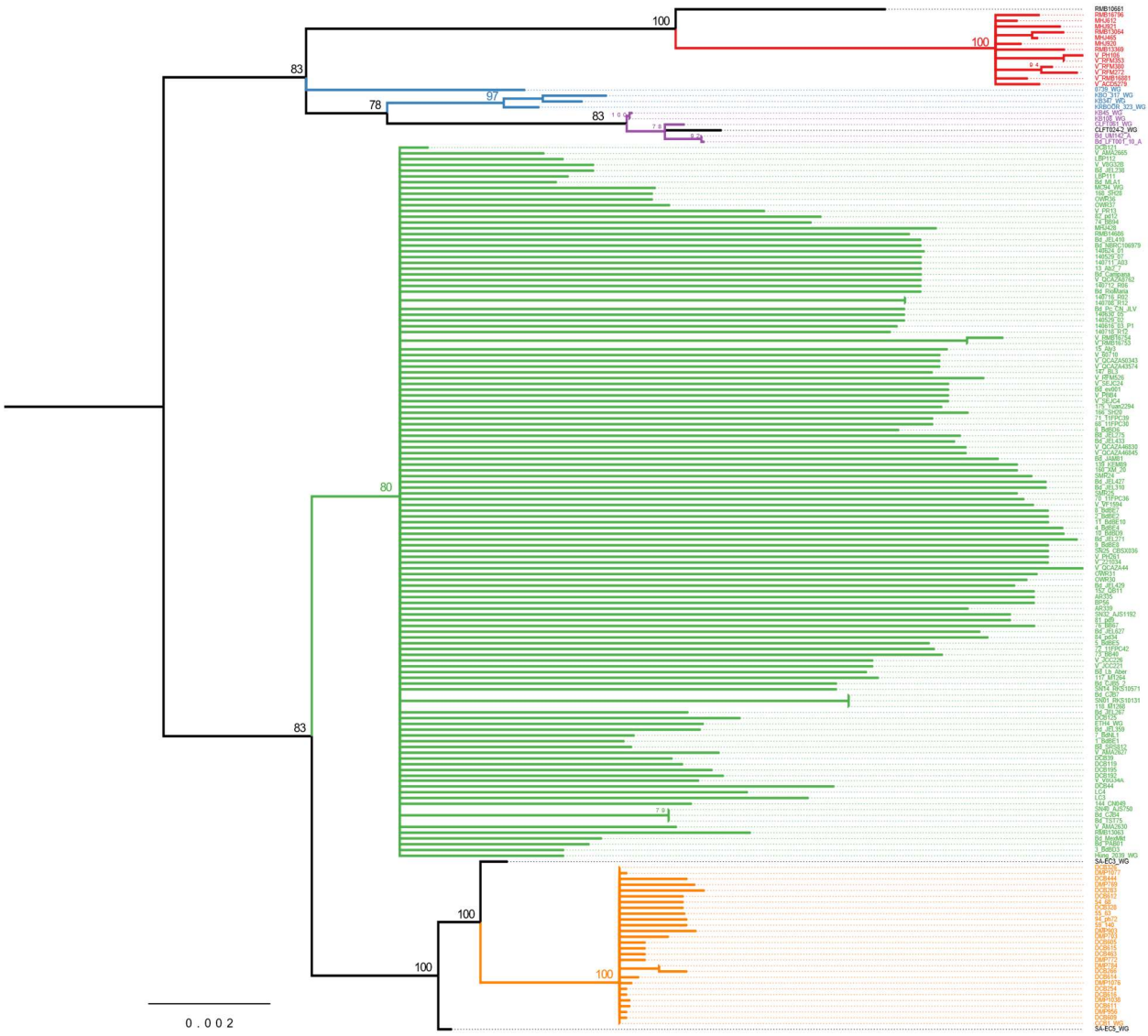

S1 Figure: Phylogeny from Figure 1B with printed tip labels.

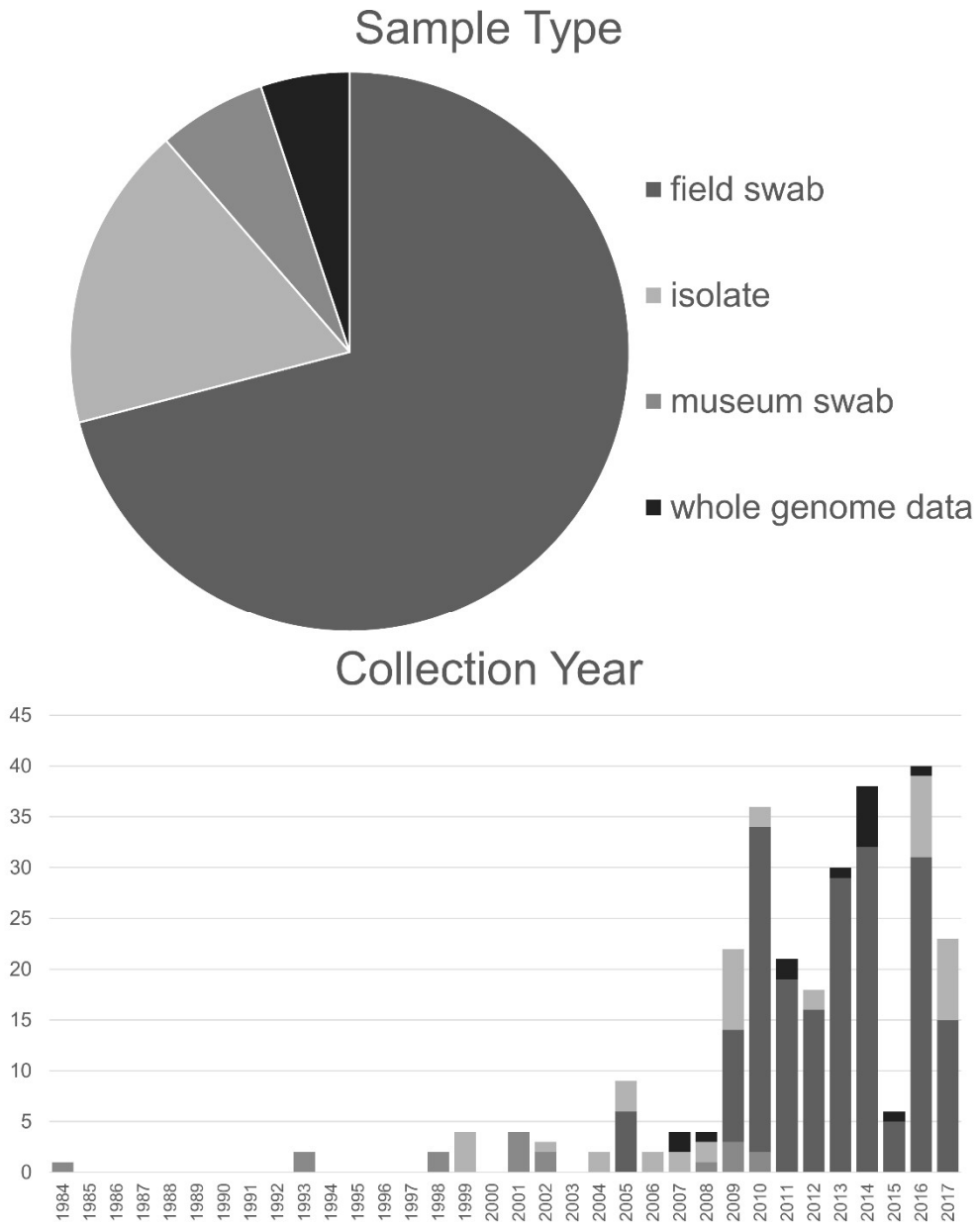

S2 Figure: Sample type and collection year for 270 samples used in this study. 222 samples are newly genotyped and 47 samples are previously-published whole genome data.

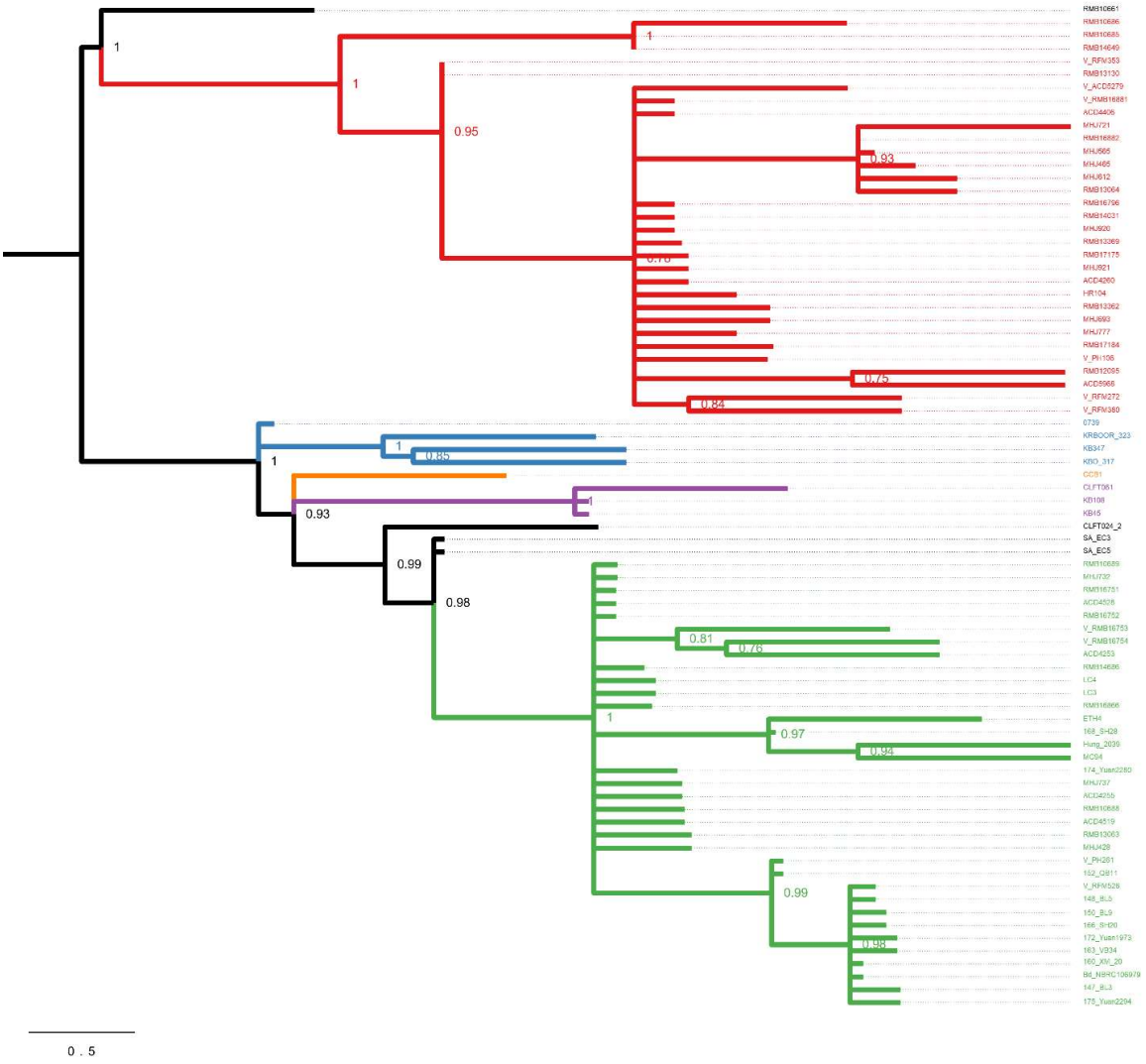

S3 Figure: Consensus tree from samples collected in Asia and representatives from major Bd clades (N=78) as pictured in Figure 1B. Tree was created using Astral (v.5.6.2; 7) and used 171 locus trees to calculate a consensus tree. Tree has a normalized quartet score of 0.807. Nodes with a posterior below 0.7 are collapsed. Tree is midpoint rooted. Major Bd clades are indicated by color (green = BdGPL, pink = BdBrazil/ASIA2, blue = BdASIA1, red = BdASIA3, orange = BdCAPE).

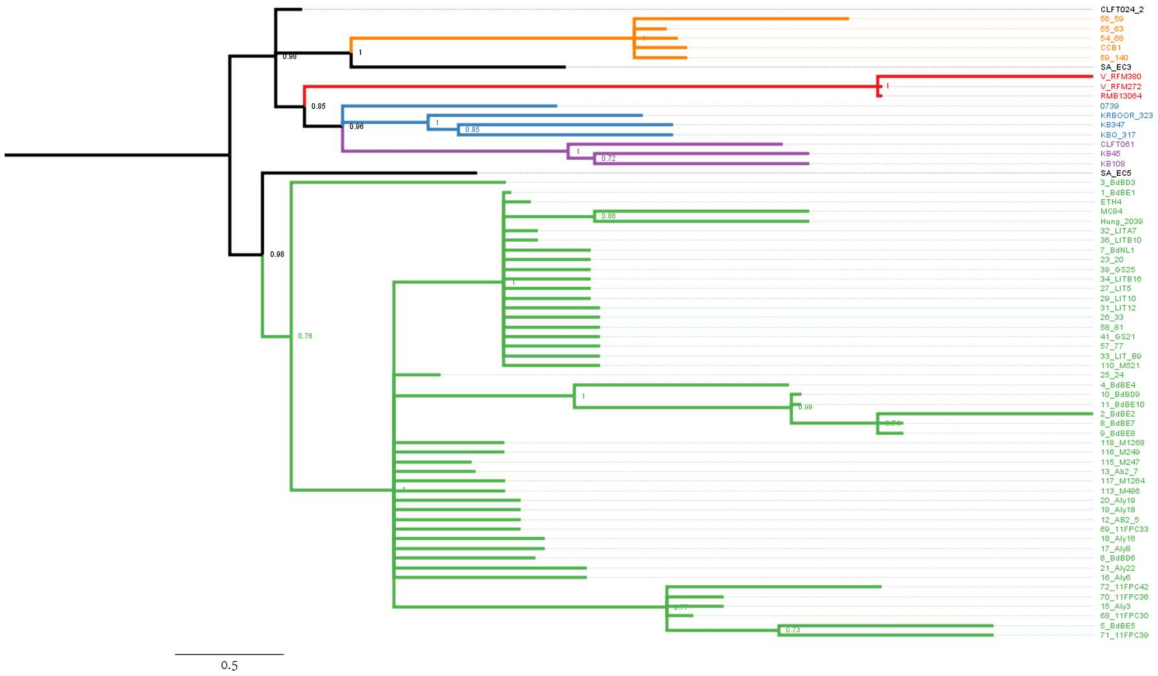

S4 Figure: Consensus tree from samples collected in Europe and representatives from major Bd clades (N=66) as pictured in Figure 1A. Tree was created using Astral (v.5.6.2; 7) and used 173 locus trees to calculate a consensus tree. Tree has a normalized quartet score (measure of the proportion of locus trees satisfied by the consensus tree before correcting for multiple individuals) of 0.746. Nodes with a posterior below 0.7 are collapsed. Tree is midpoint rooted. Major Bd clades are indicated by color (green = *Bd*GPL, pink = *Bd*Brazil/ASIA2, blue = *Bd*ASIA1, red = *Bd*ASIA3, orange = *Bd*CAPE).

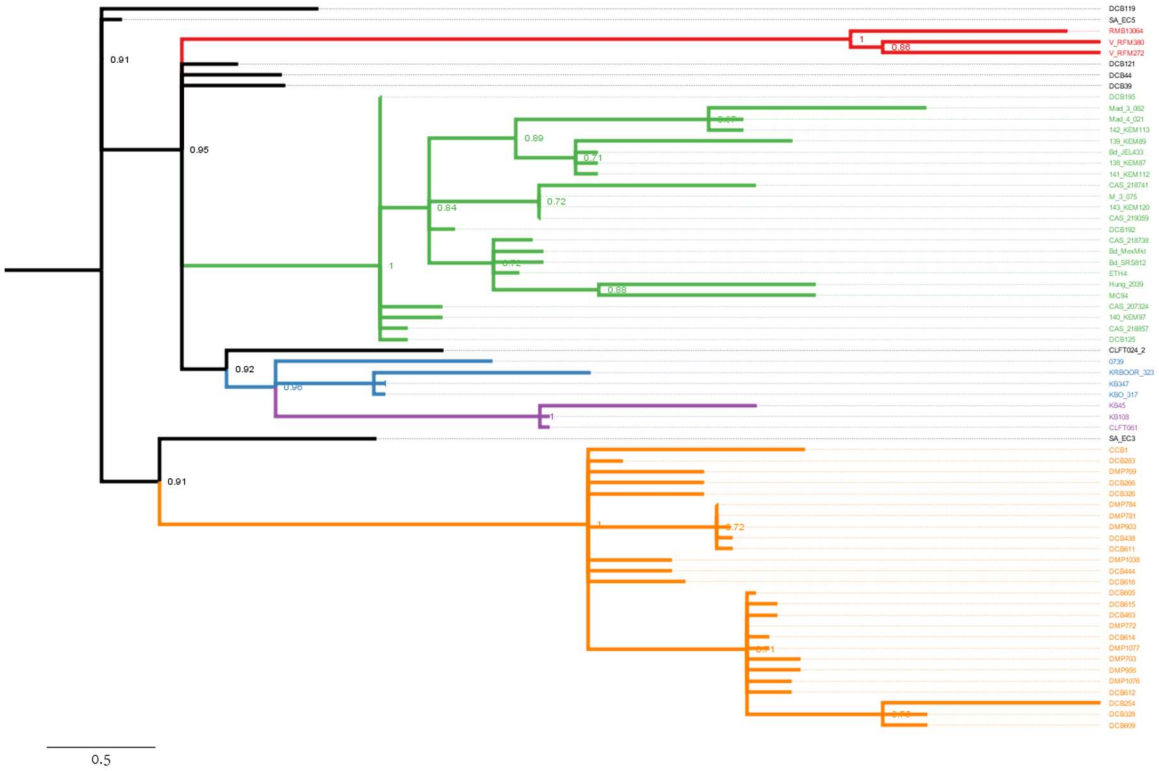

S5 Figure: Consensus tree from samples collected in Africa and representatives from major Bd clades (N=66) as pictured in Figure 1C. Tree was created using Astral (v.5.6.2; 7) and used 169 locus trees to calculate a consensus tree. Tree has a normalized quartet score of 0.813. Nodes with a posterior below 0.7 are collapsed. Tree is midpoint rooted. Major Bd clades are indicated by color (green = *Bd*GPL, pink = *Bd*Brazil/ASIA2, blue = *Bd*ASIA1, red = *Bd*ASIA3, orange = *Bd*CAPE).

S6 Figure: Consensus tree from samples collected in the Americas and representatives from major Bd clades (N=108) as pictured in Figure 1D. Tree was created using Astral (v.5.6.2; 7) and used 173 locus trees to calculate a consensus tree. Tree has a normalized quartet score of 0.736. Nodes with a posterior below 0.7 are collapsed. Tree is midpoint rooted. Major Bd clades are indicated by color (green = *Bd*GPL, pink = *Bd*Brazil/ASIA2, blue = *Bd*ASIA1, red = *Bd*ASIA3, orange = *Bd*CAPE).

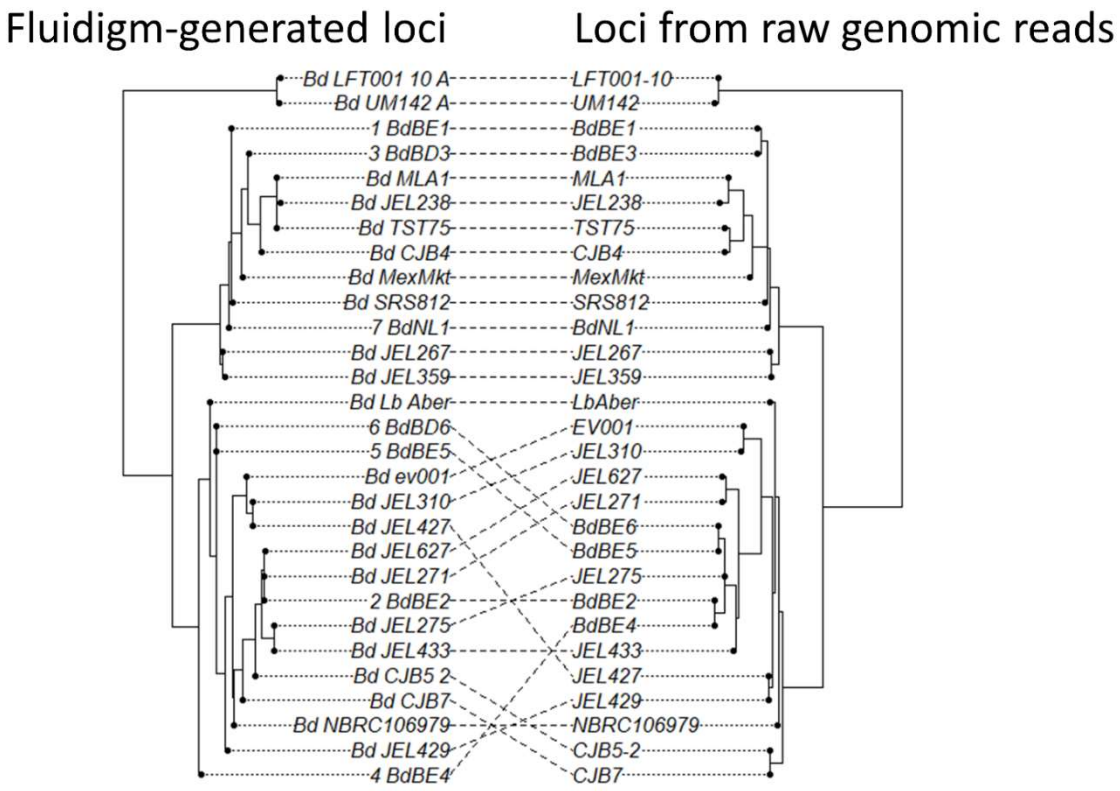

S7 Figure: Cophylogeny of whole genome data vs. Fluidigm sequence data for 29 *Bd* samples. Each tree was created using RAxML from 159 concatenated loci (22,106 bp). Trees are midpoint rooted. Whole genome data uses IUPAC ambiguity codes at a threshold of 75% from raw genomic reads and Fluidigm data uses IUPAC ambiguity codes to include all alleles present in at least 5 reads and in at least 5% of sequenced amplicons.

Appendix for Chapter 3

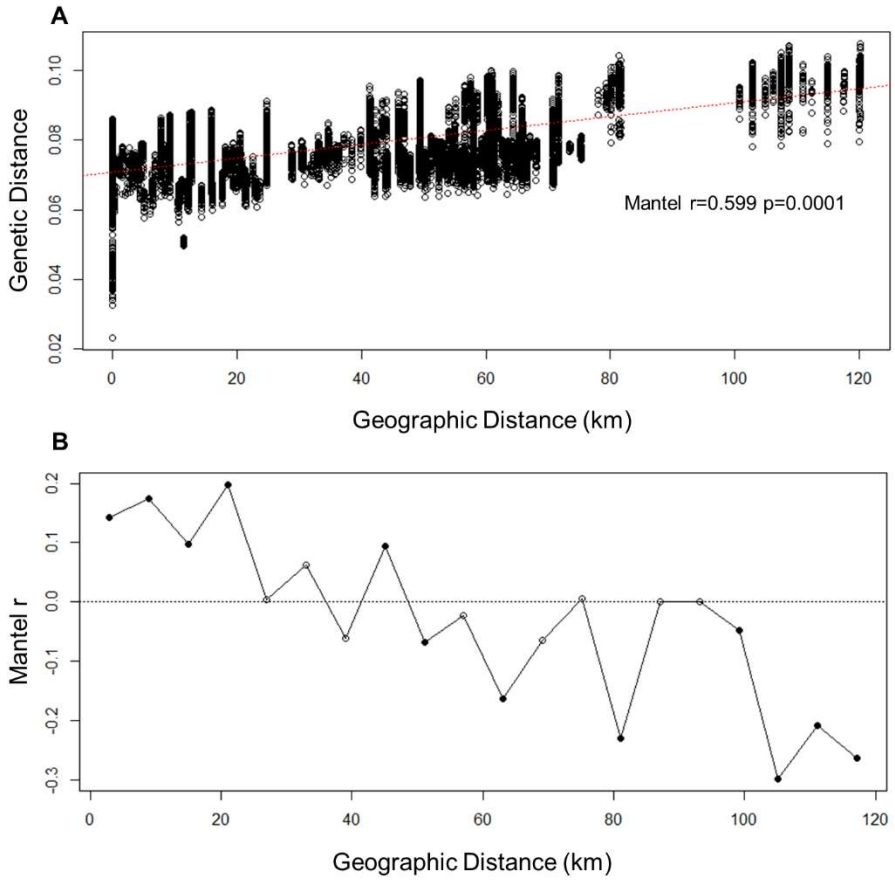

S1 Figure: Scatter plots showing a strong association of geographic and genetic distance. (A) Pairwise comparisons of geographic and genetic distance for *Atelopus varius* and *zeteki* in Panamá. Trend line shows the linear relationship of geographic and genetic distance calculated using a Mantel test (r = 0.599, p = 0.0001). (B) Mantel corellogram showing Mantel r statistic across 20 even geographic bins (each ~6km). Filled circles indicate statistical significance (α=.01).

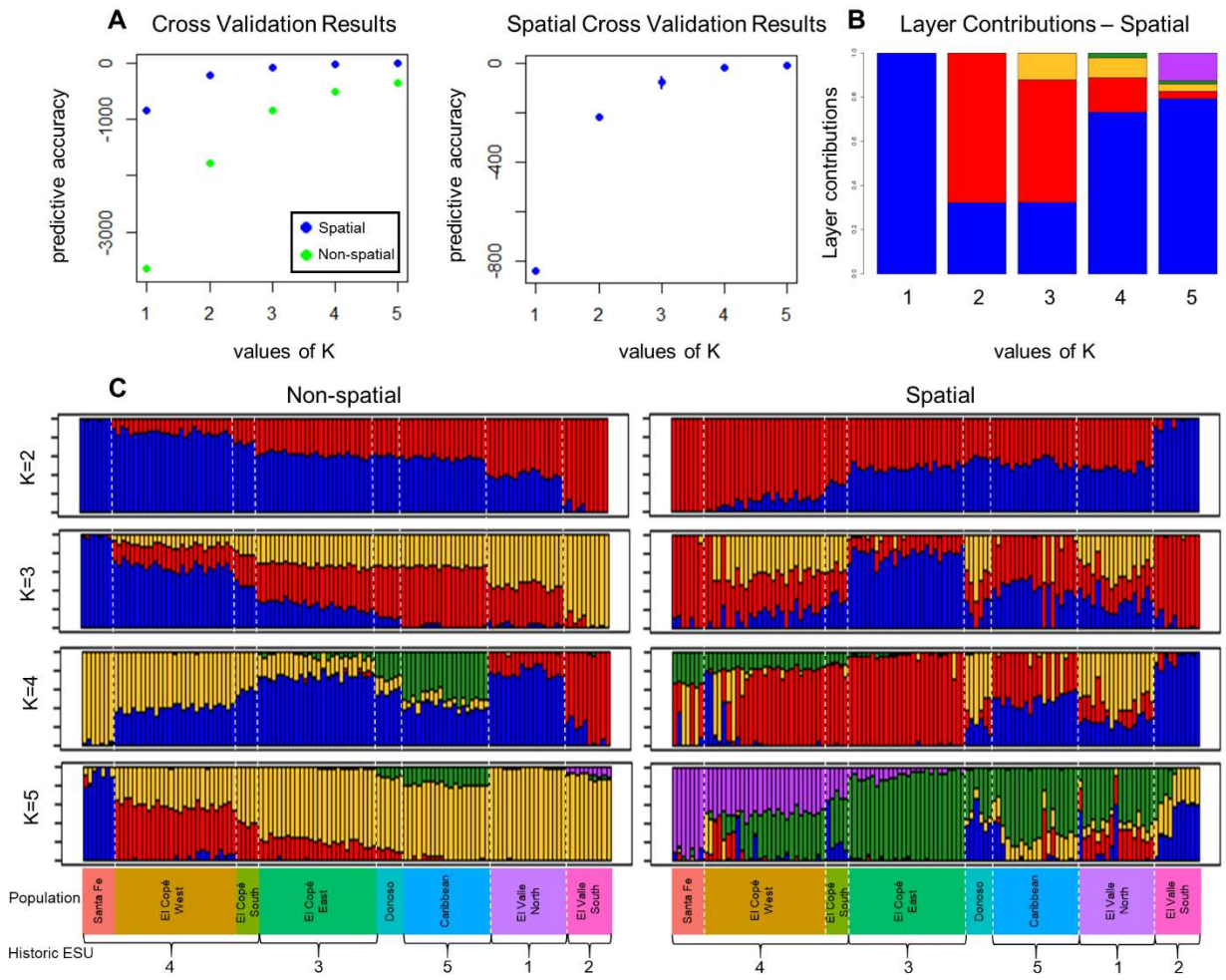

S2 Figure: ConStruct analysis reveals spatial model at K = 2 best fits the data. (A) Results from ConStruct x-validation comparing spatial and non-spatial model accuracy (left) and showing zoomed-in values for the spatial model (right). (B) Layer contributions for the spatial model for K=1 to K=5. (C) Admixture plots for K=2-5 showing non-spatial (left) and spatial (right) models. Populations are indicated below and colored as in Fig 1. Historic ESUs from Richards and Knowles (2007) (Richards & Knowles, 2007) are labeled below populations.

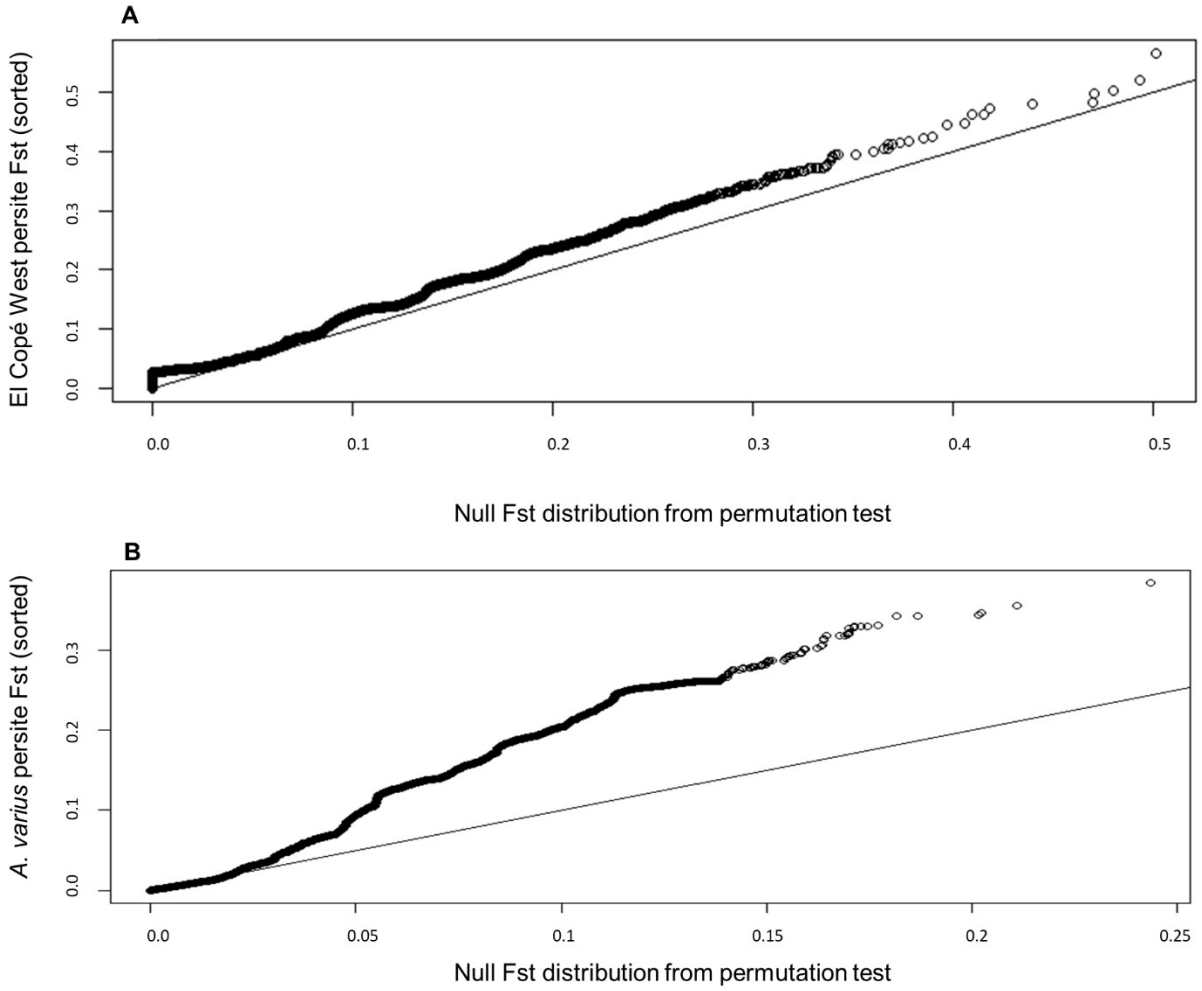

S3 Figure: Comparison of per-SNP F_{ST} values to a null F_{ST} distribution shows lack of significant Fst outliers. Null F_{ST} values generated via permutation test shows no significant outliers for the local El Copé West analysis (A) or the global analysis of all historic and contemporary *A. varius* (B).

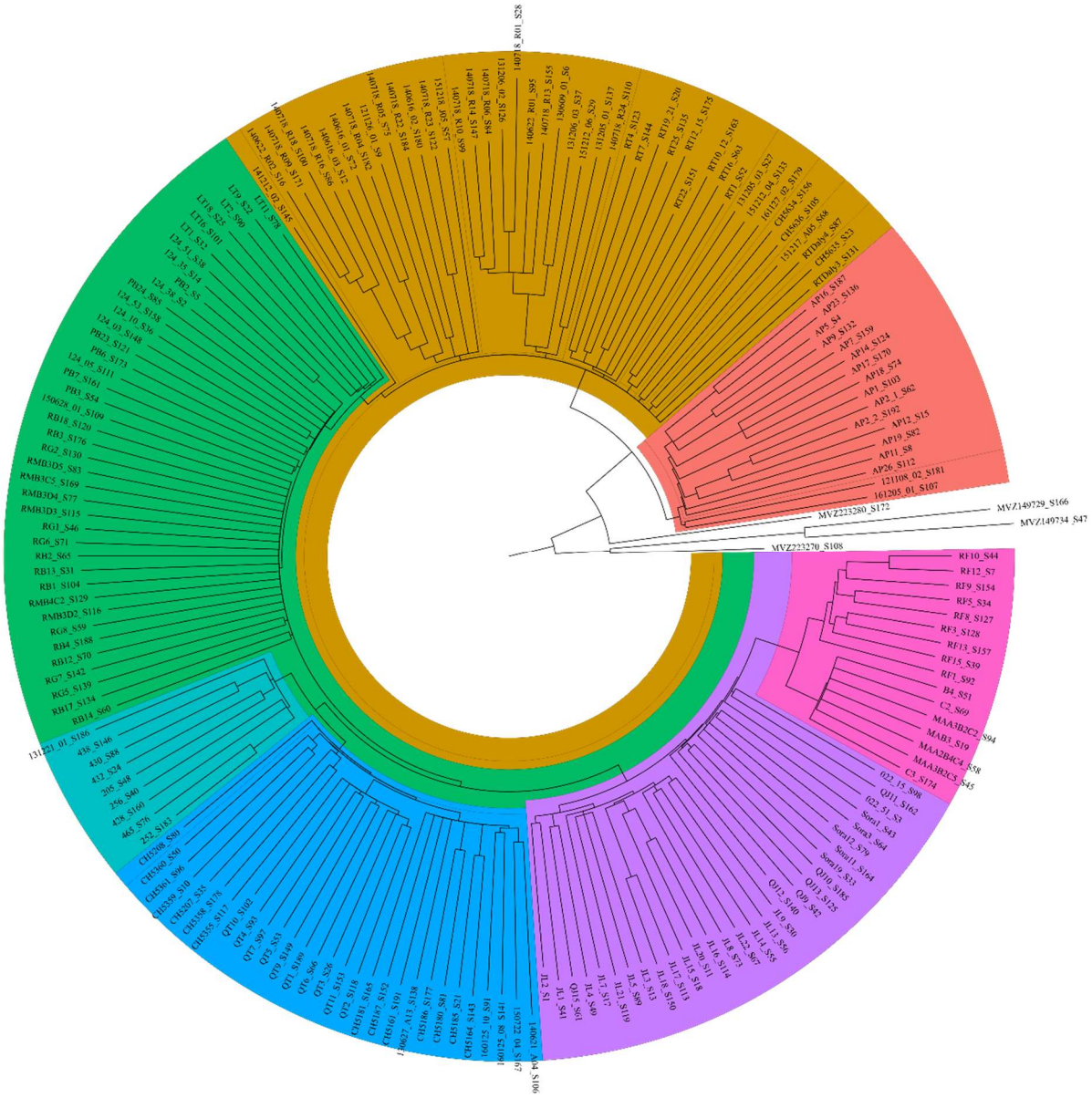

S4 Figure: Distance-based phylogeny for all samples (N=190). Consensus tree calculated from 100 bootstrap replicates of blocks of 1000 random SNPs. Tree is rooted on branch leading to outgroups from Costa Rica. Nodes with <70 bootstrap support are collapsed. Samples are colored as in Fig 2A. Branch lengths have been transformed proportionally for display purposes.

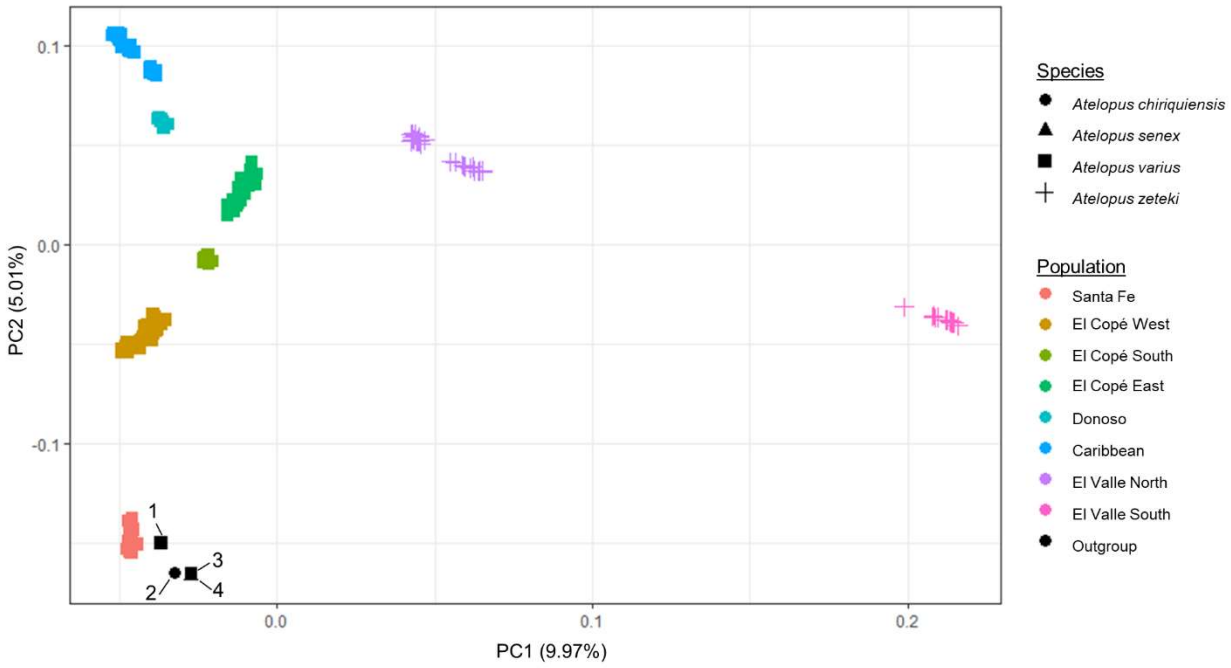

S5 Figure: PCA including 4 samples from Costa Rica shows taxonomic confusion of *Atelopus* in Costa Rica. Panamanian populations colored as in Fig 1 and samples from Costa Rica are shown in black. Sample numbers correspond to the following samples: 1) MVZ223280 2) MVZ223270 3) MVZ149729 4) MVZ149734.